A DISPERSION CURVE STUDY OF MODEL DREDGE SPOIL BASINS

Robert Male

and

David R. Basco

Coastal and Ocean Engineering Division
Civil Engineering Department
Texas A&M University

September 1974

TAMU-SG-75-201

C.D.S. Report No. 180

This research is a result of Sea Grant Project entitled "Hydraulic Characteristics of Diked Dredge Spoil Areas". It is partially supported through Institutional Grant 04-3-158-18 to Texas A&M University by the National Oceanic and Atmospheric Administration's Office of Sea Grant, U.S. Department of Commerce

$3.00

Order from:

Department of Marine Resources Information
Center for Marine Resources
Texas A&M University
College Station, TX 77843

ABSTRACT

Recent legislation relating to water quality standards has seriously affected the dredging industry, particularly the normal methods of spoil disposal. Settling basin effluents must meet the required standards, necessitating the development of improved basin operation and design.

In this study, settling tank theory and tracer testing techniques were used to compare a plain pipe inlet, various baffled inlet designs, and a reaction-jet inlet in a model spoil basin. Methods were developed to use the dye tracing technique with the tank effluent being recycled.

Baffling improved the tank performance over the uncontrolled condition. A single baffle centrally placed in front of the inlet proved to be better than (1) the same baffle with collinear baffles on each side; (2) a baffle box; and (3) a reaction-jet plate on the inlet pipe. Increasing the water depth also yielded significant improvements in behavior.

The model flow regimes were maintained similar to those in a spoil basin, so that the findings would be relevant to dredging practice. Further research work is clearly required, but the results of this study indicate that basin performance can be appreciably improved by constructing a short dike across the path of the influent and by keeping the water depth at a maximum.

Field-testing is recommended to determine dispersion curves under various conditions in the basin. A method is shown to calculate sediment

removal from the interaction of dispersion curves with a quiescent column settling curve.

ACKNOWLEDGEMENTS

The majority of the report was prepared by the first author in partial fulfillment of the requirements for the degree of Master of Science in Civil Engineering at Texas A&M University. The M.S. thesis that resulted was entitled "A Dispersion Curve Study of Dredged Spoil Basin Inlets". The second author served as graduate advisor and added some additional test results to complete the report. Support for the project was partially provided by the NOAA Sea Grant Program at Texas A&M University and by the Texas Engineering Experiment Station.

The authors wish to express their appreciation to William Moore and Chris Mauritzen for their help in testing and data reduction. The time and effort spent in reviewing the report by Dr. Wesley James and Dr. Takashi Ichiye is also appreciated. Thanks are extended to these and many other people in the Hydraulics Laboratory and the Environmental Division who contributed in material and technical ways.

TABLE OF CONTENTS

LIST OF TABLES

LIST OF FIGURES

Figures Page

I. INTRODUCTION

During the past five to ten years, public concern for the environment has been expressed in the form of environmental policy acts and regulations. A very serious restraint has been placed on the dredging industry, particularly in relation to the disposal of dredged materials. The previously employed methods of spoil disposal in unconfined areas on land and in open water are no longer accepted and the spoil must be confined. Concurrently, increased dredging is required to keep ports competitive and waterway capacities in step with demand. The effects of these requirements are reflected in the present policy for the Great Lakes region (18)*, where all the spoil must be confined. The additional costs to be incurred in that region over ten years vary from $2.62 million to $12.87 million according to the confinement scheme.

In the USA, most of the dredging projects are under the control of the Corps of Engineers. The Corps has recognized the problem and is actively engaged in an extended study of the whole field of dredge spoil disposal (4, 12). An extract from the summary of a Corps report (2) underlines this position:

> Although confined disposal of dredged material is secondary in terms of quantity to unconfined disposal, confined disposal is increasing because of recent requirements for containment of dredged materials which are considered polluted and the resulting curtailment of

*Numbers in parentheses refer to articles listed in the Reference section of the report.

> much open water disposal. A diminishing number of suitable disposal areas, brought about by filling of existing sites and difficulties of acquiring sites because of environmental or cultural restraints on their use, has become a major problem of CE districts in their dredged material disposal programs.

In 1972, about 30% of all Corps projects depended at least in part on confined disposal, the total volume being confined per year was approximately 67,000,000 cubic yards (51,000,000 m^3) (4). To cope with this quantity in the vicinity of 7,000 acres (2800 ha) of new land are required each year. In the Great Lakes area, land is scarce but the spoil quantities are relatively small and the soil foundations sound so that high fills are possible. Along the southern Atlantic and Gulf coasts, the spoil quantities are high but the foundations are poor. Consequently, the disposal problem is much more acute in these southern regions.

Clearly, more efficient usage must be made of those areas available for spoil disposal. The purpose of this study is to take a first step towards developing methods for the improved performance of diked spoil disposal areas. The specific objectives are:

1. To use the tracer dispersion curve technique to study the hydraulic behavior in a model diked spoil basin, with various inlet configurations.
2. To appraise the documented information related to the study.
3. To recommend means of improving spoil basin

performance and the direction of subsequent study in this field.

II. REVIEW

Diked Spoil Disposal Basins

In order to establish a basis for a review, it is advantageous to briefly state the functional requirements and features of spoil basins. The functional requirements are:

1. To accept spoil during a design life.
2. To prevent solids from escaping with the effluent.
3. To be economical.

This is a basic list, there are further quantitative requirements including discharge rates, effluent quality, spoil volumes, etc., but the three listed above are fundamental.

The major features of a spoil basin are:

1. The containment walls of dikes (usually soil).
2. The inlet structure(s).
3. The outlet(s).

Other features are added in order to improve the performance of the basin: these are usually concerned with the inlets and outlets.

As simple as the above requirements and features are, the operational performances are anything but good. The Corps of Engineers include "shut down" clauses in their contracts so that disposal may be stopped in the event of dike failures or if effluent quality requirements are not being met (12). The same report states that there are few efficient well-designed diked basins. The last two statements indicate a general lack of understanding

of spoil basins. In the past, it has normally been the contractor's responsibility to construct and operate the diked basins with minimal guidance from the specification. With this situation, very little information has been accumulated from many years of experience. Few records have been kept and only one or two attempts have been made to experiment with operating basins (12).

Previous studies of basin performance have been concerned with water quality of the effluent (12, 18, 20), although some have been directed at settling velocities (4, 11). The conclusions of these studies rely heavily on the concepts adopted from settling tank theories and very little on comprehensive testing of the diked basins. There are reports that poor performances were due to short detention times (4, 12) and that an increase in depth and hence detention time produced a markedly improved solids removal (4, 12, 20). This can usually be attributed to two causes: either a flocculating suspension or the shallow depth may have been causing high velocities and, therefore, scour or a different flow pattern. The reports do not state which cause is affecting the basin, but in some cases small depths of 6 in. (20) are noted and also the fact that the water surface covered only a fraction of the complete basin area (12, 20). The fall in recovery of basins as they fill with sediment has been recorded (12) and attributed to decreased detention times. An uncertainty is evident about the factor which caused the change in recovery.

Murphy and Zeigler (12) report tests on the feasibility of using flocculating agents in a spoil basin. To meet a maximum increase in total density of 8 gm/liter above a representative ambient of 1004 gm/liter the effluent must have 2% solids (by weight) or less (for a solids SG=2.7). For a useful flocculating process the initial solids concentration should be about 1% (by weight) or less, half that of an acceptable basin effluent. The flocculating process is therefore discounted as a means to improve basin performance.

To meet a 2% solids effluent quality, removals of 80 to 90% are required. An influent slurry at 21% must be reduced by 19% so that removal is 90.5%, whereas a more usual 12% slurry requires a removal of 83%. It is clear that the operational regime of spoil basins is quite different from that of the settling tanks used for water supply and sewerage treatment.

The formation of channels in the settled material is a major problem in diked basins (12). It is associated with locally high velocities over the material which settles close to the inlet. The effect is a short circuit between the inlet and the outlet. To combat "channelization" cross and spur dikes have been used to modify the flow field in the basin, although only moderate success has been gained. Other improvement techniques are used and include the establishment of vegetation in the basin, the use of energy dissipators on the inlet pipe, and the setting of minimum crest lengths for outlet weirs. Only this last is based on a measured experience, in a Corps district (12), although all

these methods may be helpful to some degree.

Settling Tanks

Boyd et al. (4) considered that a spoil basin should be regarded as a settling pond; this is also supported in other discussions (12, 20). Little is said beyond statements that detention time is important or that local high velocities are detrimental. A considerable body of information does exist in the field of water and sewerage treatment. A review of this information is valuable in view of the scarcity which exists for spoil basins.

General Concepts

Hazen (10) established the basis of the "ideal" theory which is still used. This theory assumes a uniform water velocity distribution across the tank and particles settling as the water carries them along the tank. Given a particle settling velocity, the time required to completely settle all the material can be calculated. If in the same period, a water cross section travels the full length of the tank, the maximum discharge will be achieved for which complete settlement is still maintained. This theory concludes that the flow through the tank per unit water surface area should be set equal to the vertical settling velocity of the sediment particles. Neither depth nor detention period appear in this result, and the conclusion drawn is that the tank should be as shallow as possible without causing scour.

Camp (6) supported Hazen's hypotheses and developed them into a useful theory for settling basins. He also made a distinction between sediment particles which flocculate and those which do not. Granular suspensions can be characterized by a distribution of settling velocities. If the particles flocculate the settling velocities will change and are also affected by turbulence, the detention time and flow depth.

Camp introduced the concept of an "ideal basin" having the characteristics:

> 1. The direction of flow is horizontal and the velocity is the same in all parts of the settling zone (hence, each particle of water is assumed to remain in the settling zone for a time equal to the detention period namely, the volume of the settling zone divided by the discharge rate.)
>
> 2. The concentration of suspended particles of each size is the same at all points in the vertical cross section at the inlet end of the settling zone.
>
> 3. A particle is removed from suspension when it reaches the bottom of the settling zone.

He then postulated four zones in a settling tank; an inlet zone, a settling zone, an outlet zone and a sludge zone. This concept formed the basis of many studies where estimates were made of the effective fractions of a basin in each zone (8, 9, 13).

By considering the distribution of settling velocities for a suspension in an ideal basin, Camp developed an expression for solids removal. He modified this result for the effect of turbulent dispersion. Not many investigators have continued with this last idea, although El Baroudi (9) did, since the effect is secondary to the

main behavior. The relationship between settling velocities and flow was taken up by Villemonte et al. (19) and developed as an empirical method of computing removal and also to compare tanks. (This will be discussed later in section IV.)

Finally, Camp discussed dispersion curves in an explanation of short circuiting. The curves were noted to provide a measure of the flow pattern and means of comparing the hydraulic characteristics of tanks. The parameters t_i/T and t_m/T were preferred, although later investigators have developed a longer list of parameters used (2, 9).

Non-Ideal Tanks

Hazen and Camp worked on the assumption of ideal behavior in the tank. Except for Camp's consideration of eddy turbulence, their mathematical models considered only ideal water flows. Later investigators included non-ideal effects into their methods. The generally observed departures from ideal flow conditions are the following:

1. Dead spaces resulting in a reduction of the effective volume of the tank.
2. Short circuiting, being a direct current pattern from the inlet to the outlet. This is generally coupled with either dead spaces, recirculation or density currents.
3. Recirculation of the main flow in the tank.

4. Density currents due to a difference in density between the influent and the fluid already in the tank.
5. Mixing caused by turbulent eddies.

One to four are the result of the flow field in the tank and do not affect the settling velocities of the sediment. Mixing actually inhibits settling but may have little association with any particular flow pattern, although it is a flow property. Mixing may also improve flocculation of suitable particles.

Density currents can be beneficial if the influent floats on the tank water. Sediment need only settle into the "dead" water below to be effectively trapped. If the influent settles to the bottom, a bottom current develops and bed scour is aggravated. Most methods of analyzing settling basins cannot differentiate between these two conditions since they assume that velocity is constant with depth. Dispersion curve techniques assume a uniform vertical profile of velocity, but the results are affected by nonuniform profiles. For example, a top layer flow would have the same result as short circuiting, even though the actual sediment removals would be quite different. By comparison, Clements (7) developed a theory based on horizontal variations in velocity. Vertical profiles of velocity were measured and then averaged. Density currents do not alter the result whereas short circuiting has a detrimental effect. The required velocity measurements are extensive and rarely considered worthwhile.

Efforts to improve settling tanks are aimed at reducing the

non-ideal activity. The inlet zone is most important since it is the high energy region of the flow and has the greatest capacity for detrimental behaviour. Considerable effort has been concentrated on inlet devices to dissipate energy and disperse the influent uniformly into the tank (2, 7, 19). In settling tank practice, the inlets are usually submerged as opposed to the dredging situation where the pipeline discharges above the water level. However, if the inlet zone can be reduced to a minimum, the basin can be expected to improve significantly.

The appraisal of modifications to settling tanks is generally based on the interpretation of experimental dispersion curves (1, 2, 3, 8, 9, 13, 19). The interpretation techniques vary considerably and are discussed in section IV. The dispersion curve is a frequency distribution of the detention times of water particles passing through the tank.

Summary

The ideal theory of Hazen and Camps' is a useful concept. Consideration of departures from ideal behavior is made with experimental testing by the developed methods.

The major differences between the knowledge of dredging spoil basins and that of normal settling tanks is that a great deal of experimental effort has been put into the latter, and combined with the accumulated monitoring of performance. The result is a reasonably good empirical understanding of these tanks. For spoil basins,

the ideal theory is used but almost no empirical data are available.

Physically, spoil basins are large, wide and relatively shallow. The baffling and inlet and outlet weirs normally built in settling tanks are not suitable for spoil basins. Additionally, the wide shallow shape is not conducive to efficient settling. Outlet weirs are already used to good effect. With the high energy influent, the inlet is clearly the zone with the highest potential improvement.

III. EXPERIMENTAL ARRANGEMENT

Model Planning

Due to the generality of the application of this study, no particular diked basin could be considered as the prototype. A rational approach was to establish from available data the sizes and shapes in common practice, and the usual flow regimes. The model could then be sensibly planned.

Existing Diked Basins

An examination of spoil basins reported in literature (12, 16, 18, 20) lead to the adoption of a rectangular plan shape. Although many basins were irregular in plan the most common simple geometrical shape was a rectangle. To study the proportions and overall sizes Figure 1 was developed. It can be seen that most of the basins plotted were between 25 and 200 acres (10.1 to 81 ha) in area with the sides proportioned between 1:1 and 2:1. In many cases the plotted points represent an approximated effective rectangle so that irregular plan shapes could be included.

The positioning of inlets and outlets varied according to the site and from one use to the next. The only consistency was an attempt to separate the two points sufficiently. For the purposes of study, a pipe inlet and an overflow weir outlet were assumed. Pipe inlets are typical of cutter suction dredge practice while weir outlets are being used more generally as water quality standards

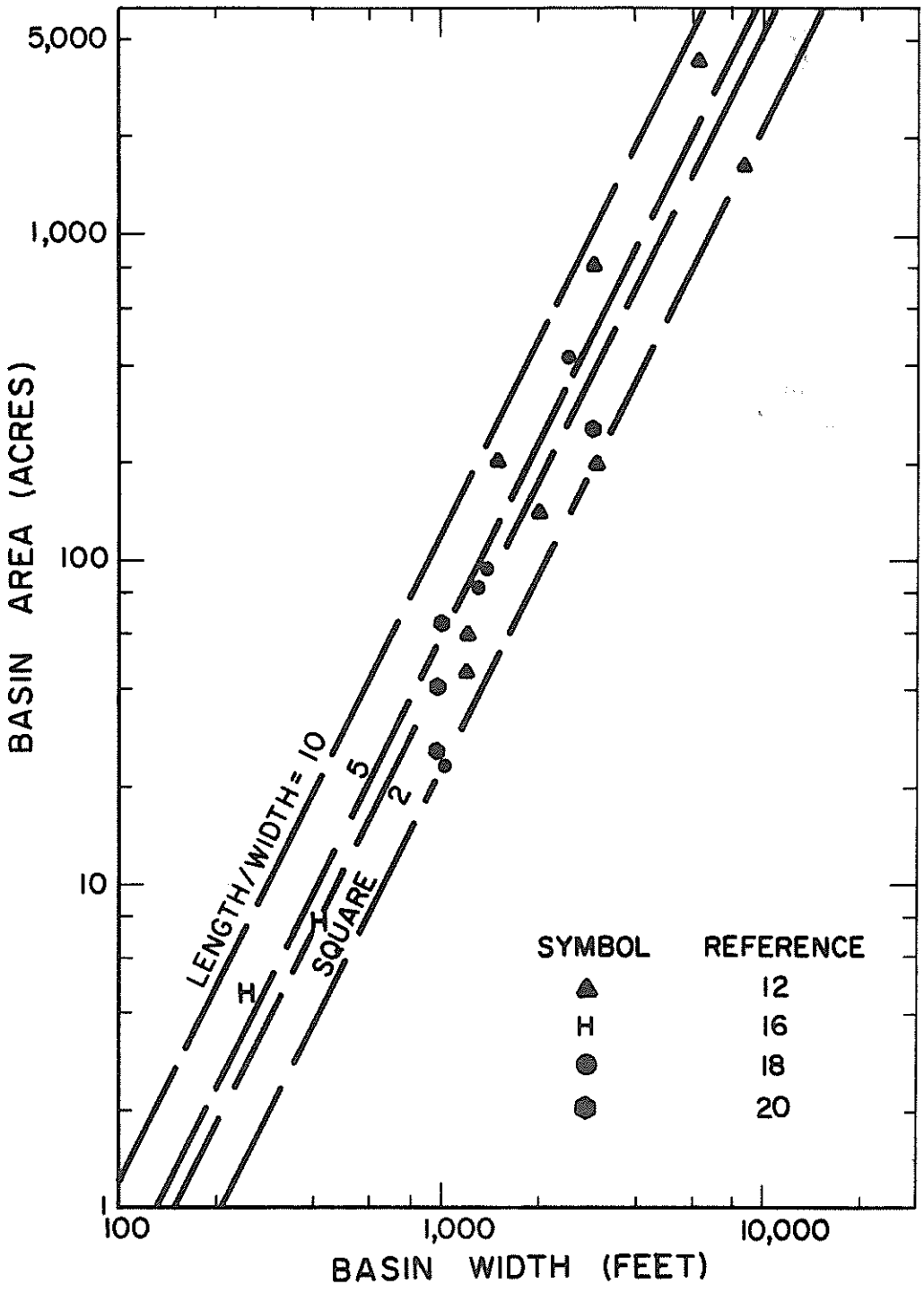

Figure 1-Dimensions of Diked Basins

are enforced.

The flow discharging into a basin depends on the dredging equipment and is independent of the basin, provided that the basin is not overloaded. Commonly used large dredges are in the size range of 24 in. to 27 in. (61 to 67.5 cm) diameter of the discharge pipeline. Extremes can be taken as 12 in. and 36 in. (30.5 and 91.5 cm) diameter pipelines. Practical velocities for the slurry in the pipe are 12 to 20 ft/sec (3.65 to 6.1 m/s). Common discharges can then be estimated at 17,000 gpm (38 cfs, 1 m^3/s) to 36,000 gpm (80 cfs, 2.24 m^3/s) with an extreme low at 4,200 gpm (9.4 cfs, 0.26 m^3/s) and an extreme high at 65,000 gpm (140 cfs, 3.9 m^3/s). Using these flow rates and assuming ideal flow (plug flow) through the basin, the practical operating region can be plotted as shown in Figure 2. The boundaries of the region should be considered as blurred and inexact, and only the critical portion of the region is plotted. Note that the flow is usually turbulent and subcritical.

The Model

To maintain the model in a similar flow regime while using water for the fluid, the largest available tank was used. Its dimensions were 82 ft x 32 ft x 2 ft maximum depth (24.4 x 9.75 x 0.61 m) (see Figure 3). In accordance with the flow regime restraints and capacities of the various components of the model, the eight testing conditions shown on Figure 2 were selected.

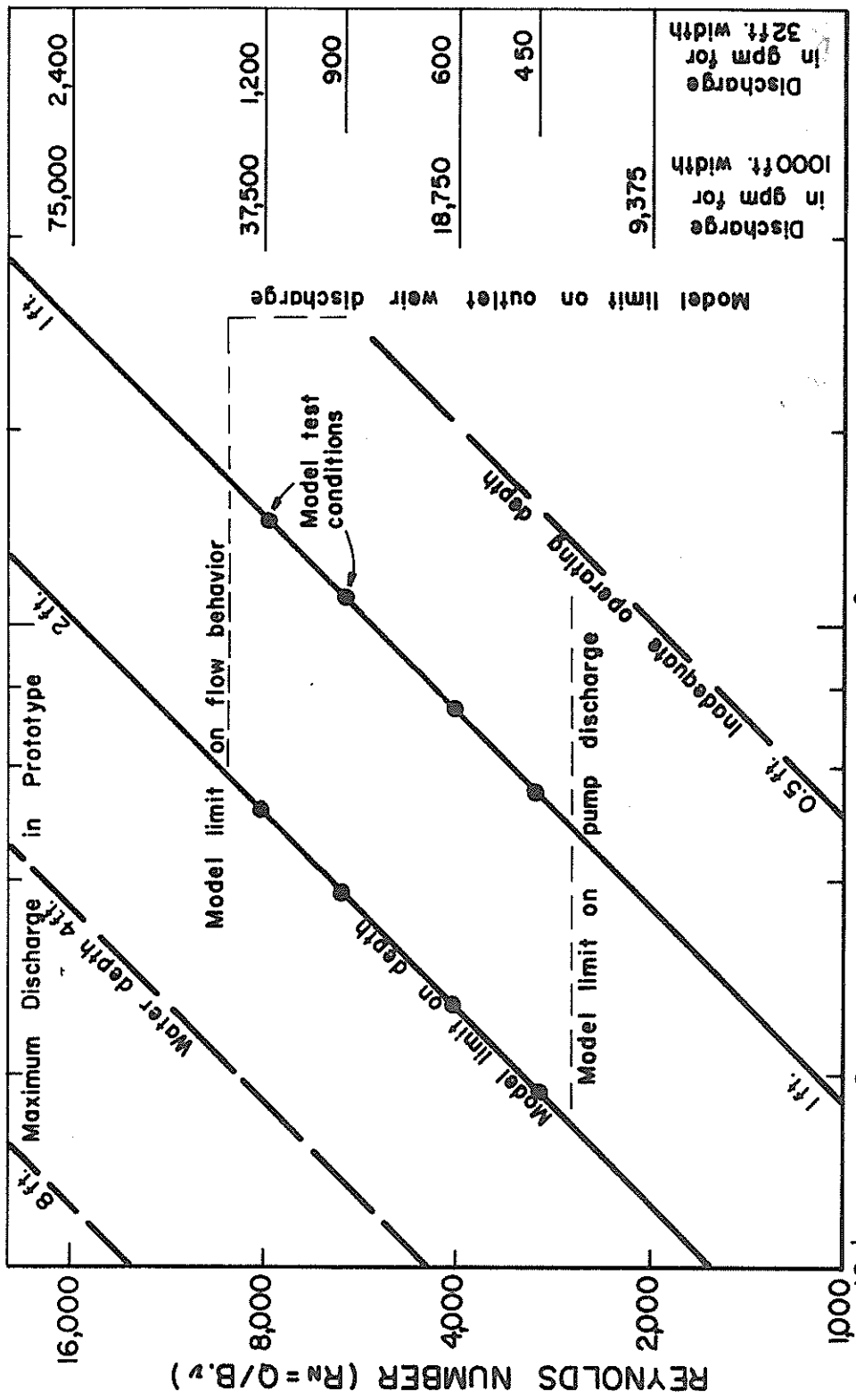

Figure 2-Operating Flow Regimes of the Model and Diked Basins

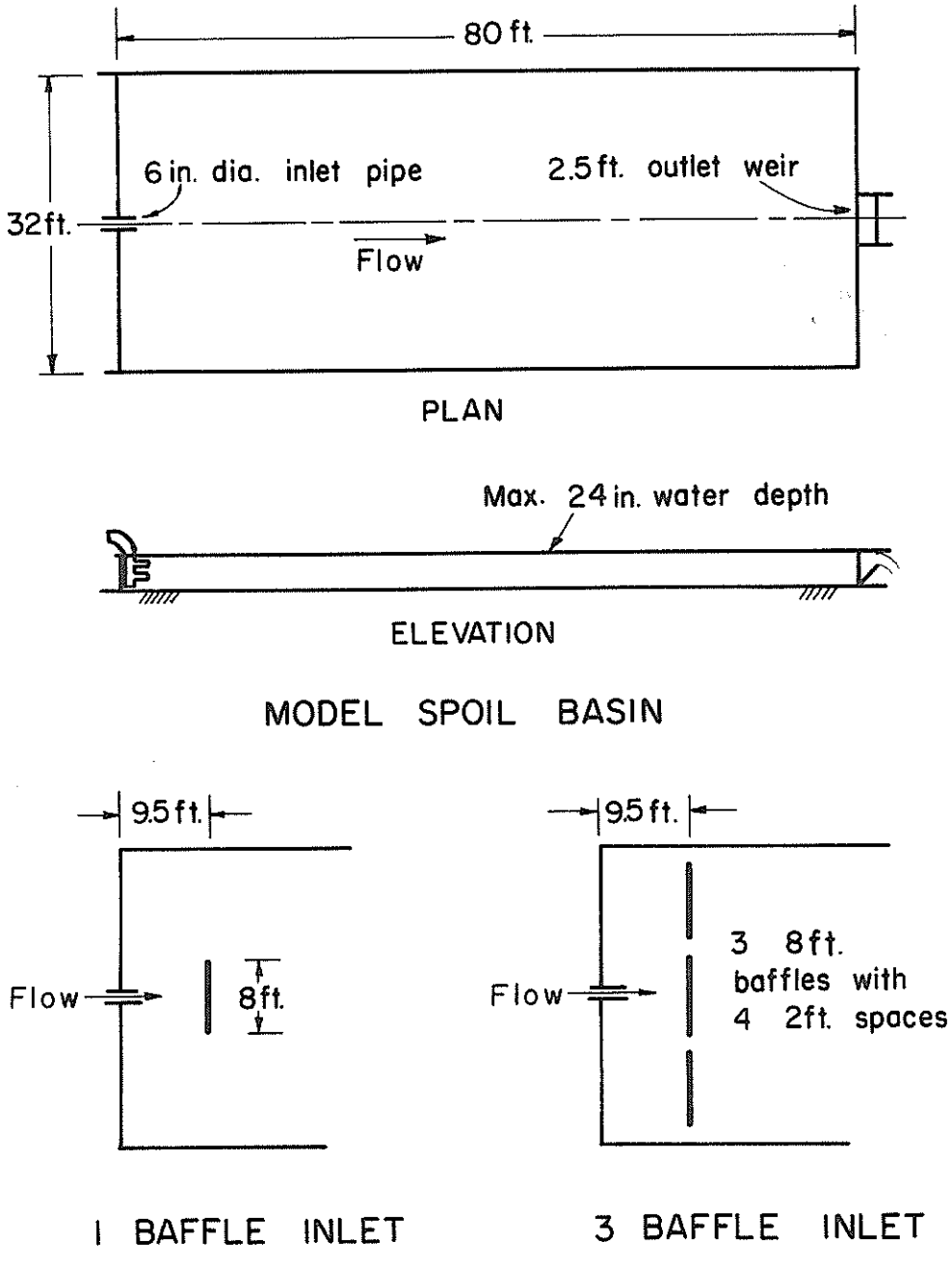

Figure 3(a)-Model Spoil Basin and Inlet Arrangements

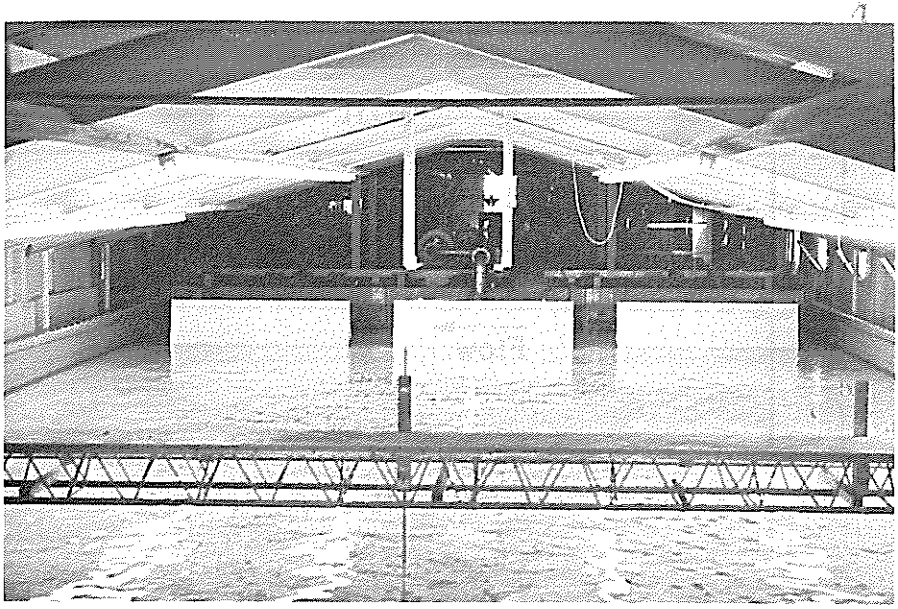

Three Baffle Inlet, 12-inch depth

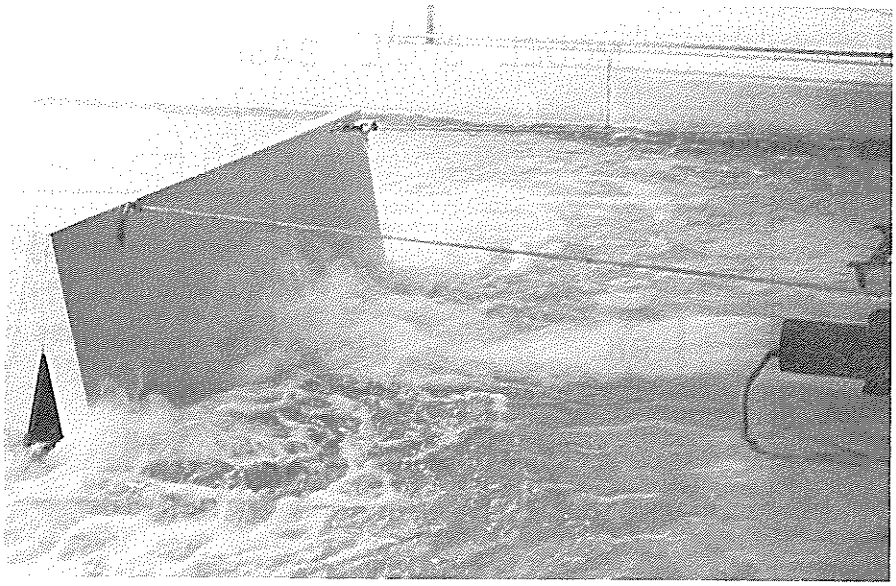

Single Baffle Inlet, 12-inch depth, 1200 gpm.

Figure 3 (b)-Model Spoil Basin and Inlet Arrangements

Model Details

The basic components of the model were the tank (located in the Hydrodynamics laboratory), the inlet and outlet, the inlet baffles, the dye injection and sampling devices, a fluorometer and a recorder, and the centrifugal pump and its sump on the floor below.

The tank is sufficiently described in Figure 3, except to note that the wall at the inlet end was, in fact, a wave paddle, immobilized and sealed at the edges.

Water Circuit

Water was circulated by a centrifugal pump, drawing from the laboratory sump, and pumping into the inlet of the tank. From this point the water flowed through the tank, over the weir and down a chute to the sump. The water was, therefore, being recirculated. When operating, the sump contained about the same volume of water as the tank but a large portion of the sump water resided in an uncirculated channel section. The circuit arrangement is shown in Figure 4.

A calibrated magnetic flowmeter was employed to continuously record the flow throughout the test.

The water level in the tank was controlled by the overflow weir shown in Figure 5. The weir was set at predetermined levels and adjusted to bring the water to the correct level.

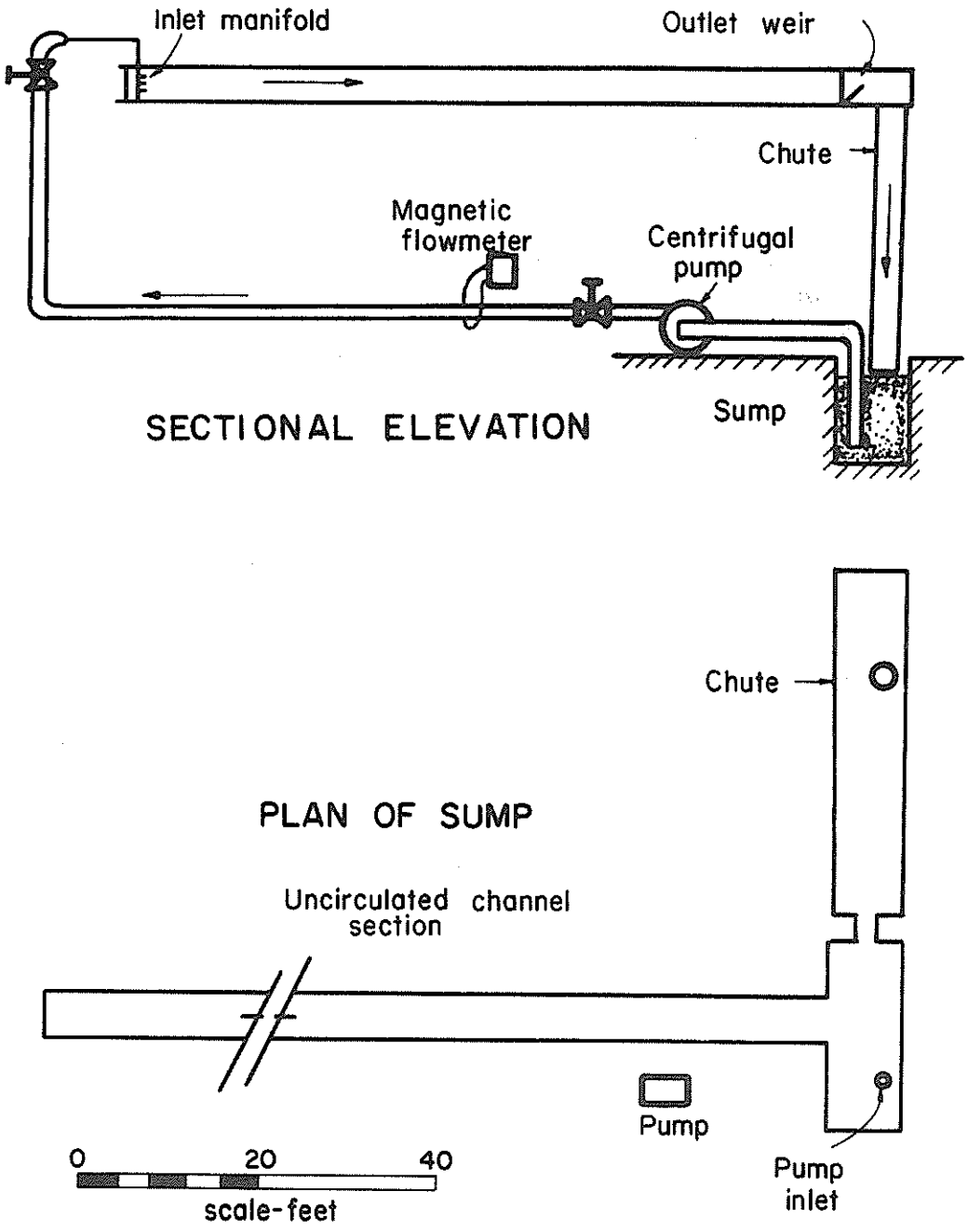

Figure 4-Water Circuit

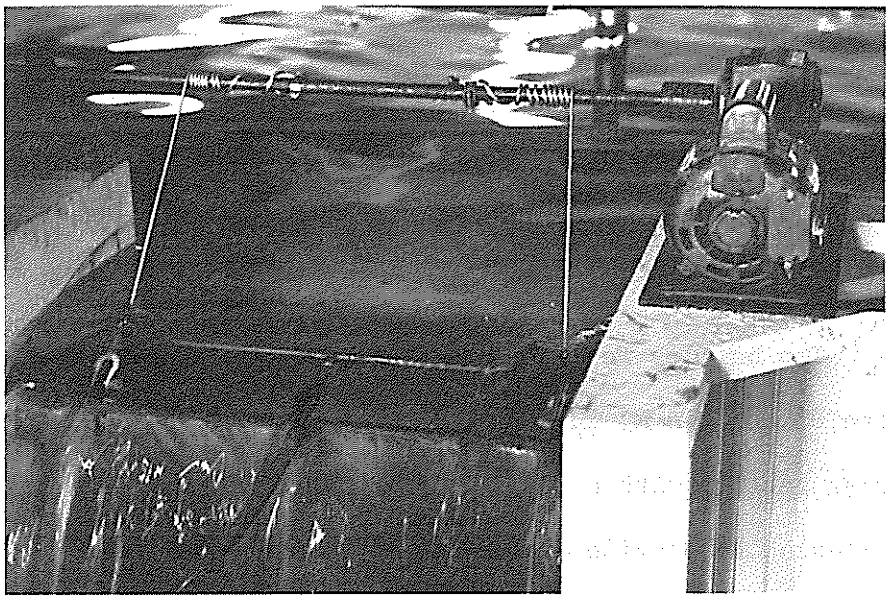

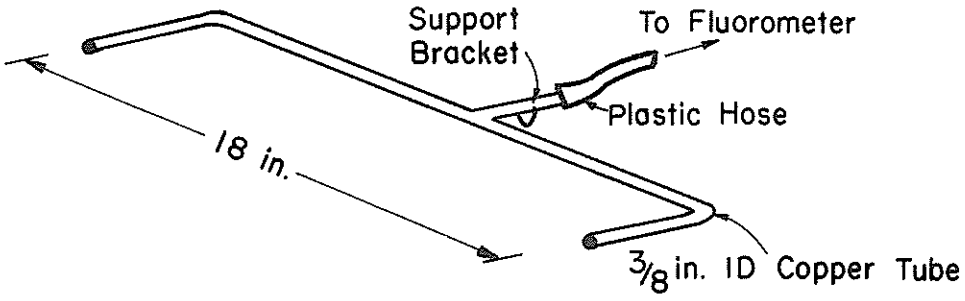

SAMPLER DETAILS

Figure 5-Outlet Weir and Sampler

Water entered the tank through an inlet manifold. This had three outlets as shown in Figure 6, although only two levels were used. The unused outlets were covered with blank flanges and the active outlet was fitted with a 6 in. (15 cm) nozzle including the dye injectors and a flow straightening section.

Inlet Baffles

The baffles were constructed from timber and plywood. They were 8 ft (2.44 m) long and 3 ft (.915 m) high of triangular cross section with a 1.5 ft (.456 m) base width. The baffles were ballasted to provide stability; the center one was additionally restrained with ropes to prevent movement. With this design the baffles could be rearranged at will and manhandled into position.

Dye Tracing Equipment

Dye was held in a pressure tank (Figure 7) from which it passed under pressure to the dye injectors on the inlet manifold (see Figures 6 and 7). A valve was used to control the dye, and a switch was available to start the recorder. A pressure of 75 psi (520 kN/m^2) was used to inject the dye solution. A 100 ml dose of 1 ppt dye was diluted to about 6000 ml and injected in 10 sec.

The inlet sampler was located in the flow straightener section of the 6 in. (15 cm) nozzle. The sampler diverted water through the fluorometer and back into the tank. A small pump was used to maintain an adequate flow through the sample tubing.

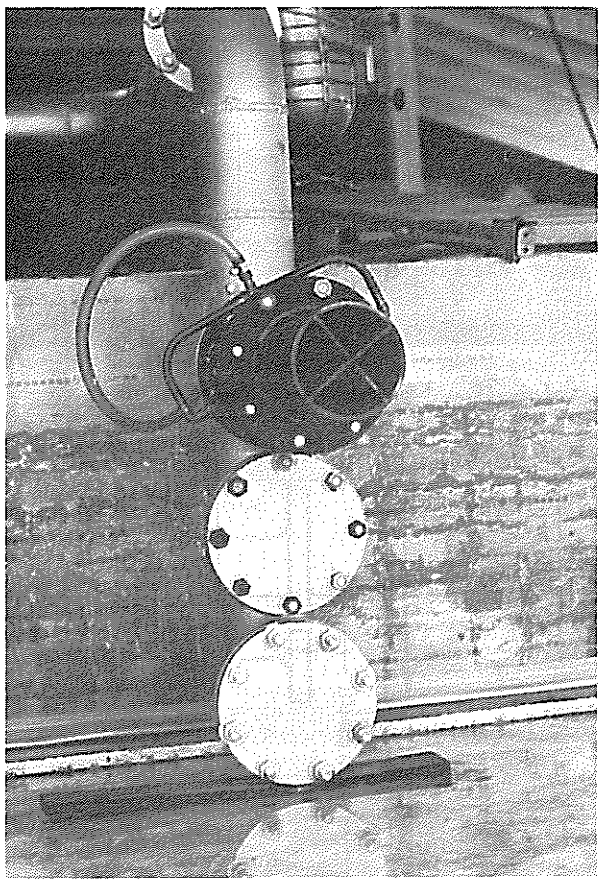

Figure 6-The Inlet Manifold

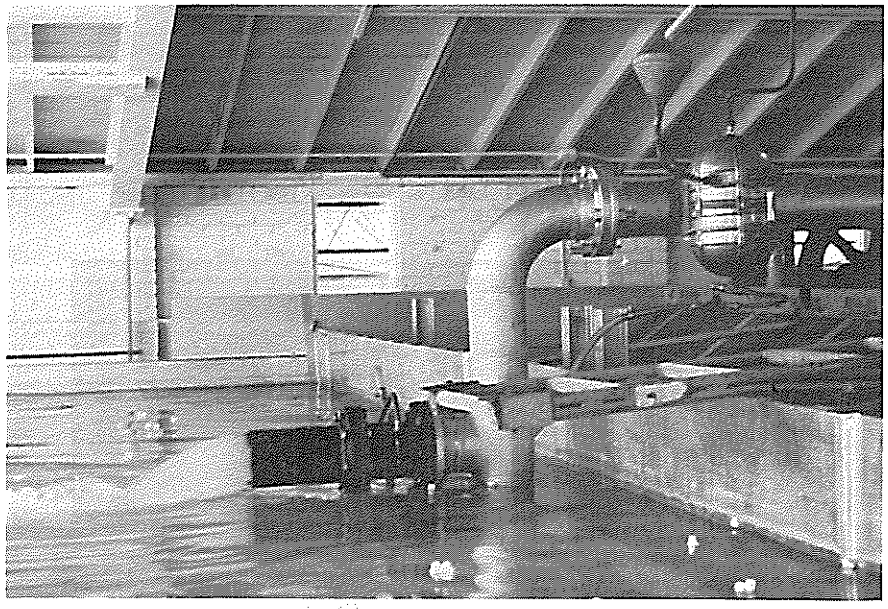

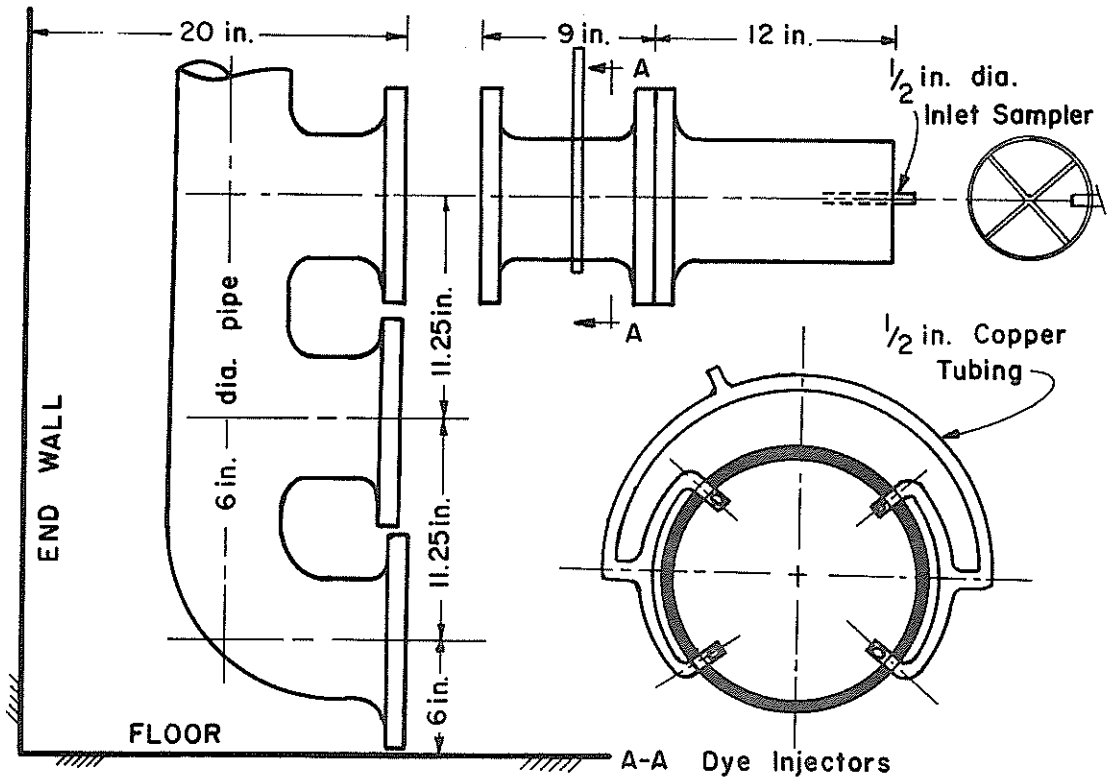

Figure 7-Inlet Manifold Details

The outlet sampler was positioned on the tail gate as shown in Figure 5 (p. 21). Tubing carried the sample to a fluorometer from which it passed into the chute. Advantage was taken of the fall down the chute by syphoning the sample at this end. It was much easier to clear bubbles from the syphoned sampler than from the pumped one; even though the fluorometer was on the suction side of the pump. Bubbles cause extraneous readings on the fluorometers.

Dye concentrations were measured continuously by a Turner Model 111 fluorometer, and recorded on an X-Y plotter. A special slow advance was fitted to the plotter so that the time scale was 500 sec/in. The fluorometer filters used were an I - 60 plus a 58 on the primary side and a 23A on the secondary side. No neutral density filters were used and the aperture was set at 10X. For further details on fluorometers see the references (5, 14) and also the manufacturer's publications.

IV. PROCEDURES AND TECHNIQUES

Test Procedures

Test Plan

The following test plan was followed, having been developed to fulfill the objectives of the study subject to the limitations noted in section III.

1. Test the unmodified tank with the plain inlet.
2. Test the tank with each of the four inlet modifications. as shown in Figure 3 (p. 17) and Figure 17 (p.58).
3. For each of these inlet configurations the tank was tested at all combinations of the discharge rates of 450, 600, 900 and 1200 gpm and the water depths 12 in. and 24 in.

Radical changes in performance were sought rather than the optimal positions for any one inlet arrangement. The results could also be analysed for the comparable effects of discharge rate and depth of water.

Test Method

Rhodamine WT dye was used since it has relatively low degradation and suffers only small losses by absorption. The water supply from which the sump was filled was chlorinated and therefore oxidized the dye. Chlorine was neutralized in the water by sodium

thiosulfate ($Na_2 S_2 O_3 \cdot 5 H_2O$) according to the reaction:

$$2 Na_2 S_2 O_3 \cdot 5 H_2O + Cl_2 \rightarrow Na_2 S_4 O_6 + 2Na Cl + 10 H_2O.$$

The relative weights are sodium thiosulfate, 496 and chlorine, 71. To neutralize an estimated chlorine content of 1.25 ppm, approximately 6 lbs (2.7 kg) of thiosulfate was added to 80,000 gallons (300 m^3) of water. A chlorine assay confirmed that all the chlorine was removed. Thiosulfate was used because it does not reduce the alkalinity as other processes do (1); a residual alkalinity is preferred with Rhodamine WT.

The tank was filled to level and the steady state flow conditions established over a 1 to 3 hour period. A fluorometer was used to monitor the residual fluorescence, the test was not started until this residual was constant.

The test was initiated by opening the dye valve and starting the recorder simultaneously. The instruments then recorded the dye concentrations continuously until the test was terminated 8 to 9 hours later.

Because only one set of instruments was available, each test had to be run twice to measure the concentrations at both the inlet and the outlet. Furthermore, if a doubtful curve was obtained the test was repeated.

The total volume of water in the system had to be adjusted to ensure repeatability of the inlet and outlet test conditions. Problems occurred when water was either added or drawn from the sump

during a test. If the priming valve on the pump was left open, chlorinated water was admitted and the test had to be repeated.

Interpretation of Dispersion Curves

The tracer technique to develop dispersion curves for the flow through a basin is well tried. With modern equipment and suitable tracers the procedure has been automated so that the raw data from the experiment is a plotted curve of concentration against time.

Despite the progress in the experimental technique, the physical interpretation of the curve is still qualitative and in many cases based on intuitive concepts. Difficulties arise around terms such as hydraulic efficiency because they have not been defined and cannot be quantified. Generally the object is to compare the resultant curve with other curves in an attempt to infer the degrees of short circuiting, large scale circulation and so on, being characteristics of the hydraulic flow conditions in the tank.

Time Ratios Method

Basco (2) and Villemonte et al. (19) provided a description of one major category of interpretation. The dispersion curve was viewed as a function of the velocity field in the tank. Several ideal flow dispersion curves were developed for comparison (see Figure 8). A normalized dispersion curve was then used, and characteristic time parameters were calculated or read from it. Several variations have been developed over the years; Basco (2)

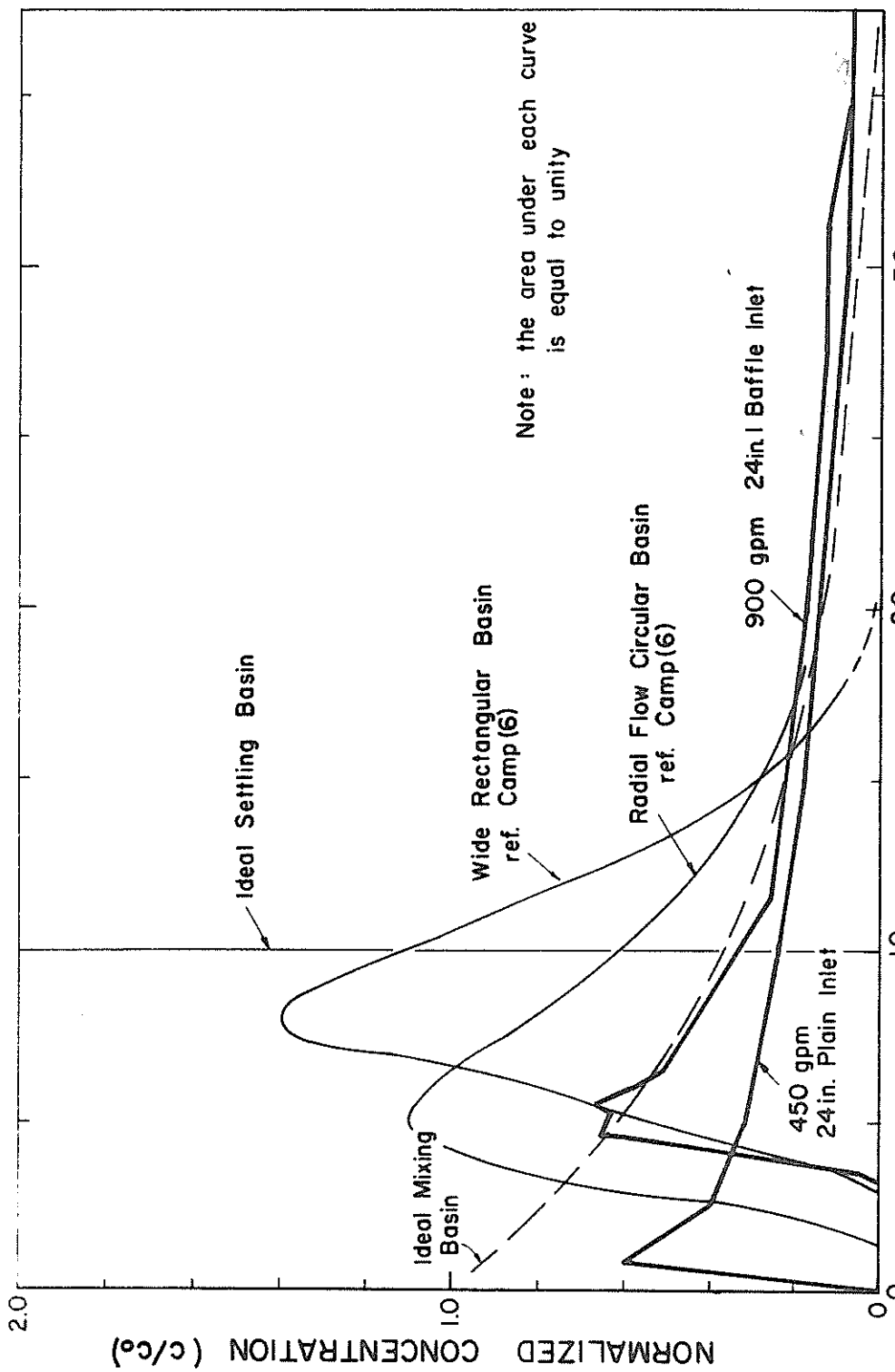

Figure 8-Comparison of Dispersion Curves with Typical and Ideal Curves

discussed many of them. The following extract from Villemonte et al. (19) is an illustration of the developed parameters. (See Appendix I for definitions of t_c, etc.)

$T_i = t_i/T$-Measures severe short circuiting. Equals 1.0 for ideal settling and zero for ideal mixing.

$T_p = t_p/T$-Measures dead or stagnant regions. Equals 1.0 for ideal settling and zero for ideal mixing.

$T_c = t_c/T$-Related mostly to eddy diffusion caused by turbulence. Equals injection time ratio for ideal settling and about 0.7 for ideal mixing.

$T_b = t_b/T$-Related to turbulence and large recirculation eddies. Equals injection time ratio for ideal settling and about 2.3 for ideal mixing.

$T_e = \frac{(t_t - t_p) - (t_p - t_i)}{T}$ -Measures the eccentricity of the curve and thus in a function of the recirculation. Equals zero for ideal settling and 2.3 for ideal mixing.

It is presumed that the closer these criteria approach their ideal values, the better will be the flow net for optimum settling conditions.

Villemonte et al. also developed a method to relate the dispersion curve to removal efficiency, and a correlation is indicated between good removal efficiency and the approach of the parameters to ideal values.

Other investigators used variations of the parameter techniques. The AWWA handbook (1) described a factor n used in a removal ratio formula based on the sequential basins concept,

$$\frac{y}{Y_o} = 1 - \left[1 + \frac{V_o}{n(Q/A)}\right]$$

where n - number of hypothetical basins,
set = $t_{mean}/(t_{mean} - t_{mode})$,

Yo - initial concentration of settling particles with settling velocity Vo,

y - removed concentration

and t_{mean} was noted to be approximately equal to the theoretical detention time.

Camp (6) mentioned some of the earlier parameters with their associated assumed governing factors. More importantly, in the discussion of Camp's paper, Eliassen made a very valid point. Short circuiting as such does not necessarily indicate poor settling conditions. Vertical velocity profiles like Figure 9 (a) in fact are mentioned by Camp to be advantageous. It should be noted that this velocity profile will produce short circuiting due to the dead regions. Figure 9 (b) however, has a detrimental velocity profile since scour will be aggravated. The usual concept of short circuiting and/or dead regions is shown 9 (c). Having recorded only a dispersion curve, there is no way of knowing to what degree the component velocity distributions contributed to the apparent short circuiting. Consequently, the method combining the dispersion curve with a cumulative settling curve (9) cannot be a consistent indicator of removal efficiency, although it will always be conservative.

For mere comparison of one dispersion curve with another, the parameters described above are intuitively useful. Many investigators have reported their results in terms of the time ratios, so it is still valuable to calculate the ratios for comparative purposes.

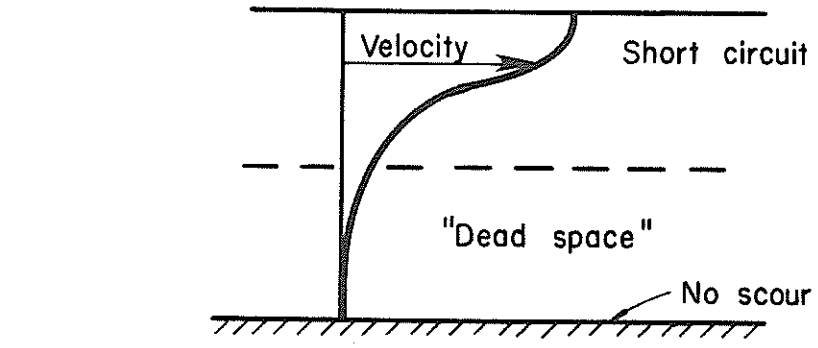

(a) A VELOCITY PROFILE

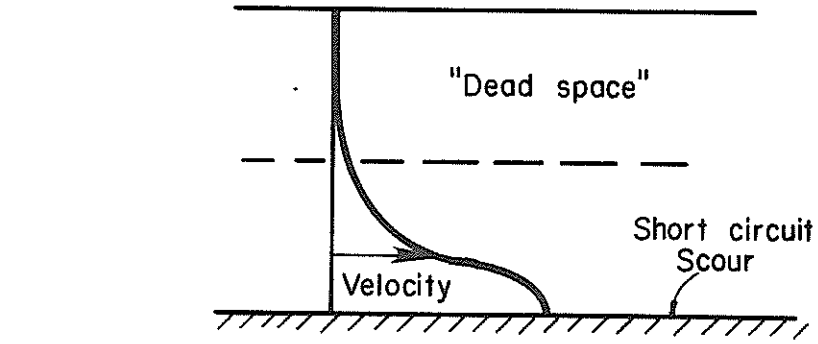

(b) A VELOCITY PROFILE

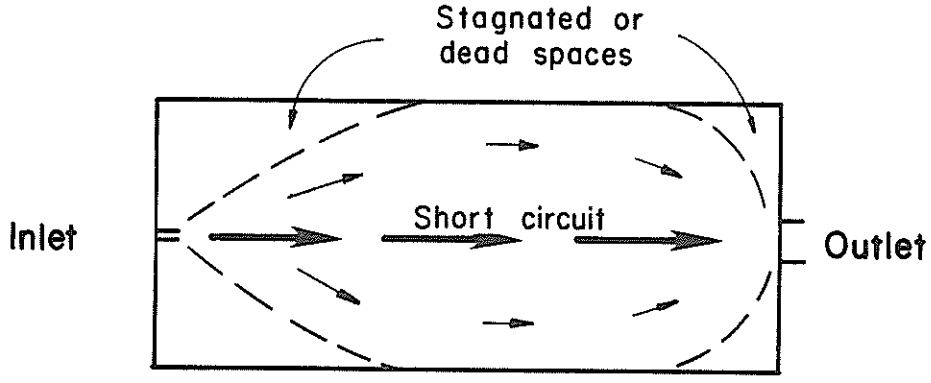

(c) PLAN OF A FLOW FIELD

Figure 9-Short Circuits and Dead Spaces

Cumulative Flow Curve

Various reporters (2, 15) and Hall in a discussion of Camp (6) mention statistical methods. Sayre (15) used the method of moments to fit a Pearson Type III distribution to his dispersion curves. Basco (2) and Hall both referred to the fitting of log normal distributions. A quoted reason to use this method is to cope with scattered results, but this is only one reason, as even a stable, reproducible flow curve when represented in the cumulative distribution form is more easily fitted with a standard curve.

The cumulative plot provides a method with advantages over the time ratio methods. Once a close fitting function has been determined, this function yields a complete description of the flow curve. For comparison of one curve with another the cumulative plot, with the scale adjusted to produce a straight line plot (probability paper), provides an easy way to appraise the differences. With the appropriate function paper, curves satisfying that function, plot as straight lines. The plotted data appear as points on or near the continuous cumulative model, as shown in Figure 10.

Since the dispersion curves are generally skewed, a skewed model is required. Due to their mathematical tractability and their availability in both tabular and probability paper form the variable skew functions of the log normal and gamma distributions are good prospects. These functions are used in statistics for the same reasons, plus the academic justification that the gamma

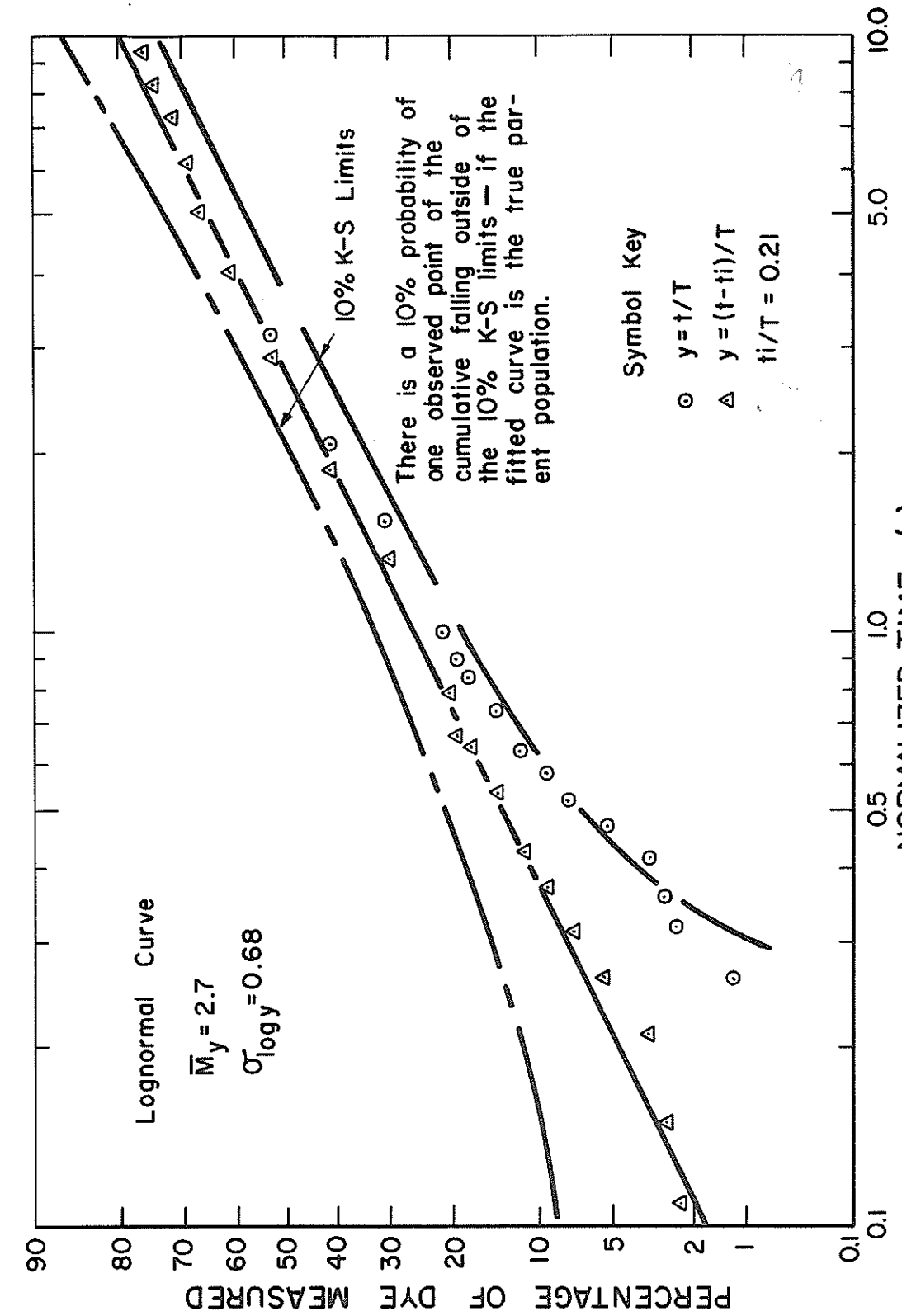

Figure 10-Typical Cumulative Plot of a Dispersion Curve

distribution can be developed from consideration of the distribution of time to the kth arrival in a Poisson process. The dispersion curve can be viewed with this attitude; that is a detention time distribution or the distribution of flow through times for elements of water entering the system. Each dispersion curve is a sample from the parent population.

It should be noted that the gamma distribution is also called Pearson Type III and one particular case is called the Erland distribution (3). A common application is in queueing theory for the distribution of waiting times between arrivals.

Once the cumulative models have been fitted it is not a great step to quantify the comparison of two flow curves by calculating the probability that they both came from the same population or are alternatively significantly different. Several tests of this nature are available (3). The cumulative model also enables the distribution parameters to be determined so that the curve can be fully defined, for example, as log normal with a given mean and standard deviation. Additionally, these parameters are estimated on the portion of the curve recorded but extrapolated according to the best fit model. This extrapolation is not possible when calculating standard deviation or the mean with the normal methods directly using a dispersion curve. The lack of consideration for detention times longer than the testing time is not important with near ideal behavior, but with particular long-tailed curves, the truncation error is considerable.

Comparison with Computed Curves

The time ratios comparison approach has been developed by methods which yield more basic results. Instead of resorting to ideal extreme cases such as pure plug flow, the experimental curve is compared against a closely fitting computed curve for which the input characteristics are known. By inference, the experimental curve is due to these same characteristics. The result is that, corresponding to an experimental curve, specific quantitative statements can be made of the system in which it occurred.

Sayre (15), El Baroudi (8, 9) and Rebhun and Argaman (13) developed mathematical models for the dispersion curve. In one case (13) the model was a poor one with the peak concentration at time t = o which is directly incompatible with the experimental model. However, the model was attractively simple with the results expressed in a desirable form of plug flow mixing and dead space fractions.

By making judicious assumptions El Baroudi (8) was able to approximate the dominant characteristics of each zone in a high rate settling tank. These characteristics were described mathematically and combined sequentially to develop a general equation for the dispersion curve in terms of the relative proportions of each zone to the total volume.

Sayre (15) investigated the dispersion of silt as it was transported in an open channel. His theoretical model predicted

the mean position, the variance and skewness coefficient of the distribution of the dispersant. Using these first, second and third moments he selected a gamma distribution. This distribution was in space at a particular time. His experimental results were a distribution of concentration in time, measured at one point, also expressed as a gamma distribution. The two distributions were compared to confirm the validity of the model.

In the above examples, the system under investigation in each case was relatively simple compared with the spoil basin model. The single high velocity entrance to the model developed a very complex and unstable flow pattern. This complexity and particularly the instability render the calculation of the flow curve a difficult problem. However, the simple Rebhun and Argaman method could be applied because it simply does not consider the unstable jet induced flow.

Data Analysis

Determination of the Dispersion Curve

The raw test records were the time histories of dye concentrations measured at the inlet and the outlet. A dispersion curve can be considered as a unit impulse response, or the time domain system characteristic. The input, output and system characteristic are related by convolution:

$$y(t) = \int_{-\infty}^{\infty} x(\tau)\, h(t - \tau)\, d\tau$$

where

$y(t)$ = response (output

$x(t)$ = input

$h(t)$ = unit impulse response (characteristic)

if $y(t) = 0$ and $h(t) = 0$ for $t < 0$

$$y(t) = \int_{0}^{t} x(\tau)\, h(t - \tau)\, d\tau$$

or in discrete terms, sampled at intervals of Δt

$$Y_i = \sum_{j=1}^{i} X_j\, H_{i-j+1} \qquad i = 1,m.$$

(This is descriptive of the test conditions since $y(t) = 0$ before the dye slug is injected at $t = 0$.) The last expression can be set up in matrix form

$$\begin{bmatrix} H_1 & o & \cdots & o \\ \vdots & & & \vdots \\ H_m & \cdots & \cdots & H_1 \end{bmatrix} \begin{bmatrix} X_1 \\ \vdots \\ X_m \end{bmatrix} = \begin{bmatrix} Y_1 \\ \vdots \\ Y_m \end{bmatrix}$$

or

$$\begin{bmatrix} H_1 & \cdots & H_m \\ o & & \vdots \\ \vdots & & \vdots \\ o & \cdots & H_1 \end{bmatrix} \begin{bmatrix} X_1 \\ \vdots \\ X_1 \end{bmatrix} = \begin{bmatrix} Y_m \\ \vdots \\ Y_1 \end{bmatrix}$$

then by back substitution

$$H_i = \frac{1}{X_1} \left(Y_j - \sum_{j=2}^{i} X_j \, H_{i-j+1}\right.$$

This algorithm formed the basis of the deconvolution computer program in Appendix 2. The program corrected the data for temperature (5, 14) and calibration, executed the above calculations and printed a normalized series of values for H_i and the cumulative area under the H_i curve (the dye recovery to any time). Time was normalized as t/T where T is the theoretical detention period. The response was normalized so that the area under the curve to any point was equal to the recovery at that time. This normalization produced curves identical with the t/T and c/c_o normalizations used by others (2, 6, 8, 9, 13, 19) and is similar to Sayre's (15) method.

For the analyses run during this project the sampling interval Δt was set at 100 sec. The value X_1 was the dye slug impulse while the rest of the X_i record was due to feedback. X_1 was calculated as follows because it could not be measured. The impulse was assumed triangular over one time interval Δt. The calibration

factor α and the temperature correction factor β are defined:

$$\alpha \, X_{25°c} = \text{concentration (c)}$$

$$\beta \, X_{temp} = X_{25°c}$$

where $X_{25°c}$ = fluorometer dial response at 25°c for concentration c.

the dye passed in any time Δt is S

$$S = Q \int_{t}^{t+\Delta t} c \, dt$$

where Q = discharge rate.

Then for the assumed triangular impulse over 100 sec.

$$S = Q \, \alpha \, \beta \, 50 \, X_1$$

Since S is known (100 ml of 1 ppt solution has 0.1 gm of dye) X_1 can be calculated. The value of X_1 is the only program input which carries the fluorometer calibration information.

Comparison of the Dispersion Curves

The calculated dispersion curves were plotted as shown in Figure 8 (p. 29) for some typical examples. The calculated points on the cumulative curve were plotted on log normal probability paper both directly and with the origin shifted by t_i/T as shown in Figure 10 (p. 34). The graphical form of the Kolmogorov-Smirnov test (3) was used to select the best fitting log normal model for the shifted curve. The K - S function is the distribution

of the maximum absolute difference between observed cumulative distributions and the population distribution. The curves plotted on the graph are positioned so that there is a 10% chance of one observation falling outside the included region. For the selected model the values of the median ($t_{\bar{m}}/T$), mean (t_m/T), standard deviation (t_σ/T), and skewness coefficient (t_γ/T) were calculated.

A second form of K - S test was used to test the significant level of the difference between two observed cumulatives.

Six curve parameters, t_i/T, t_p/T, $t_{\bar{m}}/T$, t_m/T, t_σ/T and t_γ/T were tabulated according to depth, flow and inlet configuration. An analysis of variance was run on each parameter to estimate the relative significance of each variable (depth, flow and inlet). The six parameters were also plotted on the Reynolds number-Froude number region shown in Figure 2 (p. 16) to check for a correlation with either of these numbers.

The gamma distribution was not employed as a dispersion curve model because graphical methods with probability paper suited the procedures, and gamma paper was not available for the extremely skewed distributions encountered in this study. Additionally, the gamma paper is prepared only for discrete values of the shape parameter and, hence, skewness. For these reasons, the log normal curve was used.

V. EXPERIMENTAL RESULTS

General Discussion

Initially, 11 tests were conducted to determine practical dye dosages and fluorometer setting. These tests also served to confirm the practicality of the testing program flow rates and to prove the model equipment. At the completion of testing with the fourth inlet arrangement, 93 tests had been run with an average pumping time of about 10 hours per test. Testing time was, therefore, in the order of 900 hours.

The records taken of the tests were the dye concentration histories measured at the inlet and the outlet. Examples of these raw records are shown in Figures 11 and 12. These recordings were made at a horizontal advance of 500 sec/in. (197 sec/cm) and they are reduced from an original size of 15 in. (38 cm) long by 10 in. (25.4 cm) wide.

In Figure 11, a small peak can be seen where the dye slug was injected. This is severely attenuated for two reasons. The fluorometer had a reasonably slow response, especially at the low end of the scale, so that the jet of dye could pass before the instrument responded. Secondly, the dye slug was concentrated to such an extent that the color density absorbed light and so reduced the fluorescence response.

Following the dye injection the concentration returned to zero until the recirculated water began to reintroduce dye into the tank. The feedback concentration fluctuated for a few hours and eventually

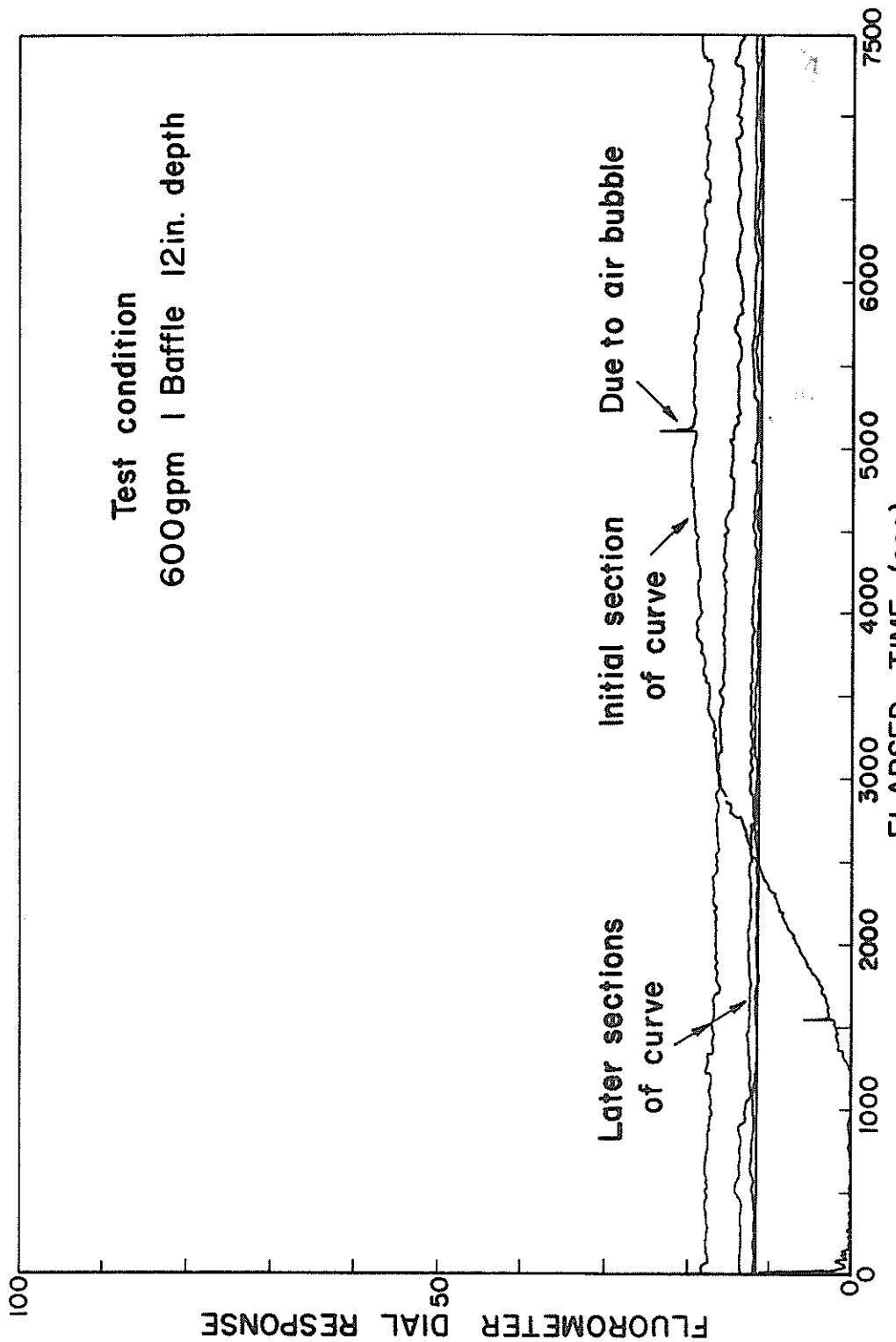

Figure 11-Typical Test Record - Inlet

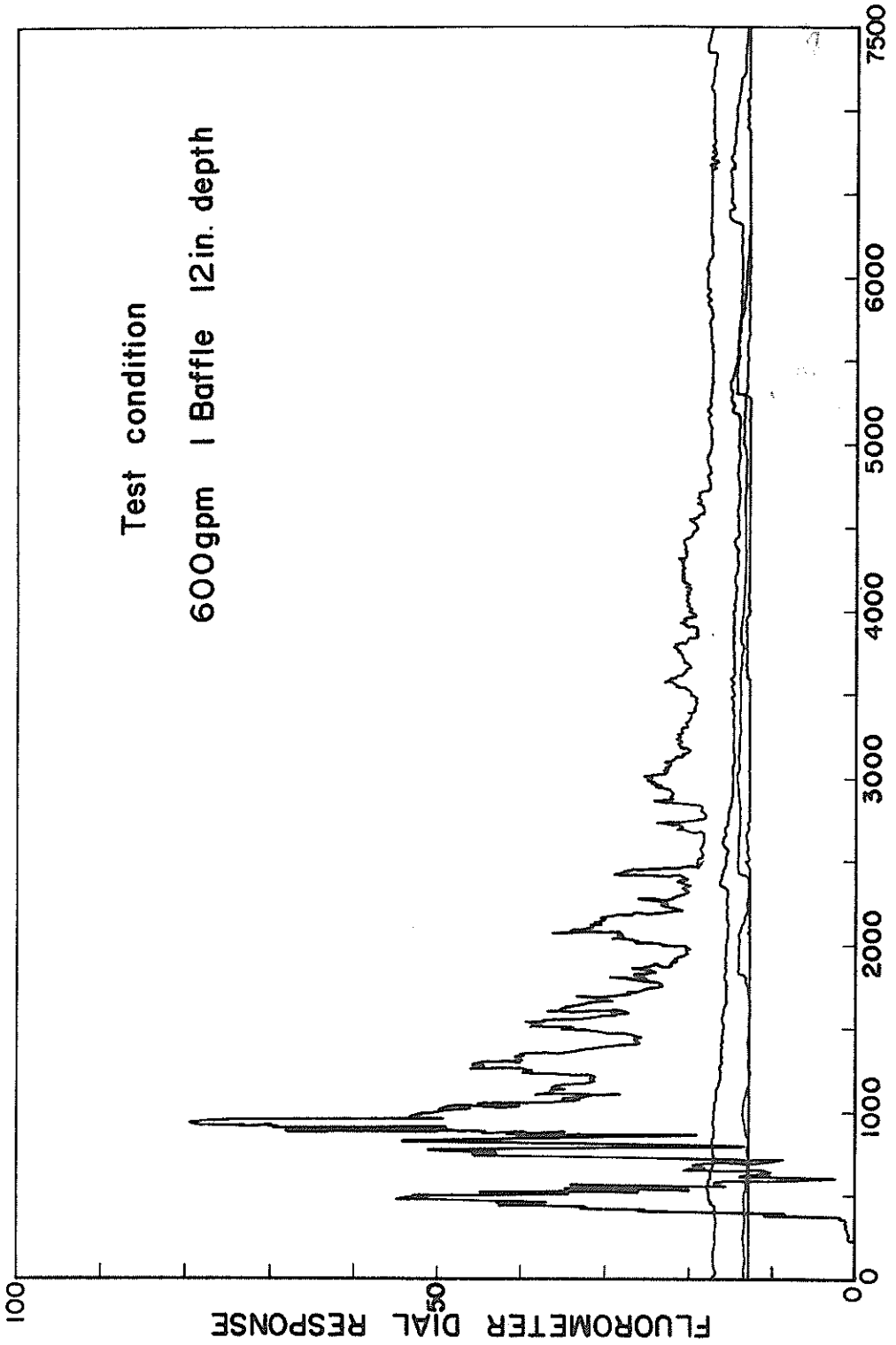

Figure 12-Typical Test Record - Outlet

settled down to an equilibrium concentration. After several tests the residual dye concentration in the system became high enough that proportionately small fluctuations rendered quite significant bumps on the recorded curves. At that stage the dye concentration was reduced, usually by the addition of freshly chlorinated water.

The outlet end concentrations were notably different as shown in Figure 12. The interval of time before the first dye arrived at the weir can be easily seen. In the period following the first arrival, the concentrations fluctuated greatly as eddies swept into the outlet. Two larger scale peaks can be seen, above the eddies, with an interval of about 400 sec between them; these were most likely caused by a circulation current in the tank.

These raw data records were reduced to the normal dispersion curve form by extracting dial response values every 100 sec and processing this information with the deconvolution computer program. The normalized response curve calculated from the data in Figures 11 and 12, is shown in Figure 13. The same peaks as those on Figure 12 can be recognized.

Because the plotting was not so detailed after one detention period, further peaks are not evident, they were however calculated and accounted for in the cumulative curve.

Dye recovery values are an indication of experimental accuracy. The recovery values calculated for Figure 13 were: 60% after 4 detention periods; 70% after 7 detention periods; and 87% after 15 detention periods. Other test recovery values ranged from a

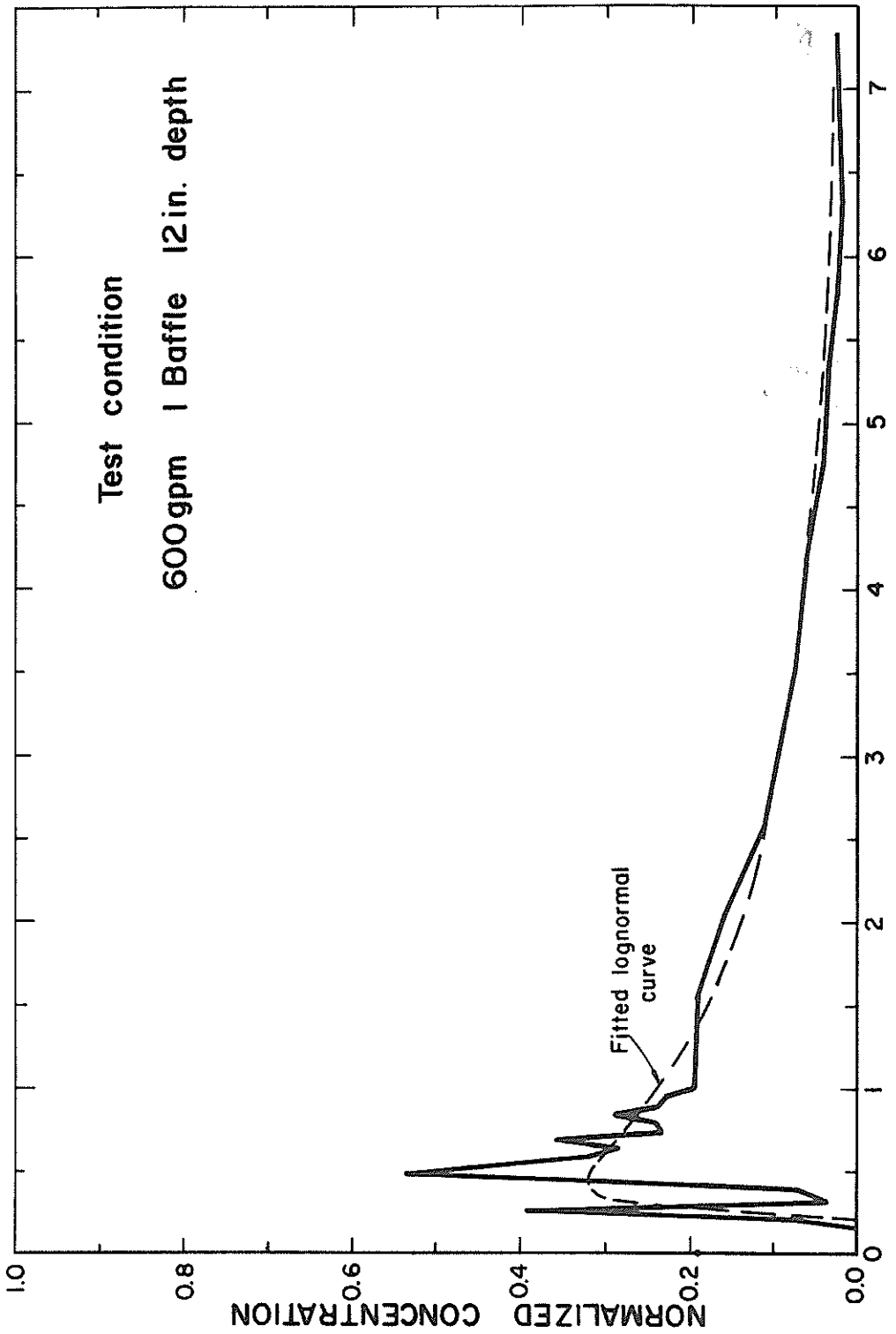

Figure 13-A Dispersion Curve Calculated from Test Records

low of 61% for a test terminated at 11 T to a high of 129% for a test terminated at 30 T, however, most values at test completion fell between 80% and 100%. The recovery figures for the long-tailed curves occurring in this study are much more sensitive to small errors because of the long duration of the test. Additionally, many of the curves do not have a definite end point at which to check the recovery.

Errors can be attributed to three major sources (3).

1. The natural or fundamental probabilistic behavior of the flow field which has been repeated with some variation, but the fine structure is completely random.
2. The statistical or sampling errors.
3. The method or procedural errors, due to incorrect assumptions and perhaps too coarse a time interval in the data reduction.

The errors due to 2. and 3. can be reduced by human effort with more samples and greater refinement of methods. The first source is, however, inherent in the behavior and cannot be reduced. Since reasonably large variations in settling tank performance were being sought in this study, it was considered that the procedures adopted produced a tolerable accuracy above which the behavior variations could be detected.

A complete set of the plotted response curves for all tests is presented in Appen. V. This was considered as the most usable form of the complete test results. A "best" and a "worst" curve were plotted

with other comparable curves in Figure 8 (p. 29). It can be seen that the curves from this study have low peaks and very long tails. This is to be expected since a high velocity point source was used in the model, whereas most settling tanks have baffled overflow or submerged weirs. Hamlin in discussion of Villemonte et al. (19) depicts similar low long-tailed curves for a "high-speed" inlet, even though it was in fact a full tank width weir.

Cumulative curves were plotted on log normal probability paper, and a log normal "model" fitted as shown in Figure 10 (p. 34). Not all the curves could be fitted quite that well; some exhibited a definite concave curving, suggesting that the gamma distribution would be a better fit. No particular group of curves fell clear of all the others in the cumulative form. Procedures for comparing cumulative density functions were employed, but these methods could only compare two curves at a time, and the general variability could not be considered. The cumulatives were therefore used as a method to estimate the mean, the standard deviation and the skewness coefficient. (The relationships on which these estimates were based are included in Appen. III.)

Comparison of Plain, One Baffle, and Three Baffle Inlets

The plain inlet will be compared separately with two other inlet types in order to avoid confusion regarding the results. Initially the one and three baffle results will be discussed.

Values of t_i/T and t_p/T were taken directly from the raw outlet curves, and t_m/T was taken from the cumulative curve. These values with t_m/T, t_σ/T and t_γ/T are presented in Table 1. The ideal values of the first four parameters are all 1.0, while the last two are zero for a

Table 1-Experimental Values of Dispersion Curve Parameters for Plain, One Baffle and 3 Baffle Inlets

	t_i/T	t_p/T	$t_{\bar{m}}/T$	t_m/T	t_σ/T	t_γ/T
Plain 24"	(.062)	(.116)	(2.01)	(6.26)	(22)	(52)
450	.054	.099	2.06	6.58	22	45
600	.062	.079	1.70	5.21	16	38
900	.060	.115	2.20	4.71	14	33
1200	.074	.171	2.07	8.53	36	94
Plain 12"	(.064)	(.095)	(2.41)	(9.39)	(40)	(88)
450	.079	.118	2.78	7.95	23	34
600	.047	.071	2.04	7.56	29	65
900	.063	.102	2.56	14.3	81	200
1200	.060	.090	2.27	7.76	28	55
1 Baffle 24"	(.245)	(.455)	(1.55)	(3.57)	(8.02)	(22.7)
450	.29	.413	1.53	3.02	7.4	22
600	.15	.290	1.35	3.94	13	45
900	.32	.591	1.72	3.78	7	12
1200	.22	.527	1.60	3.54	4.7	12
1 Baffle 12"	(.16)	(.31)	(2.34)	(8.22)	(31)	(65)
450	.16	.320	2.56	11.30	53	118
600	.21	.490	2.91	9.15	31	49
900	.11	.157	1.91	6.45	22	49
1200	.17	.263	2.00	5.98	20	45
3 Baffles 24"	(.173)	(.292)	(1.51)	(4.91)	(16.5)	(44.4)
450	.142	.40	1.70	7.86	35	105
600	.157	.244	1.82	5.2	14	27
900	.236	.315	1.02	1.72	2.34	6.7
1200	.158	.211	1.50	4.87	14.6	39
3 Baffles 12"	(.138)	(.22)	(2.5)	(10)	(46)	(91)
450	.177	.295	2.70	16	94	220
600	.131	.22	2.60	9.55	34	55
900	.138	.158	2.20	8.5	40	63
1200	.137		2.50	6.9	17.4	25

NB: bracketed figures are group averages

perfect settling tank. It is, therefore, clear that the one baffle inlet at 24 in. depth yields the best dispersion curves. The plain inlet at 12 in. depth has the worst results.

An analysis of variance was run for each time ratio. The full tables are included in Appendix IV and a summary of the significance testing is presented in Table 2. Here it can be seen that flow was not a significant factor, at least in view of the error variance, for any time ratio. The water depth and the inlet were very significant. The inlets affected mainly the t_i/T and t_p/T ratios while depth affected the shape of the curve, that is the t_m/T, t /T and t /T values. A probable explanation is that the inlets prevented gross short circuiting by the inlet jet whereas a greater depth tended to absorb and dissipate the inlet energy and partially arrest the circulation. Circulation is almost certainly the cause of the long tails on the curves.

A second series of analyses of variance testing was run to compare only the two types of baffled inlets herein discussed. The significance tests summary is given in Table 3. In this analysis the great difference between the plain and baffled inlets has been avoided. The significance of variations in the time ratios due to the inlet factor reflect only the change from one baffle to three. It can, therefore, be concluded that the single baffle inlet was significantly better than the 3 baffle inlet. The reader should refer to the bracketed averages in Table 1 and the significance of differences between these averages, given in Table 3. For example t_p/T shows an average of (0.455 + 0.31)/2 for the 1 baffle inlet and (0.292 + 0.22)/ for a 3 baffle inlet, and the

Table 2-Analysis of Variance Summary for All Three Inlet Arrangements

	Depth		Inlet		Flow
t_i/T	*	(*)	**	(***)	
t_p/T	*	(*)	**	(***)	
$t_{\bar{m}}/T$	***	(***)			
t_m/T	**	(***)			
t_σ/T	***	(**)			
t_γ/T	*	(*)			

Variance ratio F test: Significance Levels

*	10%	Significant
**	1%	Very significant
***	.1%	Extremely significant

(Bracketed tests refer to tests where all non significant effects have been pooled as error)

Notable Correlations:

median/mean	0.78-correlation coeff.
initial/peak	0.895
mean/standard dev.	0.968
mean/skewness	0.90
standard dev./skewness	0.972

Table 3-Analysis of Variance Summary for the Two Baffled Inlets

	Depth		Inlet		Flow	
t_i/T		(*)				
t_p/T				(*)		
$t_{\bar{m}}/T$	*	(***)				
t_m/T	**	(***)	*	(*)		(*)
t_σ/T	**	(**)	*	(*)	*	(*)
t_γ/T	*	(**)	*	(*)		(**)

Variance ratio F test: Significance Levels

*	10%	Significant
**	1%	Very significant
***	.1%	Extremely significant

(Bracketed tests for pooled error)

Notable Correlations:

initial/peak	0.83-correlation coeff.
median/ mean	0.79
mean/standard dev.	0.967
mean/skewness	0.89
standard dev./skewness	0.96

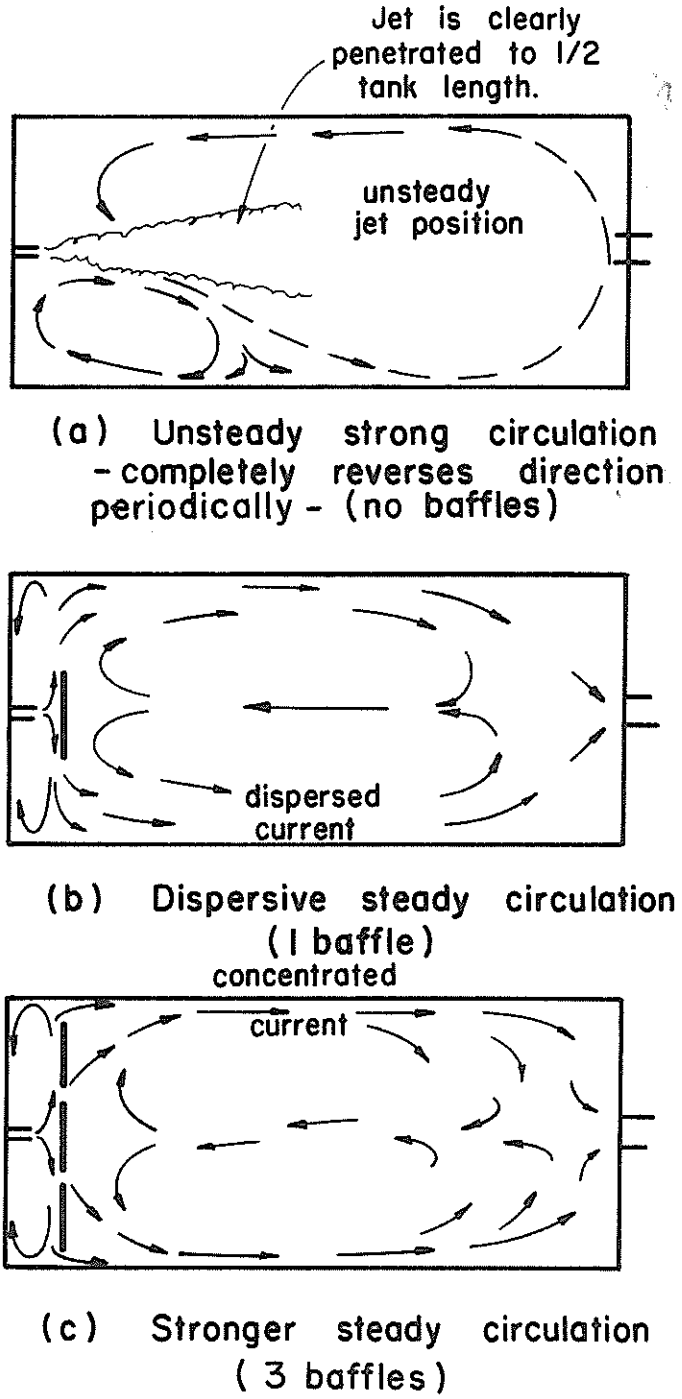

Figure 14-Observed Flow Patterns

difference is noted as significant.

The comparison of these inlets alone reduced the importance of depth and the formerly insignificant variations due to flow could now be resolved. The plain inlet tank was more sensitive to depth than the baffled entrances, and the general behaviour was more erratic. Visual observations support this finding; Figure 14 shows the general current patterns observed during testing. With the plain entrance the inlet jet was coherent to at least the half length of the tank and wandered from one side to the other periodically. The direction of circulation reversed as the jet changed sides. Baffling the inlet arrested the jet and confined the gross turbulence to a well-defined region behind the baffle. A lateral current, however, developed and split at the wall forming a double recirculation behind the baffling and a wall current with double recirculation in the main rank region. Water escaping through the two interior gaps of the 3 baffle inlet still had lateral momentum and so continued to move laterally as shown and join the wall current. Figure 15 (a) shows the 1 baffle inlet with a strong lateral current. Sediment can be seen on the tank floor, having settled in the slower current regions. Figure 15 (b) shows the sediment more clearly after the test was terminated. The divergent streamlines of the return current near the baffle are clearly evident. The reader should refer to Figure 3 (b) (p. 17), top for a view of the other side of the baffle, operating during the same test. The baffle clearly confines the turbulent area.

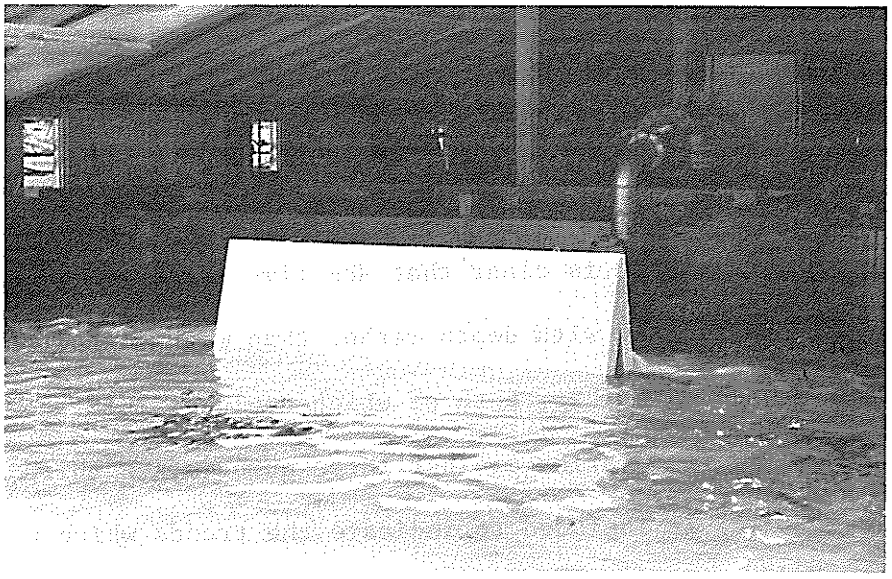

(a) 12-inch depth, 1200 gpm.

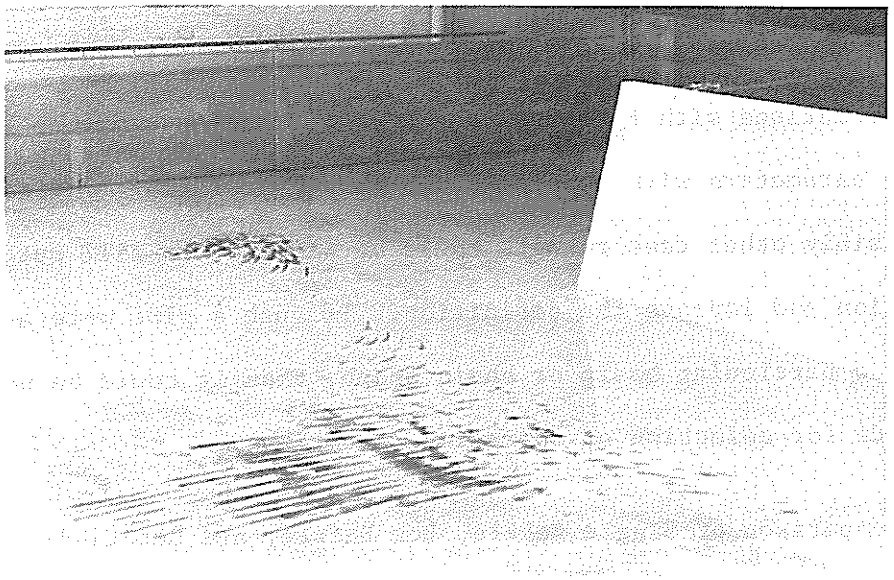

(b) Residual Sediment Patterns

Figure 15-Tank Circulation - Sediment Patterns

An attempt, lacking in success, was made to extend the data by plotting it on the Reynolds and Froude number domain previously shown in Figure 2 (p. 16). Due to the scatter in the data, and that only eight points were determined on each plot, meaningful contour diagrams could not be made. The two most definitive plots are shown in Figure 16 (a) & (b) to illustrate the possible results. From these plots it is clear that the time ratios shown were strongly correlated with depth rather than with either Reynolds number or Froude number, both of which could be inferred by graphing the time ratios against these numbers. A third example Figure 16 (c) is included to indicate the trends which would become evident on this type of plot, if sufficient confidence could be put on the individual values plotted or if a greater number of points were determined.

The purpose of these plots was to graphically investigate the correlations with F_N and R_N and also to develop a way to average the parameters with consideration for the relative test conditions. Possibly other test results could be plotted, to fill out the region and improve the definition. If such a plot were available for a particular basin or basin shape, then it could be used as a guide for selection of operating conditions.

Comparison of Single Baffle, Box Baffle, and Reaction-Jet Inlets

Additional tests were undertaken to compare the two inlet arrangements (box baffle and reaction-jet inlets) shown in Figure 17 with the results obtained for the single baffle inlet.

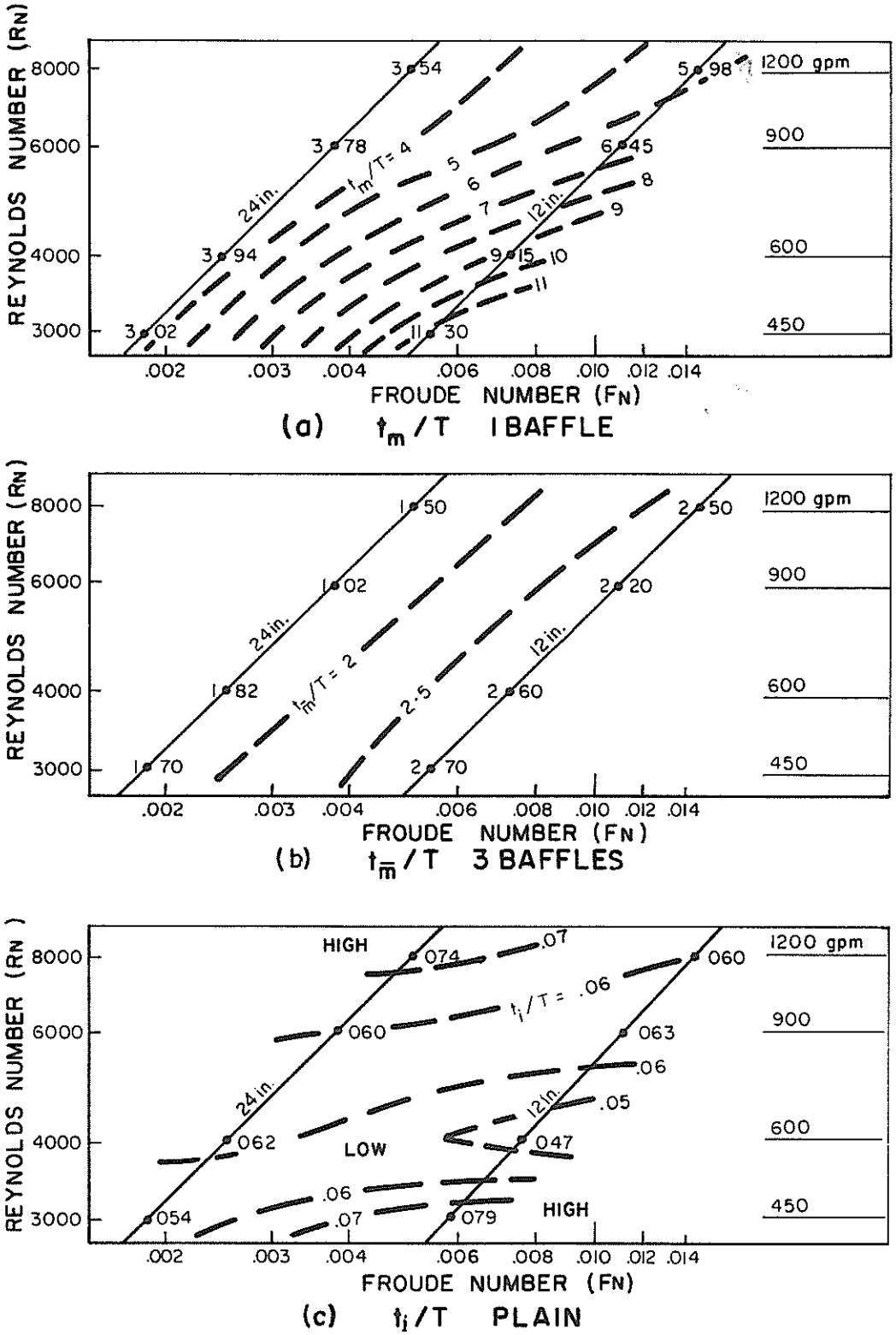

Figure 16-Time Ratio Plots on R_N - F_N Domain

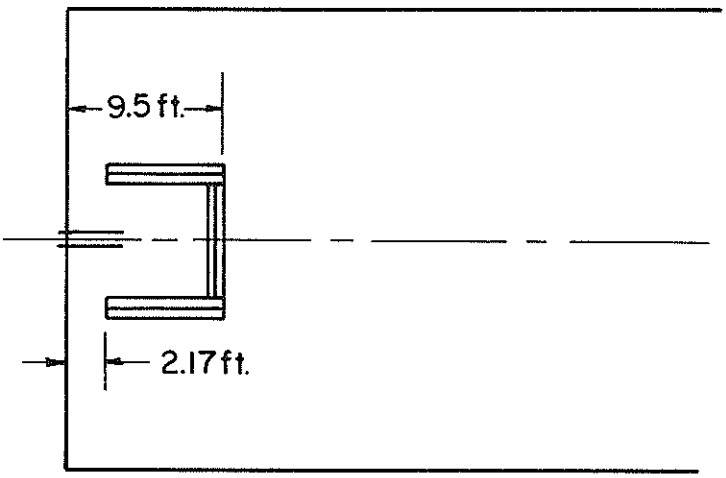

BOX INLET

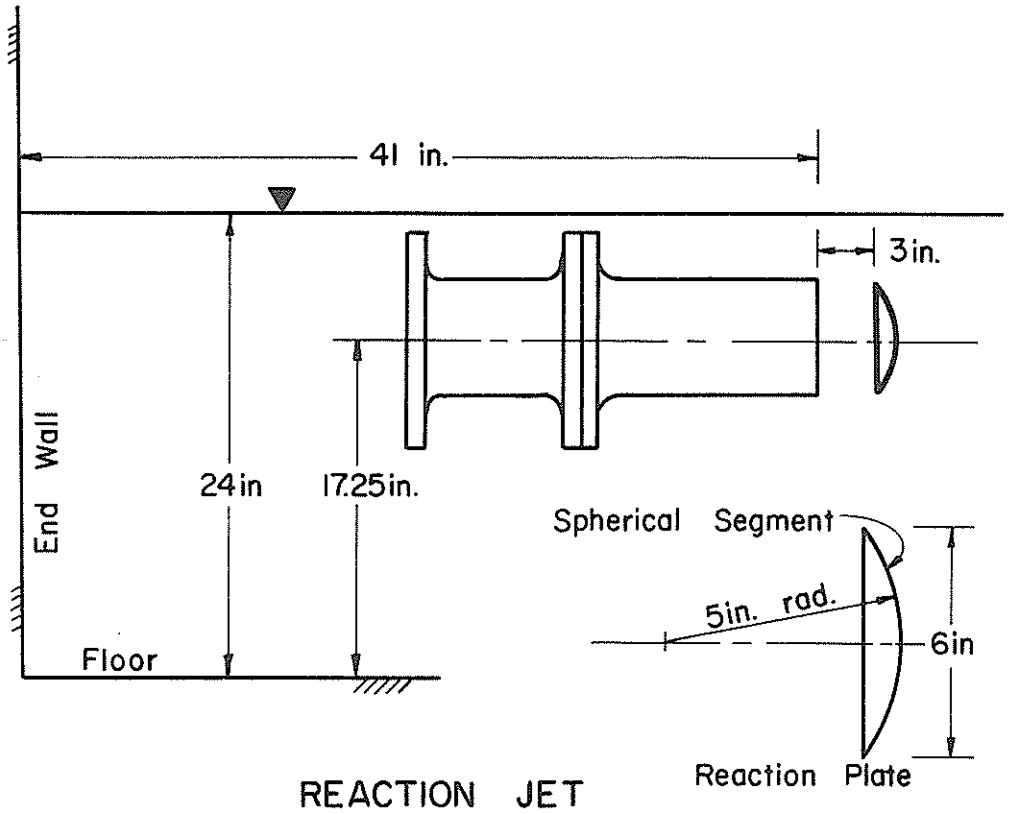

REACTION JET

Figure 17-Box and Reaction Jet Inlets

The testing and data reduction followed the methods of the previous work. The results are presented in Tables 11, 12, 13, and 14. Dispersion curves were plotted and are included in Appendix V.

Examination of Table 11 leads to the conclusion that the reaction-jet inlet allowed short circuiting to occur and that circulation is evidenced by the skewed curve with a long tail. By comparison, both the box baffle and the single baffle inlet (discussed in the previous section) are superior, particularly with regard to the t_i/T and t_p/T values.

The single and box baffle inlets were compared by running an analysis of variance on their curve parameters. A summary of these analyses is presented in Table 12. It is apparent that the inlet differences are not discernable above the experimental error. Depth is the major factor, although for t_i/T and t_p/T there is an interaction between depth and inlets. These dependencies can be seen on Table 11, and Table 12 highlights and quantifies the effects. Using only t_i/T and t_p/T, it follows that the box inlet is "better" at 12 in. depth while the single baffle is "better" at 24 in. depth. Since the other parameters do not yield significant differences in results, it must be concluded that the performance of the two inlets is very similar, but that the single baffle at 24 in. depth provided the best dispersion curves.

Since the box inlet is more complex and would be more expensive to construct, it is reasonable to conclude that the single baffle is the most preferable inlet and must be recommended above all others tested.

	t_i/T	t_p/T	$t_{\bar{m}}/T$	t_m/T	t_σ/T	t_γ/T
Box Baffle 24 in.	(.098)	(.223)	(1.37)	(2.73)	(5.43)	(14.3)
450	.088	.172	1.28	3.43	9.30	27.9
600	.092	.145	1.31	2.71	5.35	13.7
900	.098	.157	1.38	2.40	3.81	8.8
1200	.105	.420	1.50	2.38	3.25	6.7
Box Baffle 12 in.	(.226)	(.633)	(2.28)	(7.68)	(31.17)	(88.9)
450	.335	.710	2.13	4.99	12.88	25.0
600	.179	.685	2.93	11.17	44.00	72.8
900	.165	.441	2.31	5.35	12.21	18.7
1200	.227	.695	1.73	9.19	55.60	239
Reaction Jet 24 in.	(.046)	(.077)	(1.24)	(2.87)	(6.42)	(17.7)
600	.039	.058	1.21	2.37	4.19	10.8
1200	.053	.095	1.27	3.37	8.65	24.7
Single Baffle						
24 in.	(.245)	(.455)	(1.55)	(3.57)	(8.02)	(22.7)
12 in.	(.160)	(.310)	(2.34)	(8.22)	(31.00)	(65.0)

NB: Bracketed figures are group averages

Table 11-Dispersion Curve Parameters

	INLET	DEPTH	FLOW	INLET *DEPTH	DEPTH *FLOW
t_i/T		* (*)		* (**)	
t_p/T		** (***)		** (***)	* (*)
t_m/T		* (***)			* (*)
t_σ/T		* (**)			
t_γ/T		(*)			

* 10% Significant

** 1% Very Significant

*** .1% Extremely Significant

Brackets refer to pooled analyses

Notable Correlations	Correlation Coefficient
Initial/peak	0.76
median/mean	0.84
mean/standard deviation	0.95
standard deviation/skewness	0.86

Table 12. Summary of Analysis of Variance between Single and Box Baffle Inlets

SOURCE	DF	SUM OF SQUARES	MEAN SQUARE	SIGNIFICANCE
t_i/T				
Inlet	1	0.0072675625	0.0072675625	
Depth	1	0.0023280625	0.0023280625	
Inlet*Depth	1	0.0454755625	0.0454755625	*
Flow	3	0.0079206875	0.0026402292	
Inlet*Flow	3	0.0027081875	0.0009027292	
Depth*Flow	3	0.0129046875	0.0043015625	
Inlet*Depth*Flow	3	0.0168171875	0.0056057292	
Corrected Total	15	0.0954219375	0.0063614625	
t_p/T				
Inlet	1	0.008742250	0.008742250	
Depth	1	0.068382250	0.068382250	*
Inlet*Depth	1	0.310249000	0.310249000	**
Flow	3	0.039105500	0.013035167	
Inlet*Flow	3	0.029464250	0.009821417	*
Depth*Flow	3	0.123679250	0.041226417	
Inlet*Depth*Flow	3	0.019702500	0.006567500	
Corrected Total	15	0.599325000	0.039955000	

Table 13-Analysis of Variance, Single and Box Baffled Inlets

SOURCE	DF	SUM OF SQUARES	MEAN SQUARE	SIGNIFICANCE
$t_{\bar{m}}/T$				
Inlet	1	0.06375625	0.06375625	
Depth	1	2.89850625	2.89850625	**
Inlet*Depth	1	0.01265625	0.01265625	
Flow	3	0.36891875	0.12297292	
Inlet*Flow	3	0.08706875	0.02902292	
Depth*Flow	3	0.92601875	0.30867292	*
Inlet*Depth*Flow	3	0.14046875	0.04682292	
Corrected Total	15	4.49739375	0.29982625	
t_m/T				
Inlet	1	1.918225	1.9182250	
Depth	1	92.064025	92.0640250	*
Inlet*Depth	1	0.087025	0.0870250	
Flow	3	10.521225	3.5070750	
Inlet*Flow	3	9.528525	3.1761750	
Depth*Flow	3	8.146325	2.7154417	
Inlet*Depth*Flow	3	18.637025	6.2123417	
Corrected Total	15	140.902375	9.3934917	

Table 13-Continued

SOURCE	DF	SUM OF SQUARES	MEAN SQUARE	SIGNIFICANCE
t_σ/T				
Inlet	1	8.52640	8.52640	
Depth	1	2423.10062	2423.10062	*
Inlet*Depth	1	5.17563	5.17563	
Flow	3	340.31945	113.43982	
Inlet*Flow	3	697.11495	232.37165	
Depth*Flow	3	265.38562	88.46187	
Inlet*Depth*Flow	3	896.49562	298.83187	
Corrected Total	15	4636.11830	309.07455	
t_γ/T				
Inlet	1	229.5225	229.5225	
Depth	1	13712.4100	13712.4100	
Inlet*Depth	1	1030.4100	1030.4100	
Flow	3	5774.2275	1924.7425	
Inlet*Flow	3	10863.6275	3621.2092	
Depth*Flow	3	7595.8200	2531.9400	
Inlet*Depth*Flow	3	12287.6200	4095.8733	
Corrected Total	15	51493.6375	3432.9092	

Table 13-Continued

	DF	SUM OF SQUARES	MEAN SQUARE	F VALUE	SIGNIFICANCE
t_i/T					
Inlet*Depth	1	0.045475	0.045475	12.72	**
Error	14	0.095422	0.00357		
t_p/T					
Depth	1	0.068382	0.068382	6.58	*
Inlet*Depth	1	0.310249	0.310249	32	***
Depth*Flow	3	0.123679	0.041226	4.24	*
Error	10	0.097014	0.009701		
t_m/T					
Depth	1	2.898506	2.898506	47.4	***
Depth*Flow	3	0.926019	0.30867	5.5	*
Error	11	0.672869	0.0611		
$t_{\bar{m}}/T$					
Depth	1	92.0640	92.0640	26.4	***
Error	14	48.8384	3.49		
t_σ/T					
Depth	1	2423.10	2423	15.35	**
Error	14	2213.01	158		
t_γ/T					
Depth	1	13712	13712	5.1	*
Error	14	37781	2690		

Table 14-Analysis of Variance
Single and Box Baffle Inlets, Pooled Error Terms

VI. DISCUSSION

The Model as a Settling Tank

For the purposes of a direct comparison, the results in Table 1 (p. 49) should be measured against those of other studies, shown in Table 4. Only t_i/T and t_p/T have been tabulated since these are the most reliable and consistently reported curve parameters. Camp (6) did note a value for t_m/T of 0.925 for the wide rectangular basin and this clearly distinguishes it from the curves determined in this study where values from 1.5 to 2.8 were found. The wide rectangular tank curve is plotted on Figure 8 (p. 29).

The tanks reported in Table 4 are of similar sizes to the model tank but had narrower and deeper proportions. The wide rectangular tank (6) is an exception, having L/B = 2.45 and L/D = 17.8 (2.5 and 40 to 80 for this study). The Froude numbers are broadly 5 to 50 times as high as the model values. Despite these variations, the values of t_i/T and t_p/T are in the same ranges. The reported curves (2, 6, 8, 9, 13, 19) were better shaped, however, and decreased to zero by about 4 detention periods and this could be expected since the Froude numbers were higher (6). The inlets and outlets were either full width weirs or of the reaction jet type and this with the longer tank proportions was conducive to more nearly ideal flow.

Another method of rating settling tanks is by the discharge rate per unit area. Sewerage tanks are noted to have loading in

Table 4-Results of Other Studies - Initial and Peak Times

Tank Description	L	B	D	$V/\sqrt{gD}$	t_i/T	t_p/T	Reference
Radial Flow Circulator			14.2	.865	.14		Camp (6)
Wide Rectangular	330	135	18.5	2.4	.30		Camp (6)
Rect. Reaction Jet	14	3	3	3.67	.15	.32	Villemonte et al. (19)
	14	3	3	5.4	.21	.49	
	14	3	3	7.3	.24	.47	
	14	3	3	9.2	.22	.52	
	14	3	3	11.0	.28	.57	
	14	3	3	14.7	.18	.36	
Rect. Over Weir	14	3	3	3.67	.05	.13	
	14	3	3	5.4	.07	.20	
	14	3	3	7.3	.10	.30	
	14	3	3	9.2	.08	.28	
	14	3	3	11.0	.09	.24	
	14	3	3	14.7	.07	.13	
Rect. Reaction Jet	80	18	7.7	5.1	.12	.22	
	80	18	7.7	10.2	.15	.22	
	80	18	7.7	15.3	.22	.27	
Rect. Over Weir	80	18	7.7	5.1	.05	.09	
	80	18	7.7	10.2	.11	.18	
	80	18	7.7	15.3	.09	.17	
Rect. Baffled	13	1.97	3.28	.584		.51	Rebhun and Argaman (13)
			1.38	2.15		.40	
			2.66	1.4		.38	
			2.04	2.1		.55	
			3.28	1.46		.40	
			1.38	5.4		.50	
Rect. No Baffle			3.28	1.46		.098	
Rect.(long tail curve)	80	40.5	10.25			.04	Hamlin (19)
						.15	
	80	40.5	7.5		.02		
					.11		
Rect.(long tail curve)	80	20.25	10.75			.04	
						.19	
	80	20.25	8.0				
Rect.(long tail curve)	80	32	1.0	.19	.05	.09	This Study
			2.0	1.5	.30	.59	

NOTE: Dimensions in ft
Froude number x 1000

the range 550 to 2000 gal/ft^2 as noted by Eliassen in discussion of Camp (6). Reported testing has been in the range 118 to 1270 gal/ft^2 day (9), and 500 to 2000 gal/ft^2 day (19). By comparison, the model was tested in the range from 250 to 675 gal/ft^2 day.

From these comparisons it is evident that the model tank is inherently far from optimum proportions, and that the experimentally determined dispersion curves confirm this. If the overall shape is to be retained the major improvements possible are at the inlet end due to the high energy of the influent.

Baffling of the inlet jet yielded a clear improvement over the plain pipe inlet, and of the four arrangements tested, the single baffle was the best. The inference of Figure 14 (p. 53) is that the jet is best arrested and then allowed to naturally dissipate, without further control. Provided that the energy is dissipated and the flow diffused, the effects of recirculation will be greatly diminished.

A note should be made that the reaction jet inlet was similar to a "flow splitter" mounted at the end of a spoil pipeline. The jet was operated underwater, since in a submerged position, a better performance was expected. The results, however, indicate that the reaction jet was substantially inferior to the baffled inlets. It can then be inferred that in a spoil basin a single baffle dike would improve the basin performance significantly over either a plain pipe or a pipe fitted with a flow splitter.

Sediment Removal Estimates

One inference of the dispersion curve results is that higher flow rates yielded better flow conditions. This conclusion must

be modified to consider the settling behavior of the material to be removed from the influent. Three settling characteristics curves, two derived from reported quiescent column analysis (6, 19) and one assumed, are shown in Figure 18. Calculations were made, following the methods proposed by Villemonte et al. (19), to estimate the removal of suspended sediment in the settling tank. If the settling curve is S(t) and the dispersion curve h(t), then removal, R, is:

$$R(t) = \frac{\int_o^t S(t)\, h(t)\, dt}{\int_o^t h(t)\, dt}$$

or in discrete terms

$$R_n = \frac{\sum_{i=1}^{n} S_i\, H_i\, \Delta t}{\sum_{i=1}^{n} H_i\, \Delta t}$$

A more detailed description of these calculations is given in Appendix VI.

By plotting R(t) against time an insight was gained in the interaction between the two curves, and an asymptotic value of removal could be estimated on the graph.

The following graphs, Figures 19 to 23, present a brief study of the removal percentages calculated using the three settling curves and the dispersion curves for (a) the 24 in. depth, plain tank; (b) the 24 in. depth, single baffled tank; and (c) the 12 in. depth, single baffled tank--so providing comparisons of the effects

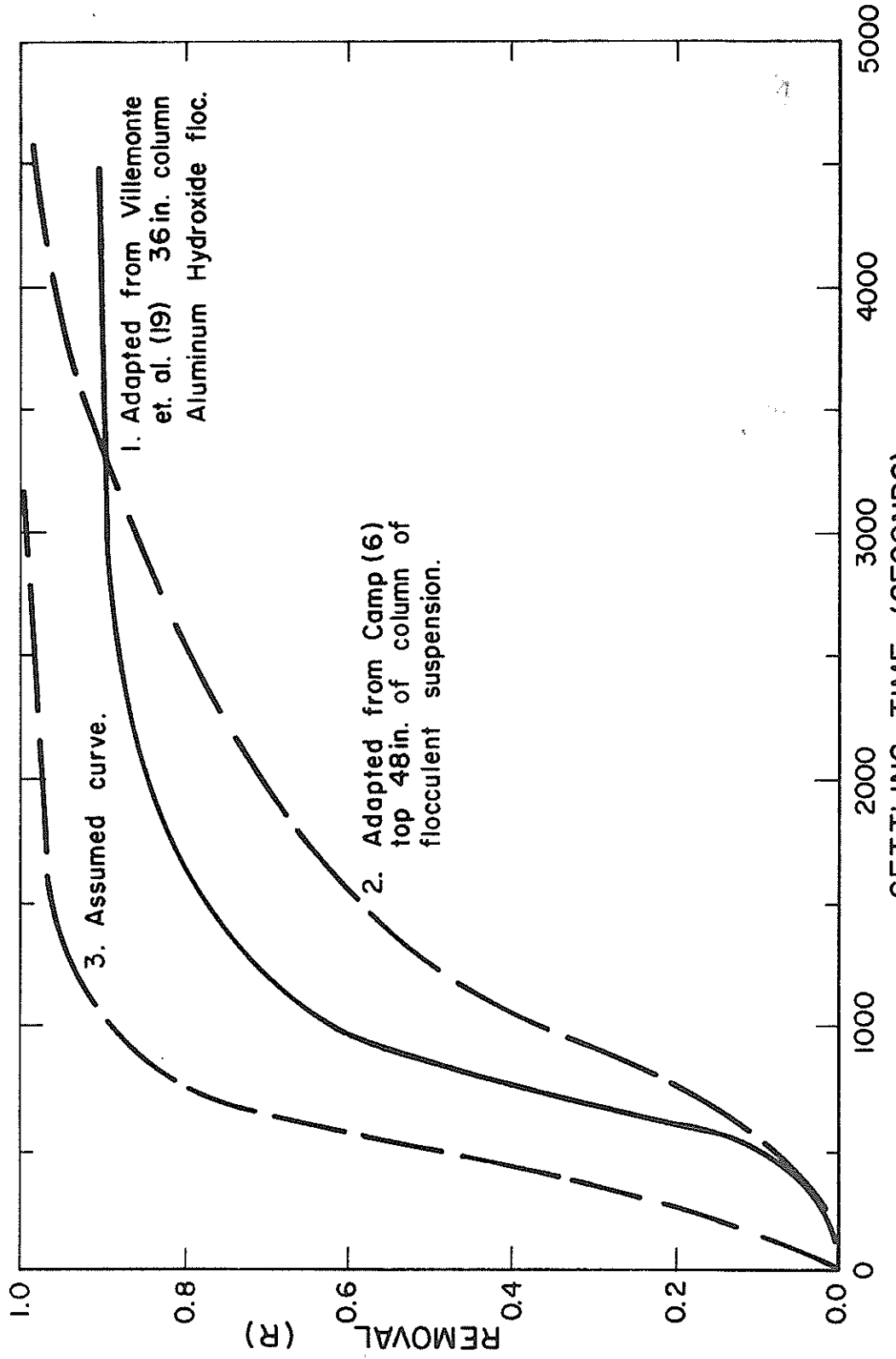

Figure 18-Settling Curves

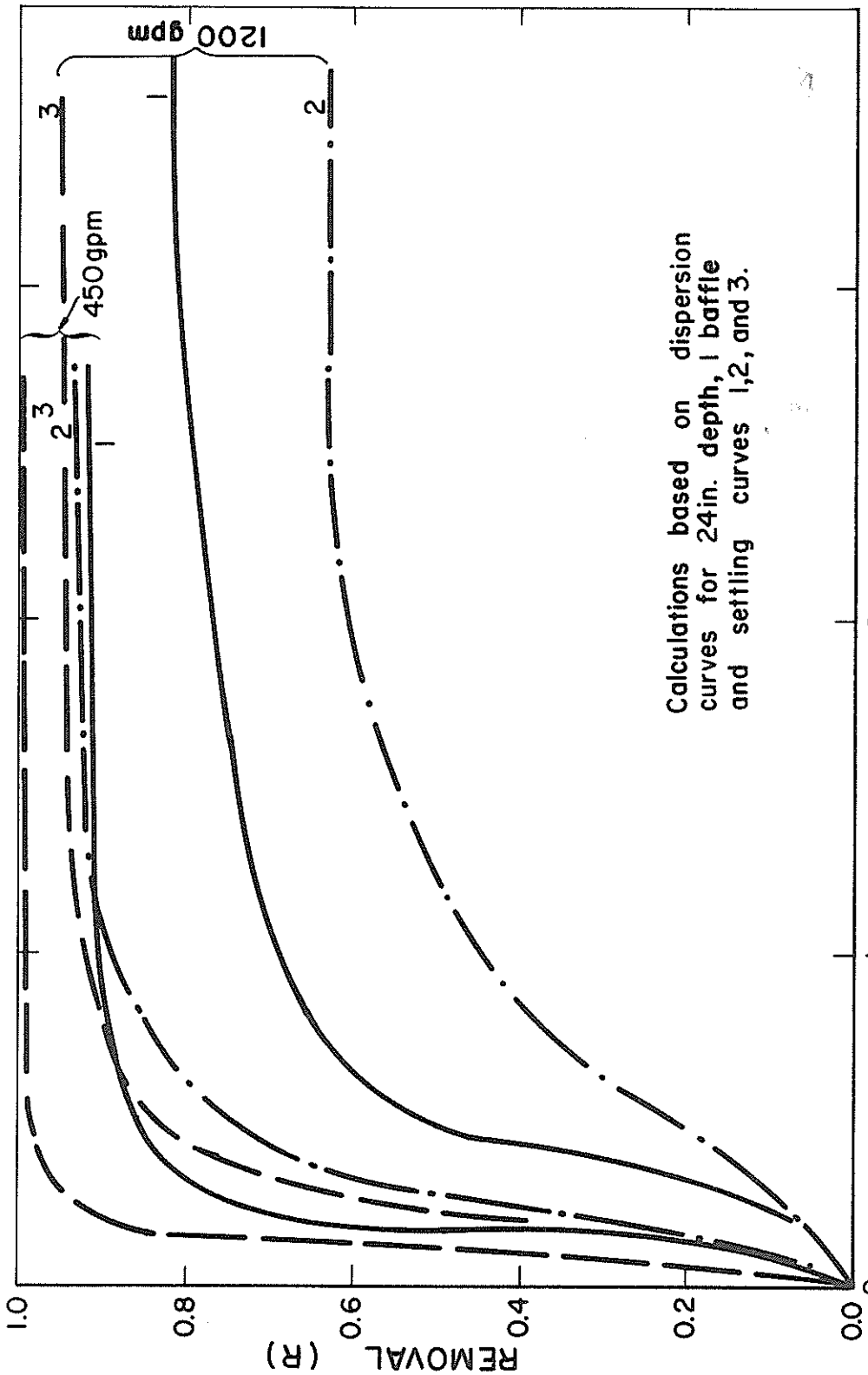

Figure 19-Effect of Settling Curves on Removal

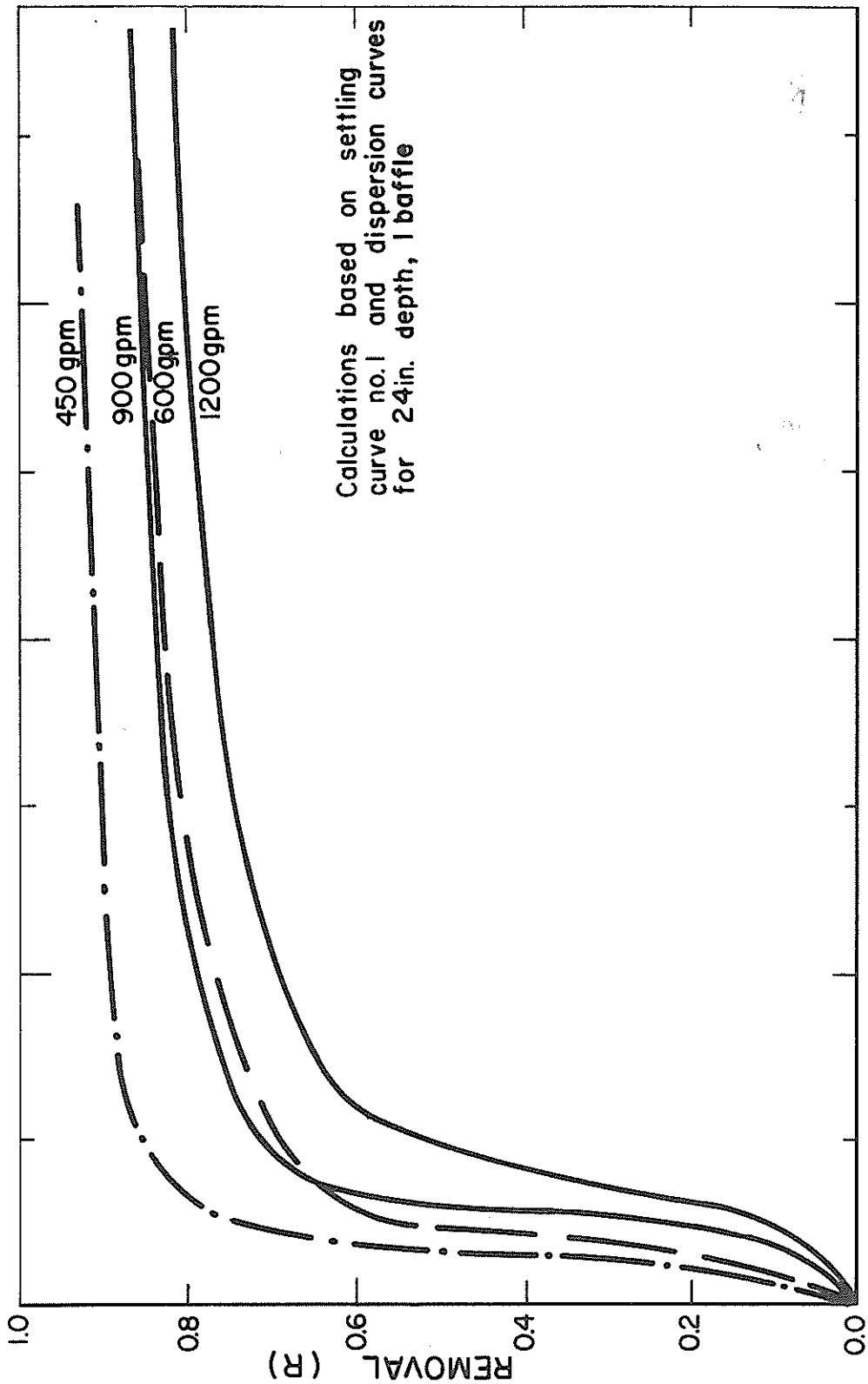

Figure 20-Removal - 24 in. Depth, 1 Baffle

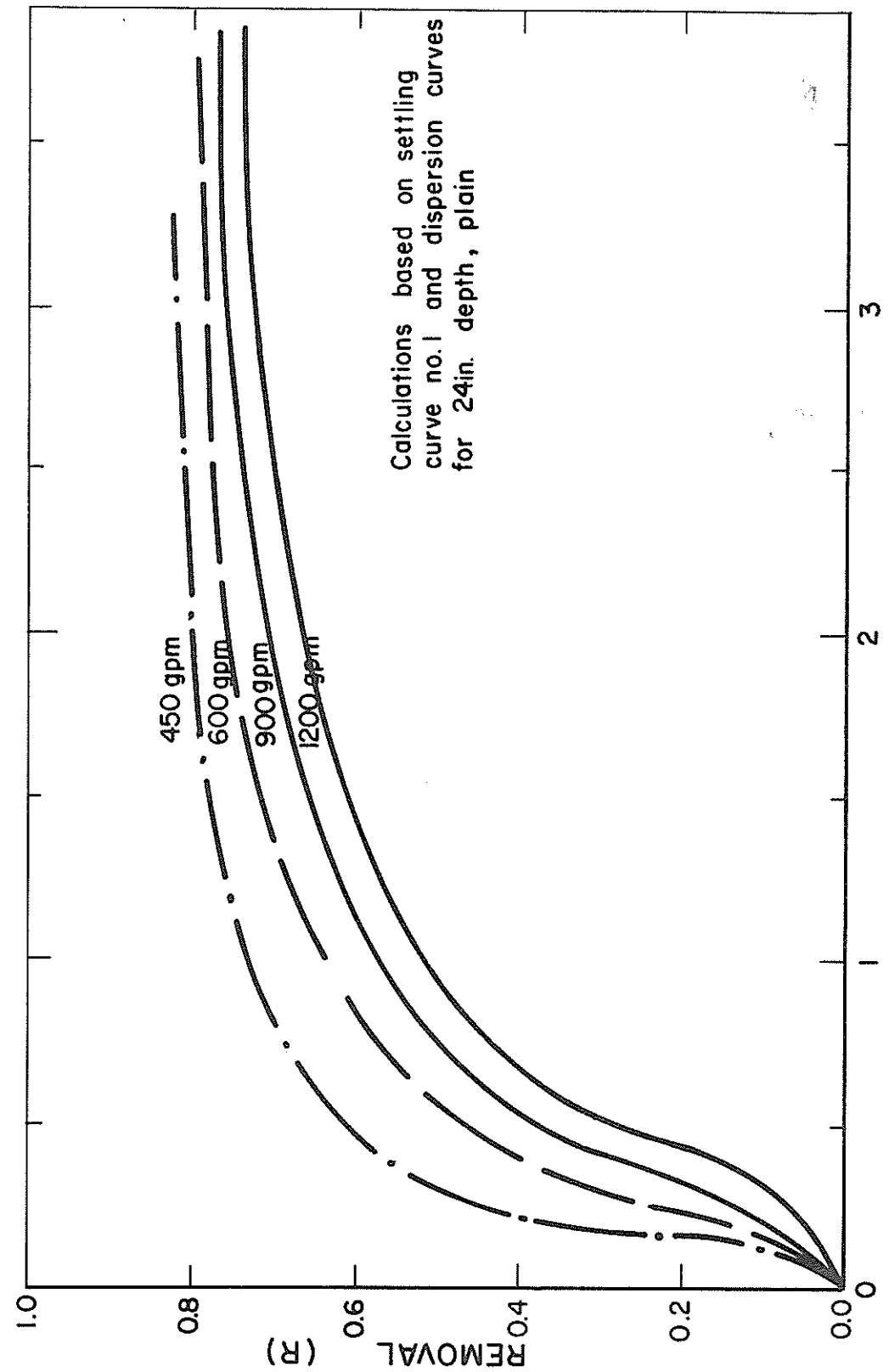

Figure 21-Removal - 24 in. Depth, Plain

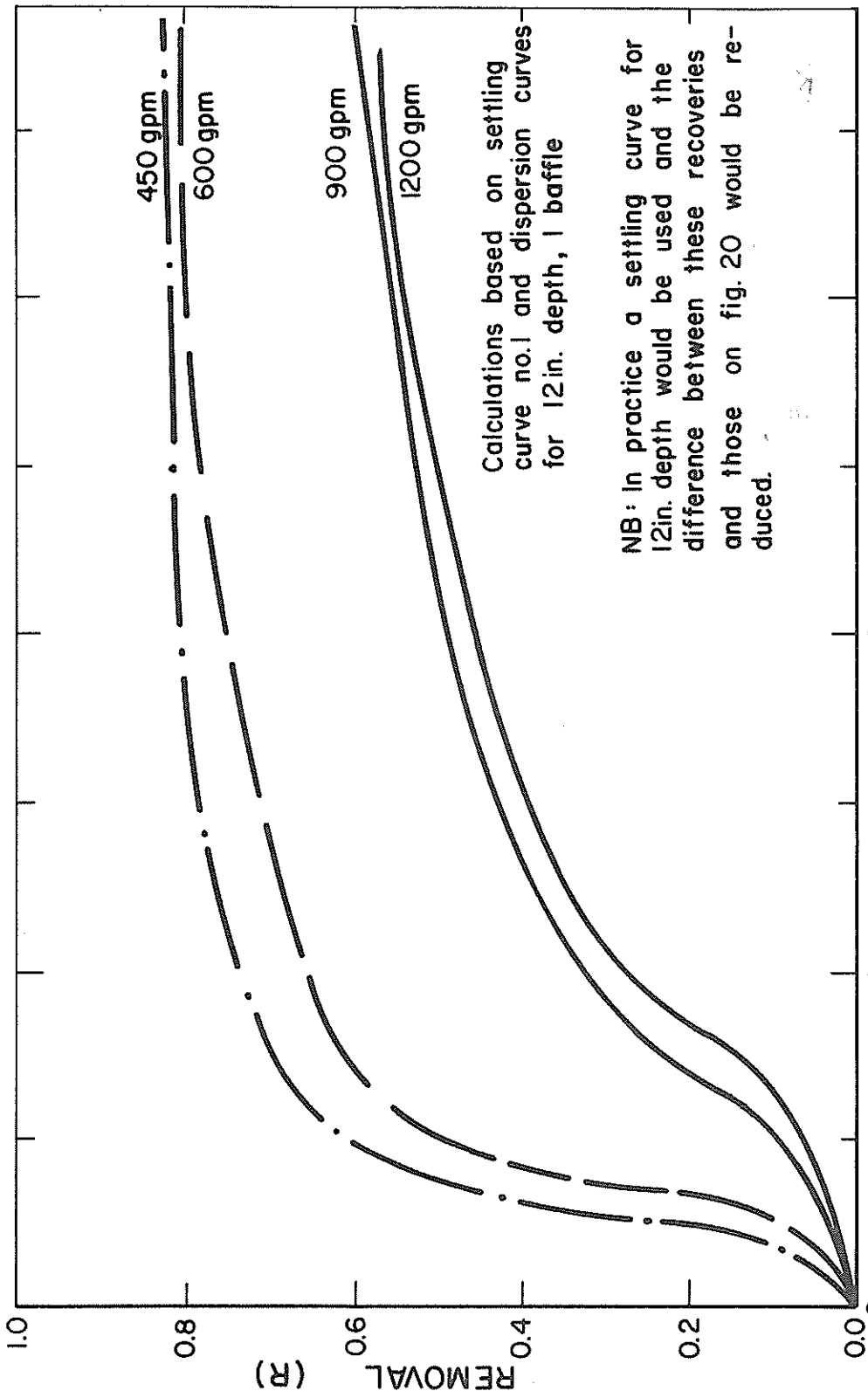

Figure 22-Removal - 12 in. Depth, 1 Baffle

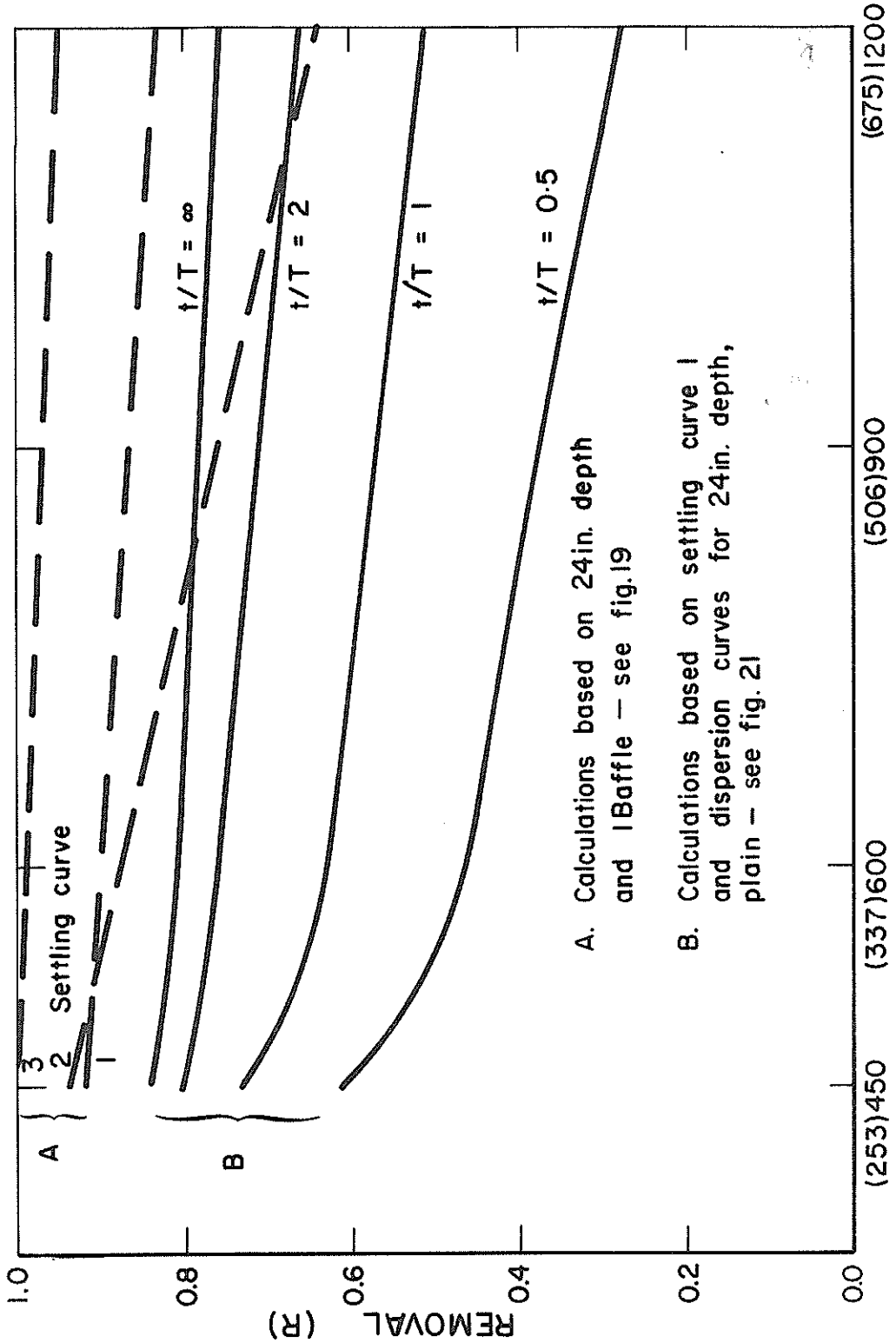

Figure 23-Variation of Removal with Discharge

of depth, flow and inlet.

Figures 19 to 23 indicate that, although the dispersion curves for high flow rates are of a better shape, in the dimensionless form, higher removals are obtained with the lower discharges. This is not always the case, as Figure 20 illustrates, where the 900 gpm curve was sufficiently superior to the 600 gpm curve to overcome the effect of the higher flow. The shape of both curves is important in determining the resultant removal.

Comparison between Figures 20 and 21 supports the concepts on which the dispersion curves were ranked. The baffled curves did yield higher theoretical removals with the same suspension. Additionally, the R(t) curves approach the asymptotic values by 3 or 4 detention periods along the dispersion curve, and the long tail section is seen to be quite ineffective in significantly increasing the removal. This happens to have some support since the long tail was caused by circulation, which inherently had a higher velocity and hence a tendency to scour and inhibit settling. The calculation and the physical argument are not held to have any connection beyond yielding the same tendency.

Figure 22 shows the removals for the 12 in. depth with the single baffle. Comparison with Figure 20 indicates the great decrease in removal wrought by the decrease in depth. This is due not only to the better dimensionless dispersion curve for the deeper case but, also, because the real time scale for the deeper curves is twice that of the shallower depth. Hence, if for both,

the $t_i/T = y$, then t_i (24 in.) = 2 X t_i (12 in.) and so on for all the parameters, this directly causes the removal to be higher for the 24 in. depth despite identical dimensionless dispersion curves. For correctness in principle, the settling curve for the 12 in. depth should be determined from a 12 in. quiescent column, and so would reflect this fact. The removal for 24 in. would not then necessarily be superior.

Figure 23 shows the variation of removal with discharge rate. The dashed curves are extracted from Figure 19 (p. 71) and indicate that discharge can interact with the settling curves so that the removals can vary in relative magnitudes. The full line plots trace the removal values through a theoretical or pseudo time to asymptotic or ultimate curves. The theoretical time relates the time elapsed since a sediment-laden water element entered the system.

The conclusion from this removal study is that removal depends not only on the dispersion curve and the settling curve but on their interaction. However, "improvements" in the dispersion curve will yield higher removals. With the required curves and using the illustrated techniques, allowable discharge rates could be determined so that the effluent would meet the required standards.

Relationship to Dredging Practice

The extension of the conclusions thus far, to a full-scale diked dredge spoil basin involves hydraulic similitude principles.

In order to minimize these problems, the model was as large as could be practically handled. The problem arises since water is used in the model so that R_N and F_N cannot be simultaneously equal in the model and the prototype. The flow over the weir and in that region was basically gravity-controlled so that Froude similitude would be the appropriate scaling. The high-speed inlet caused a great deal of turbulence, energy dissipation and frictional behavior in general, and Reynolds similitude must, therefore, be considered for this part of the tank.

Previous investigators have not been in great accord on similitude. Camp (6) stated that geometric models are quite useful in the measurement of hydraulic short circuiting and later mentioned that experimental evidence supported his statement. It should be noted that he was discussing settling tanks with submerged weir inlets where his assumption of gravity controlled flow was most probably true. In discussion of Camp's paper, Eliassen stated that Reynolds similitude should be followed due to inlet turbulence and boundary friction. In further discussion on Camp, Mulholland proposed the use of judgment and experience, which is probably the best advice, but not very helpful.

Others preferred to model the removal directly and relied on the ratio Q/LB (9, 17). Thompson (17) went so far as to state that removal is not dependent on either Froude or Reynolds numbers.

It remains for the user to judge the correct scales for himself. The model was planned on the basis of equal Froude numbers

for model and prototype, but with a distorted vertical scale. Since no one prototype was considered in this study, Figure 24 was prepared to facilitate the estimation of Froude scales. From given L_H and L_V values, the desired scale can be found, for example if $L_H = 100$, $L_H/L_V = 5$ then $Q = 1{,}000$. Care must be exercised, however, to ensure that the model and prototype both have the same flow regime. The model was tested in a turbulent subcritical flow state.

The qualitative or comparative results of the model tests can be extended to dredging practice as follows. Depth is an important factor, not only to avoid scour but because deeper water arrests the influent jet and produces a notably more stable flow. The dispersion curves are significantly better for a deeper basin (Table 1, p. 49). A major problem in diked basins is the formation of channels in the settled material. Examination of the model behavior infers that the formation of concentrated streams of water can be reduced by arresting the influent with a single short internal dike, and by raising the water depth to a maximum. The baffle dike would probably require some type of rock covering to resist the scouring force of the influent, but due to the short length, the cost would be reasonable. It is also sensible that deeper water is affected less by undulations in the bed which with shallower flow could cause a channeling effect.

Although it cannot be expected that the model dispersion curves could be directly used to plan a basin, the prototype curves

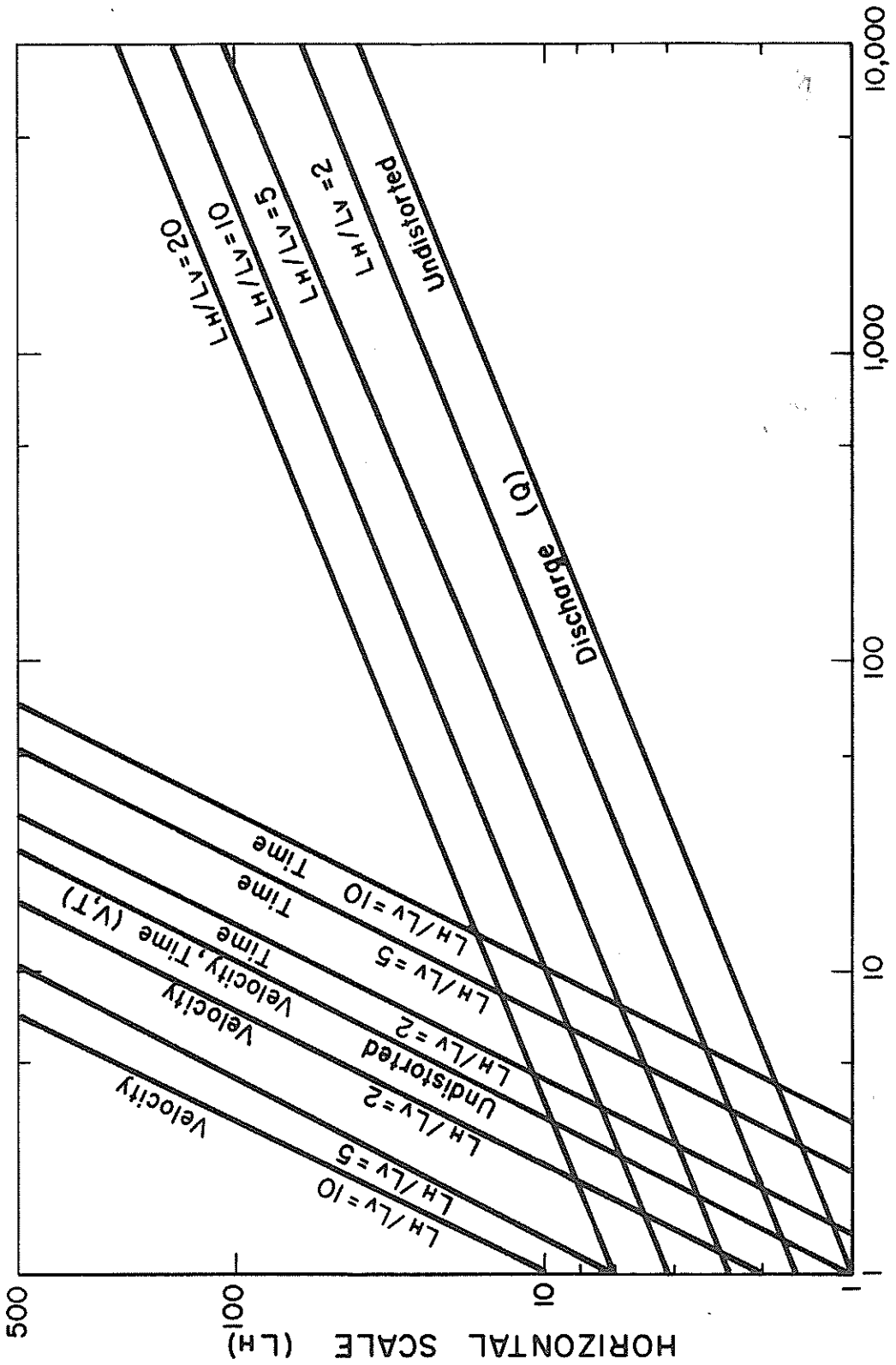

Figure 24-Froude Number Scaling

would be similar. The model curves could be used as a best approximation until some field-tested curves were available. In this way theoretical removal estimates could be made, and refined as better information was obtained.

For managing the operation of existing basins, the techniques used in the study would enable the selection of theoretical optimum depths and flow rates. The establishment of such techniques is conducive to the collection of performance information within the proposed structure. The necessary feedback for the development of a better understanding then follows. Field dispersion curves, being an integral part of the required data, should not be too difficult to determine. If a dredge is fitted with a recording flowmeter the measurements could be made in the normal course of operation. Radioactive tracers may be more appropriate than fluorescent dyes since the water would be turbid, and might inhibit the passage of light through a sample.

Finally, areal loading of diked basins is very low compared either to settling tank practice or to the model. A high flow of 65,000 gpm into a 2000 ft X 1000 ft area is approximately 50 gal/ft^2 day. This is in the order of 1% of a comparable high loading in a settling tank. Clearly there is room for improvement of the diked dredge spoil basins.

VII. CONCLUSIONS AND RECOMMENDATIONS

Conclusions

A method was formulated to determine dispersion curves for a settling tank in a closed system where the effluent was recycled as influent. The dye concentrations were measured at both the outlet and the inlet. These records were deconvolved together to yield the dispersion curve or unit impulse response.

Techniques for comparing the determined dispersion curves were studied. Statistical tests for the comparison of two observed cumulative distributions (dispersion curves) were not fruitful under the variable circumstances found. The cumulatives were, therefore, used to fit log normal curves from which the moment parameters, mean, standard deviation and skewness coefficient were estimated. Analysis of variance techniques were used on these time parameters to test for significant effects due to inlets, flows and depths.

Depth was consistently the most important factor. The inlet variations caused less significant variations. Only when two controlled inlets were compared did flow register as a significant source of variation.

On the basis of the experimental dispersion curves, the single baffle inlet showed the greatest improvement over the uncontrolled or plain inlet. The box baffle inlet was similar in performance to the single baffle but tended to be inferior. Considering costs, the single baffle is preferred. The reaction-jet inlet, as tested, was inferior. It appears that the shallow-depth and minimal submergence

did not suit this type of inlet.

Large circulation currents were caused by the high speed inlet, and were intensified in shallower water. The dispersion curves reflected the circulation in a very long tailed shape with a consequently low peak. The tail sections beyond 4 detention periods were not useful for sediment removal.

The model testing was used to select the inlet arrangement with the greater potential. It should be further tested to determine the optimum proportions. Only field-testing will, however, provide the final proof.

The behavior in the model enables qualitative predictions to be made of the behavior in a diked basin.

Previously developed methods have been used to indicate how dispersion curves interact with quiescent settling column results to yield estimates of the removal efficiency.

Recommendations

Diked basins should be operated with the water as deep as possible, unless the effluent standards are met at a lesser depth.

Further model testing should be followed by field trials of the most promising inlet arrangements.

Field-measured dispersion curves are practical and should be determined. They would provide valuable basin management information and the necessary design feedback.

It is clear that the area with the greatest potential for improvement in a diked basin is the inlet. Further efforts should be concentrated on the inlet behavior and improvement. However,

the suggestions made here would generally advance the understanding of diked basins.

REFERENCES

1. American Water Works Association, A Handbook of Public Water Supplies, AWWA, 3rd Edition, McGraw-Hill Book Co., 1971.

2. Basco, D. R., "Tracer Studies of Circular Basins with Stengel Inlets," M. S. Thesis, University of Wisconsin, 1962.

3. Benjamin, J. R., and Cornell, C. A., Probability, Statistics and Decision for Civil Engineers, McGraw-Hill Book Co., 1970.

4. Boyd, M. B., et. al., "Disposal of Dredge Spoil - Problem Identification and Assessment and Research Program Development," Technical Report H-72-8, U. S. Army Corps of Engineers, Waterways Experiment Station, Vicksburg, November, 1972, pp. 119.

5. Butts, T. A., "Fluorometer Calibration Curves and Monographs," Journal of the Sanitary Engineering Division, ASCE, Vol. 95, No. SA4, Proc. Paper 6728, Aug., 1969, pp. 705-714.

6. Camp, T. R., "Sedimentation and the Design of Settling Tanks," Transactions, ASCE, Vol. III, 1946, Paper No. 2285, pp. 895-936 and discussion, pp. 937-958.

7. Clements, M. S., "Velocity Variations in Rectangular Sedimentation Tanks," Proceedings of the Institution of Civil Engineers, Vol. 34, June, 1966, Paper No. 6923, pp. 171-200.

8. El-Baroudi, H. M., "Tracer Dispersion of High Rate Settling Tanks," Journal of the Environmental Engineering Division, ASCE, Vol. 95, No EE3, Proc. Paper 9820, June, 1973, pp. 347-368.

9. El-Baroudi, H. M., "Characterization of Settling Tanks by Eddy Diffusion," Journal of the Sanitary Engineering Division, ASCE, Vol. 95, No. SA3, Proc. Paper 6618, June, 1969, pp. 527-544.

10. Hazen, A., "On Sedimentation," Transactions, ASCE, 53, 1904, Paper No. 980, pp. 45-88 (includes discussion)

11. Kolessar, M. A., "Some Engineering Aspects of Disposal of Sediments Dredged from Baltimore Harbor," Proceedings of the Federal Inter-Agency Sedimentation Conference, Agricultural Research Service, U. S. Department of Agriculture, Misc. Publ. No. 970, 1963.

12. Murphy, W. L., and Zeigler, T. W., "Practices and Problems in the Confinement of Dredged Materials in Corps of Engineers Projects," Technical Report D-74-2, U. S. Army Engineer Waterway Experiment Station, Vicksburg, MS, Aug., 1973.

13. Rebhun, M., and Argaman Y., "Evaluation of Hydraulic Efficiency of Sedimentation Basins," Journal of the Sanitary Engineering Division, ASCE, Vol. 91, No. SA5, Proc. Paper 4523, Oct., 1965, pp. 37-45.

14. Replogle, J. A., Myers, L. E., and Brust, K. J., "Flow Measurements with Fluorescent Tracers," Journal of the Hydraulics Division, ASCE, Vol. 92, No. HY5, Proc. Paper 4895, Sept., 1966, pp. 1-15.

15. Sayre, W. W., "Dispersion of Silt Particles in Open Channel Flow," Journal of the Hydraulics Division, ASCE, Vol. 95, No. HY3, Proc. Paper 6579, May, 1969, pp. 1009-1038.

16. Sullivan, S. P., and Gerritsen, F., "Dredging Operation Monitoring and Environmental Study, Kawaihae Harbor, Hawaii," Technical Report No. 25, University of Hawaii Look Laboratory, Sept., 1972, pp. 170.

17. Thompson, D. M., "Scaling Laws for Continuous Flow Sedimentation in Rectangular Tanks," Proceedings of the Institution of Civil Engineers, Vol. 43, July, 1969, Tech. Note 11, pp. 453-361 plus discussion by Clements, M.S., Vol. 46, July 1970, pp. 387-393.

18. U. S. Army Engineer District, Buffalo, C. E., "Dredging and Water Quality Problems in the Great Lakes," U. S. Army Corps of Engineers, Buffalo, N. Y., June, 1969.

19. Villemonte, J. R., Rohlich, G. A., and Wallace, A. T., "Hydraulic and Removal Efficiencies in Sedimentation Basins," Advance in Water Pollution Research, Proceedings of 3rd Intercoastal Conference, Sept., 1966, Vol. 2, pp. 381-414.

20. White, J., Seidel, G. A., and Terzich, L., "Report to the Dredging Contractions Association of California on the Effects of Dredging Operations on Water Quality," Metcalf and Eddy, Engineers, Aug., 1968.

APPENDIX I

Notation

A	area
B	breadth
c	concentration of dye
c_o	a theoretical dye concentration (= S/∀)
D,d	depth of water
$F_y(y)$	cumulative distribution function of the variable y
F_N	Froude number (= $V/\sqrt{gd}$)
$F_u(u)$	cumulative distribution function of the standard normal variable, u
$f_y(y)$	probability density function of variable y
$f_u(u)$	probability density function of the standard normal variable, u
g	acceleration due to gravity
H_i	a discrete ordinate of a system unit impulse response
h(t)	continuous unit impulse response
L	length, as length of basin
L_H	ratio of prototype length to model length
L_V	ratio of prototype depth to model depth
m_y	mean of the distribution of y
$\bar{m}_y$	median of the distribution of y
Q	a discharge or flow rate, also discharge scale
R_N	Reynolds number (= VD/ν)

$R(t)$ sediment removal

R_i discrete ordinate of sediment removal

$S(t)$ settling curve characteristic of a suspension determined in a quiescent column

S_i discrete ordinate of settling curve of a suspension

S mass of dye (injected)

t time

t_i time to the initial response of the dispersion curve

t_p time to the peak response of the dispersion curve

$t_{\bar{m}}$ time to the median of the dispersion curves

t_m time to the mean of the dispersion curve

t_σ the standard deviation of a dispersion curve expressed in units of time

t_γ the skewness coefficient of a dispersion curve

t_c/T dispersion curve width at half peak concentration

t_b/T dispersion curve width at $\frac{1}{10}$ peak concentration

t_t/T time at the furthest point of t_b/T width

T theoretical detention time for a settling tank ($= \frac{Q}{\forall}$), also a time scale

u variable of the standard normal probability distribution

V flow velocity, also velocity scale

V_y coefficient of variation ($= \sigma_y/m_y$)

$\forall$ volume of tank

X_i discrete ordinate of a system input, fluorometer dial response at inlet

$x(t)$	continuous system input, fluorometer dial response at inlet
Y_i	discrete ordinate of a system response, fluorometer dial response at outlet
$y(t)$	continuous system response, fluorometer dial response at outlet
y	a variable substituted for t/T or $(t - t_i)/T$, or a removed concentration
α	calibration constant such that ( ) x (dial response) = c
β	temperature correction factor.
γ_1	skewness coefficient of a probability distribution
σ_y	standard deviation of the y distribution
$\sigma_{\log y}$	standard deviation of the log y distribution
ν	kinematic viscosity of a fluid

APPENDIX II

Computer Program

Input:

```
N, NN, DT, TEMPX, TEMPY, TD          (2I10, 4F10.2)
O, X(2), X(3)----------          X (16) (16F5.2)
X (17)-----------------          X (32)
      -----------------          X (N)
Y(1)                             Y (16)
      -----------------          Y (N)
NOPT, X(1)                           (I10, F12.2)
```

If the X(I) curve were smooth enough a larger DT could be tolerated to input the data. Subroutine INTERP was then used to recreate an X(I) vector of length N. Card changes were necessary:

17	READ (5,1001)	(Z(I), I = 1, M)	substitute
22	WRITE (6,1006)	(Z(I), I = 1, M)	
	CALL INTERP	(X, Z, DT)	inserted between

lines 23 and 24.

16	M = N/a	where a = N/M or the ratio

of the sampling intervals.

NB: lines 122, 123, 124 should be inserted between lines 26 and 27 and set A = β_x/β_y where β is calibration constant for a fluorometer.

(a three-page program listing follows.)

```
//TA498    JOB (T319-,2-G--,*30,002,01),' R MALE
//*WATFIV
C     PROGRAM TO REDUCE DATA
C
C
 1          DIMENSION X(1000),Y(1000),H1(1000),H2(1000),T(1000),CH(1000),
           1H1S(1000),Y2(1000),CHR(1000),HR(1000),Z(1000)
 2          COMMON N
 3        1 READ(5,1000,END=900)N,NN,DT,TEMPX,TEMPY,TD
 4          WRITE (6,1001)N,NN,DT,TEMPX,TEMPY,TD
 5          CALL MAIN (NN,DT,TEMPX,TEMPY,TD,X,Y,H1,H2,T,CH,H1S,Y2,
           1CHR,HR,Z)
 6          GO TO 1
 7       900 WRITE(6,1002)
 8      1000 FORMAT(2I10,4F10.2)
 9      1001 FORMAT ('1',2I10,4F10.2,//)
10      1002 FORMAT('1','  OUT OF DATA ')
C
C       N        NO OF SAMPLES POINTS IN DATA
C       NN       N VALUE OF FIRST NON ZERO Y
C       DT       TIME INTERVAL
C       TEMPX    TEMPERATURE AT WHICH X RECORDED
C       TEMPY    TEMPERATURE AT WHICH Y RECORDED
C       TD       DETENTION TIME
C
11          STOP
12          END

13          SUBROUTINE MAIN (NN,DT,TEMPX,TEMPY,TD,X,Y,H1,H2,T,CH,H1S,Y2,
           1CHR,HR,Z)
14          COMMON N
15          DIMENSION X(N),Y(N),H1(N),H2(N),T(N),CH(N),H1S(N),Y2(N),
           1CHR(N),HR(N),Z(1000)
16          M=N/4.5
17          READ(5,1001)(X(I),I=1,N)
18          READ(5,1001)(Y(I),I=1,N)
19          READ (5,1000)NOPT, X(1)
20           XX=X(1)
21          WRITE(6,1006) (X(I),I=1,N)
22          WRITE(6,1006) (Y(I),I=1,N)
23     1006 FORMAT(5X,16F5.1)
24           X(1)=XX
25          CALL TEMP (X,TEMPX)
26          CALL TEMP (Y,TEMPY)
27          CALL RESP (X,Y,H1,1)
28          T(1)=0.
29          DO 20 I=1,N
30          AN=I-1
31       20 T(I)=AN*DT
32          WRITE(6,1003)
33          IF(NOPT.NE.0) GO TO 100
34          NO=N/10
35          DO 17 I=1,19
36       17 WRITE (6,1004) T(I),X(I),Y(I),H1(I)
37          DO 60 J=20,N,10
38       60 WRITE(6,1004)T(J),X(J),Y(J),H1(J)
39          GO TO 90
40      100 DO 30 I=1,N
41       30 WRITE(6,1004)T(I),X(I),Y(I),H1(I)
42       90 CONTINUE
```

```
43          CALL NORM (H1,CH,DT,CHR,S)
44          DO 45 I=1,N
45          H1(I)=H1(I)*TD
46       45 HR(I)=H1(I)*S
47          DO 40 I=1,N
48       40 T(I)=T(I)/TD
49          WRITE (6,1005)
50          IF(NOPT.NE.0) GO TO 110
51          DO 18 I=1,19
52       18 WRITE (6,1004) T(I),H1(I),CH(I),CHR(I),HR(I)
53          DO70 J=20,N,10
54       70 WRITE(6,1004)T(J),H1(J),CH(J),CHR(J),HR(J)
55          GO TO 120
56      110 DO 50 I=1,N
57       50 WRITE(6,1004)T(I),H1(I),CH(I),CHR(I),HR(I)
58      120 CONTINUE
59     1001 FORMAT (16F5.2)
60     1000 FORMAT(I10,F12.2)
61     1003 FORMAT ('1',' OUTPUT DATA ',/// ,10X,'      TIMA       INPUT       OU
           1TPUT       TANK ',/,50X,' RESP    ',//)
62     1004 FORMAT(10X,6G12.4,/)
63     1005 FORMAT('1',10X,'  TIME        HNORM       CUMH        RECOV        HR
           1EC ',//)
       C
       C
       C      VARIABLES
       C
       C       X(I)     INPUT VECTOR     X(NN).NE.0   X(1).NEQ
       C       Y(I)     OUTPUT VECTOR
       C       H1(I)    VECTOR OF UNIT IMPULSE RESPONSE     TANK
       C       H2(I)    VECTOR OF UNIT IMPULSE RESPONSE     SUMP
       C       T        TIME
       C       DT       SAMPLING TIME INTERVAL
       C       N        NO OF CPTS IN VECTORS
       C       NOPT     0 FOR ONE RESULT IN 10, 1 FOR ALL RESULTS
64          RETURN
65          END

66          SUBROUTINE RESP (X,Y,H,NN)
67          COMMON N
68          DIMENSION X(N),Y(N),H(N)
69          DO 5 I=1,NN
70        5 H(I)=0.
71          H(NN)=Y(NN)/X(NN)
72          NNN=NN+1
73          DO 10 I=NNN,N
74          SX=0.
75          DO 20 J=NNN,I
76       20 SX=SX+X(J)*H(I-J+1)
77       10 H(I)=(Y(I)-SX)/X(NN)
78          RETURN
79          END

80          SUBROUTINE TEMP (H,T)
81          COMMON N
82          DIMENSION H(N)
83          DTEMP=T-25.
84          TFACT=EXP(0.026*DTEMP)
85          DO 10 I=1,N
86       10 H(I)=TFACT*H(I)
87          RETURN
88          END
```

```
      SUBROUTINE NORM (H,CH,DT,CHR,S)
      COMMON N
      DIMENSION H(N),CH(N),CHR(N)
      NM=N-1
      S=(H(1)+H(N))/2.
      DO 10 I=2,NM
   10 S=S+H(I)
      S1=S*DT
      CH(1)=0.
      CHR(1)=0.
      DO 20 I=1,N
   20 H(I)=H(I)/S1
      DO 30 I=2,N
      CH(I)=CH(I-1)+DT*((H(I-1)+H(I))/2.)*100.
   30 CHR(I)=CH(I)*S
      WRITE(6,100)S
  100 FORMAT(///,'   INTEGRAL  H*DT  =  ',G12.4)
      RETURN
      END
//$DATA
```

```
      SUBROUTINE INTERP (Y,Z,DT)
      COMMON N
      DIMENSION Y(N),Z(1000)
      DT2=4.5*DT
      DO 20 I=1,N
      T=(I-1)*DT
      J=T/DT2+1
      IF(J.GT.M) GO TO 1
      A=T/DT2-J+1
      B=1.-A
      Y(I)=B*Z(J)+A*Z(J+1)
      GO TO 20
    1 Y(I)=Z(M)
   20 CONTINUE
      A=4.35
      DO 15 I=1,N
   15 Y(I)=Y(I)*A
      RETURN
      END
//$DATA
```

APPENDIX III

Log Normal Function

1. $$f_y(y) = \frac{1}{y\sqrt{2\pi}\ 2.3\ \sigma_{\log y}} \exp\left\{-\frac{1}{2}\left[\frac{1}{\sigma_{\log y}} \log\left(\frac{y}{\bar{m}_y}\right)\right]^2\right\}$$

$$= \frac{1}{2.3\ y\ \sigma_{\log y}} f_u(u)$$

where

$$u = \frac{1}{\sigma_{\log y}} \log\left(\frac{y}{\bar{m}_y}\right)$$

$f_u(u)$ = standard normal curve

$F_y(y) = F_u(u)$ cumulative distribution function (CDF)

2. Given $\bar{m}_y$ and $\sigma_{\log y}$ from the log normal cumulative plot

$$m_y = \bar{m}_y \exp\left(\frac{2.3^2}{2} \sigma^2_{\log y}\right)$$

$$\sigma_y^2 = m_y^2 \{\exp\left(2.3^2\ \sigma^2_{\log y}\right) - 1\}$$

$$V_y^2 = \exp\left(2.3^2\ \sigma^2_{\log y}\right) - 1$$

$$\gamma_1 = 2\ V_y + V_y^3$$

3. To determine $\sigma_{\log y}$

   (a) read from the CDF plot the value of the median $\bar{m}_y$,

   (b) read from the same plot the value of $F_y(10)$ where the model intersects $y = 10$.

then since $F_y(10) = F_y(y) = F_u(u)$, u can be taken from the standard normal tables. Then

$$\sigma_{\log y} = \frac{1}{u} \log \left(\frac{10}{\bar{m}_y}\right).$$

APPENDIX IV

Analyses of Variance

Analyses were run

1. with all inlets included,
2. with baffled inlets only.

The significance levels are defined as:

*	10%	Significant
**	1%	Very significant
***	.1%	Extremely significant

Table 5-Analysis of Variance, All Inlets, t_i/T, t_p/T and $t_{\bar{m}}/T$

ANALYSIS OF VARIANCE FOR VARIABLE TI		MEAN 0.141875000	
SOURCE	DF	SUM OF SQUARES	MEAN SQUARE
INLET	2	0.083675250	0.0418376250
DEPTH	1	0.008103375	0.0081033750
INLET*DEPTH	2	0.007021750	0.0035108750
FLOW	3	0.003039458	0.0010131528
INLET*FLOW	6	0.001881417	0.0003135694
DEPTH*FLOW	3	0.009481792	0.0031605972
INLET*DEPTH*FLOW	6	0.015443583	0.0025739306
CORRECTED TOTAL	23	0.128646625	0.0055933315

ANALYSIS OF VARIANCE FOR VARIABLE TP		MEAN 0.247041667	
SOURCE	DF	SUM OF SQUARES	MEAN SQUARE
INLET	2	0.304754333	0.152377167
DEPTH	1	0.040098375	0.040098375
INLET*DEPTH	2	0.016204000	0.008102000
FLOW	3	0.006191458	0.002063819
INLET*FLOW	6	0.022815667	0.003802611
DEPTH*FLOW	3	0.053074458	0.017691486
INLET*DEPTH*FLOW	6	0.065896667	0.010982778
CORRECTED TOTAL	23	0.509034958	0.022131955

ANALYSIS OF VARIANCE FOR VARIABLE TMO		MEAN 2.05416667	
SOURCE	DF	SUM OF SQUARES	MEAN SQUARE
INLET	2	0.30463333	0.15231667
DEPTH	1	3.19740000	3.19740000
INLET*DEPTH	2	0.35490000	0.17745000
FLOW	3	0.27975000	0.09325000
INLET*FLOW	6	0.73710000	0.12285000
DEPTH*FLOW	3	0.18556667	0.06185556
INLET*DEPTH*FLOW	6	0.50963333	0.08493889
CORRECTED TOTAL	23	5.56898333	0.24212971

Table 6-Analysis of Variance, All Inlets, t_m/T, t_σ/T and t_γ/T

ANALYSIS OF VARIANCE FOR VARIABLE TME MEAN 7.08166667

SOURCE	DF	SUM OF SQUARES	MEAN SQUARE
INLET	2	17.058133	8.529067
DEPTH	1	116.336067	116.336067
INLET*DEPTH	2	4.550633	2.275317
FLOW	3	23.975967	7.991989
INLET*FLOW	6	49.079433	8.179906
DEPTH*FLOW	3	25.319900	8.439967
INLET*DEPTH*FLOW	6	29.717800	4.952967
CORRECTED TOTAL	23	266.037933	11.566867

ANALYSIS OF VARIANCE FOR VARIABLE SIG MEAN 27.4350000

SOURCE	DF	SUM OF SQUARES	MEAN SQUARE
INLET	2	706.7493	353.37465
DEPTH	1	3416.7521	3416.75207
INLET*DEPTH	2	135.3606	67.68032
FLOW	3	1260.6729	420.22429
INLET*FLOW	6	2952.2392	492.03987
DEPTH*FLOW	3	1278.7289	426.24296
INLET*DEPTH*FLOW	6	1615.4412	269.24021
CORRECTED TOTAL	23	11365.9442	494.17149

ANALYSIS OF VARIANCE FOR VARIABLE SKE MEAN 60.6958333

SOURCE	DF	SUM OF SQUARES	MEAN SQUARE
INLET	2	3378.9408	1689.4704
DEPTH	1	10387.5204	10387.5204
INLET*DEPTH	2	108.9908	54.4954
FLOW	3	8076.8279	2692.2760
INLET*FLOW	6	25153.1558	4192.1926
DEPTH*FLOW	3	8218.6612	2739.5537
INLET*DEPTH*FLOW	6	10947.1725	1824.5288
CORRECTED TOTAL	23	66271.2696	2881.3595

Table 7-Analysis of Variance, All Inlets, Pooled Error Terms

	Source	df	SSD	MS	Significance
t_i/T	INLET	2	0.0836	0.0418	***
	DEPTH	1	0.0081	0.0081	*
	ERROR	20	0.0386	0.001842	
t_p/T	INLET	2	0.3047	0.1523	***
	DEPTH	1	0.0401	0.0401	*
	ERROR	20	0.1642	0.00821	
$t_{\bar{m}}/T$	DEPTH	1	3.1974	3.1974	***
	ERROR	22	2.2211	0.101	
t_m/T	DEPTH	1	116.33	116.33	***
	ERROR	22	149.201	6.8	
t_σ/T	DEPTH	1	3416.	3416.	**
	ERROR	22	7949.	361.	
t_γ/T	DEPTH	1	10387.	10387.	*
	ERROR	22	55884.	2530.	

Table 8–Analysis of Variance, Baffled Inlets, t_i/T, t_p/T, and $t_{\bar{m}}/T$

ANALYSIS OF VARIANCE FOR VARIABLE TI — MEAN 0.181625000

SOURCE	DF	SUM OF SQUARES	MEAN SQUARE
INLET	1	0.0078322500	0.0078322500
DEPTH	1	0.0121000000	0.0121000000
INLET*DEPTH	1	0.0030250000	0.0030250000
FLOW	3	0.0039242500	0.0013080833
INLET*FLOW	3	0.0007942500	0.0002647500
DEPTH*FLOW	3	0.0154215000	0.0051405000
INLET*DEPTH*FLOW	3	0.0089765000	0.0029921667
CORRECTED TOTAL	15	0.0520737500	0.0034715833

ANALYSIS OF VARIANCE FOR VARIABLE TP — MEAN 0.317750000

SOURCE	DF	SUM OF SQUARES	MEAN SQUARE
INLET	1	0.064770250	0.0647702500
DEPTH	1	0.050400250	0.0504002500
INLET*DEPTH	1	0.005041000	0.0050410000
FLOW	3	0.008569500	0.0028565000
INLET*FLOW	3	0.017291250	0.0057637500
DEPTH*FLOW	3	0.074771250	0.0249237500
INLET*DEPTH*FLOW	3	0.041483500	0.0138278333
CORRECTED TOTAL	15	0.262327000	0.0174884667

ANALYSIS OF VARIANCE FOR VARIABLE TMO — MEAN 1.97625000

SOURCE	DF	SUM OF SQUARES	MEAN SQUARE
INLET	1	0.01322500	0.01322500
DEPTH	1	3.18622500	3.18622500
INLET*DEPTH	1	0.03802500	0.03802500
FLOW	3	0.53722500	0.17907500
INLET*FLOW	3	0.09922500	0.03307500
DEPTH*FLOW	3	0.17212500	0.05737500
INLET*DEPTH*FLOW	3	0.44932500	0.14977500
CORRECTED TOTAL	15	4.49537500	0.29969167

Table 9-Analysis of Variance, Baffled Inlets, t_m/T, t_σ/T and t_γ/T

ANALYSIS OF VARIANCE FOR VARIABLE TME MEAN 6.73500000

SOURCE	DF	SUM OF SQUARES	MEAN SQUARE
INLET	1	11.289600	11.2896000
DEPTH	1	99.500625	99.5006250
INLET*DEPTH	1	0.455625	0.4556250
FLOW	3	50.297550	16.7658500
INLET*FLOW	3	13.417850	4.4726167
DEPTH*FLOW	3	18.072725	6.0242417
INLET*DEPTH*FLOW	3	3.999225	1.3330750
CORRECTED TOTAL	15	197.033200	13.1355467

ANALYSIS OF VARIANCE FOR VARIABLE SIG MEAN 25.5900000

SOURCE	DF	SUM OF SQUARES	MEAN SQUARE
INLET	1	543.35610	543.35610
DEPTH	1	2845.15560	2845.15560
INLET*DEPTH	1	40.83210	40.83210
FLOW	3	2682.59180	894.19727
INLET*FLOW	3	694.94530	231.64843
DEPTH*FLOW	3	1026.30580	342.10193
INLET*DEPTH*FLOW	3	172.48930	57.49643
CORRECTED TOTAL	15	8005.67600	533.71173

ANALYSIS OF VARIANCE FOR VARIABLE SKE MEAN 55.7937500

SOURCE	DF	SUM OF SQUARES	MEAN SQUARE
INLET	1	2225.4806	2225.48062
DEPTH	1	7889.8806	7889.88062
INLET*DEPTH	1	14.6306	14.63063
FLOW	3	19924.0419	6641.34729
INLET*FLOW	3	6397.9419	2132.64729
DEPTH*FLOW	3	5762.8419	1920.94729
INLET*DEPTH*FLOW	3	864.9919	288.33063
CORRECTED TOTAL	15	43079.8094	2871.98729

Table 10-Analysis of Variance, Baffled Inlets, Pooled Error Terms

	Source	df	SS	MS	Significance
T_i/T	DEPTH	1	0.0121	0.0121	*
	ERROR	14	0.03997	0.00285	
t_p/T	INLET	1	0.06477	0.0647	*
	ERROR	14	0.1975	0.0141	
$t_{\bar{m}}/T$	DEPTH	1	3.186	3.886	***
	ERROR	14	1.309	0.0935	
t_m/T	INLET	1	11.29	11.28	*
	DEPTH	1	99.50	99.55	***
	FLOW	3	50.29	16.8	*
	ERROR	10	25.94	2.594	
t_σ/T	INLET	1	543.4	543.356	*
	DEPTH	1	2845.1	2845.156	**
	FLOW	3	2682.6	894.198	*
	DEPTH * FLOW	3	1026.3	342.00	
	ERROR	7	908.2	129.8	
t_γ/T	INLET	1	2225.	2225.	*
	DEPTH	1	7889.	7889.	**
	FLOW	3	19924.	6641.	**
	INLET * FLOW	3	6397.	2132.	*
	DEPTH * FLOW	3	5762.	1920.	*
	ERROR	4	879.6	214.9	

APPENDIX V

Model Dispersion Curves

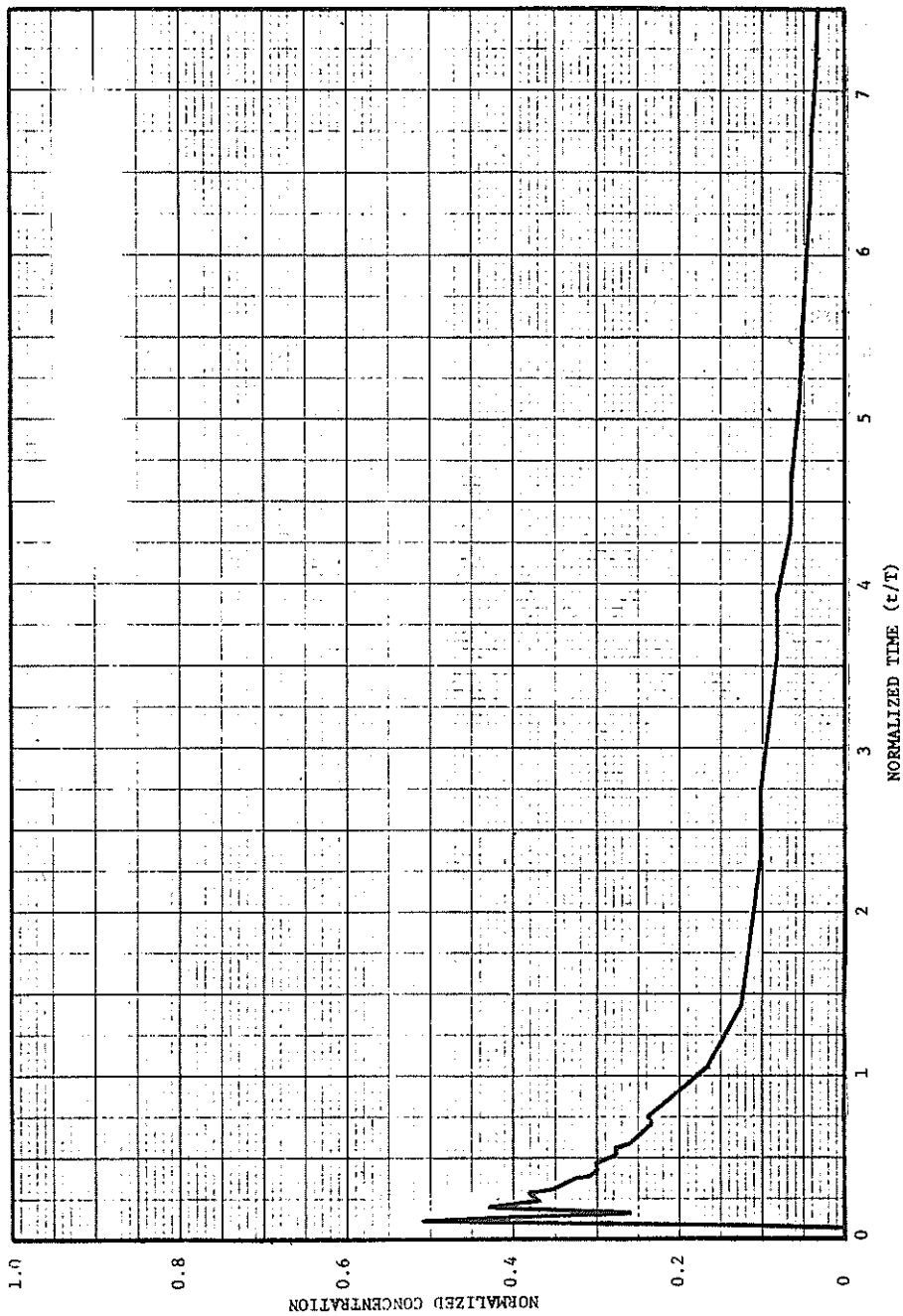

Figure 25-Dispersion Curve - 12 in., Plain 450 gal/min

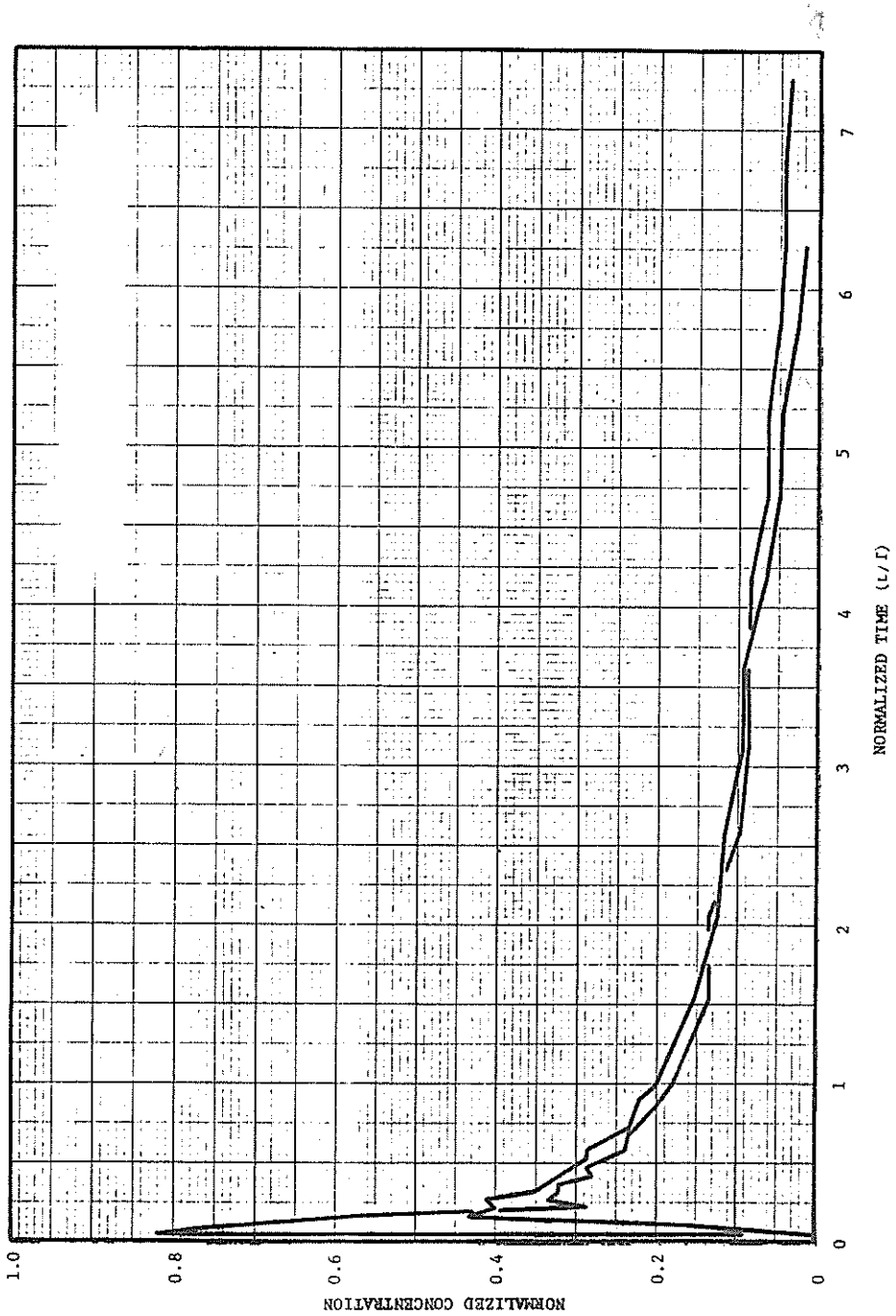

Figure 26-Dispersion Curve - 12 in., Plain 600 gal/min

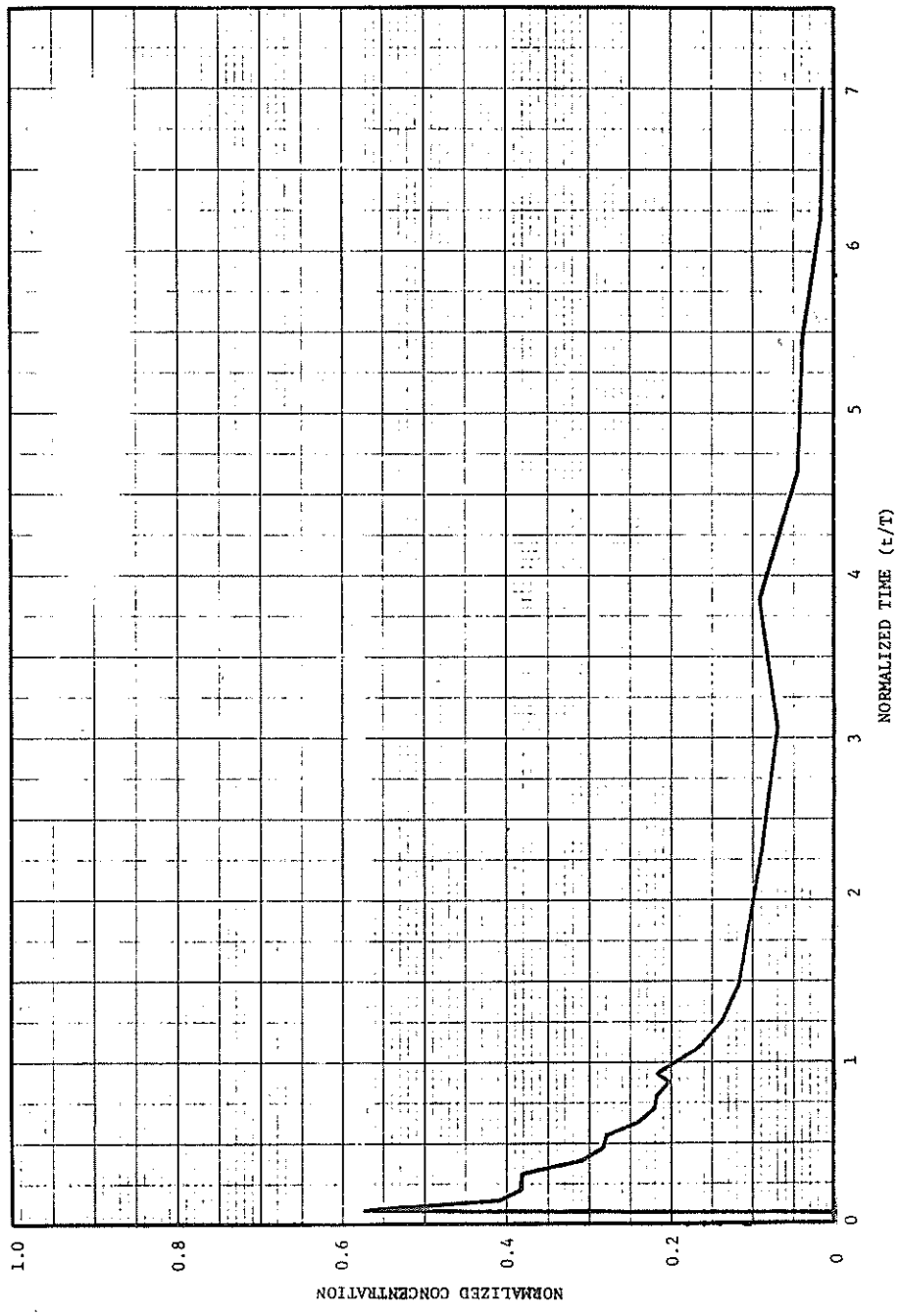

Figure 27-Dispersion Curve - 12 in., Plain 900 gal/min

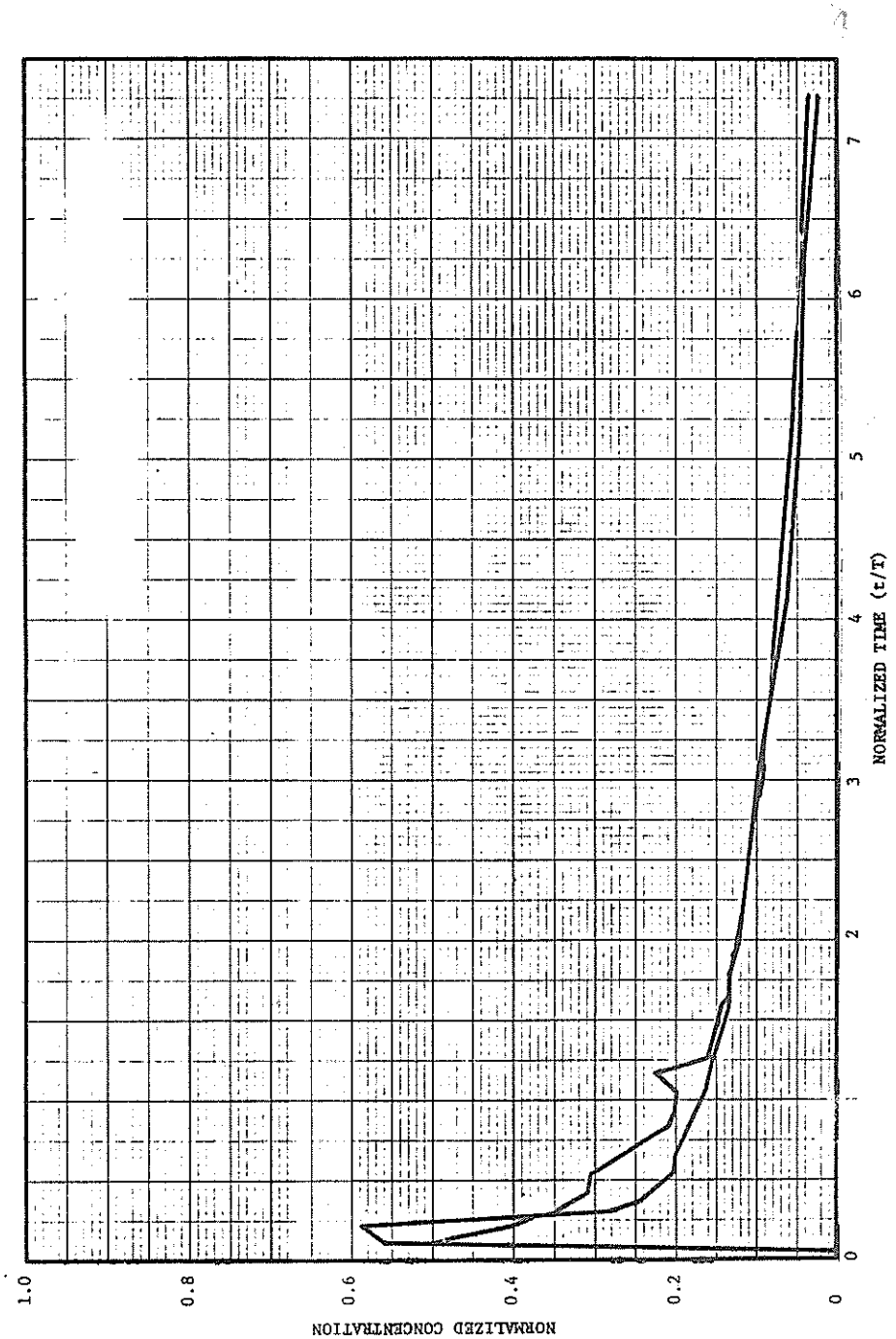

Figure 28-Dispersion Curve - 12 in., Plain 1200 gal/min

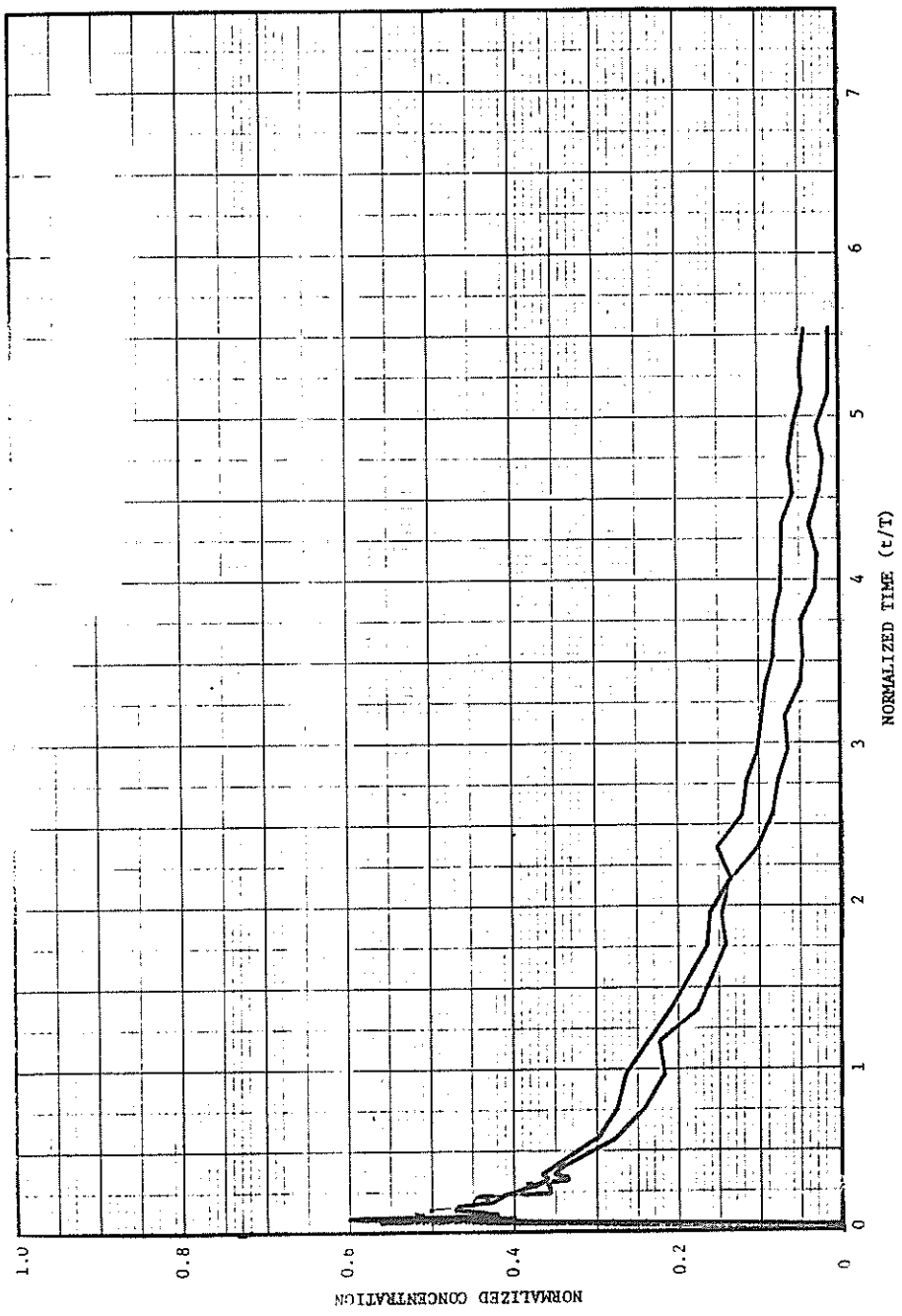

Figure 29-Dispersion Curve - 24 in., Plain 450 gal/min

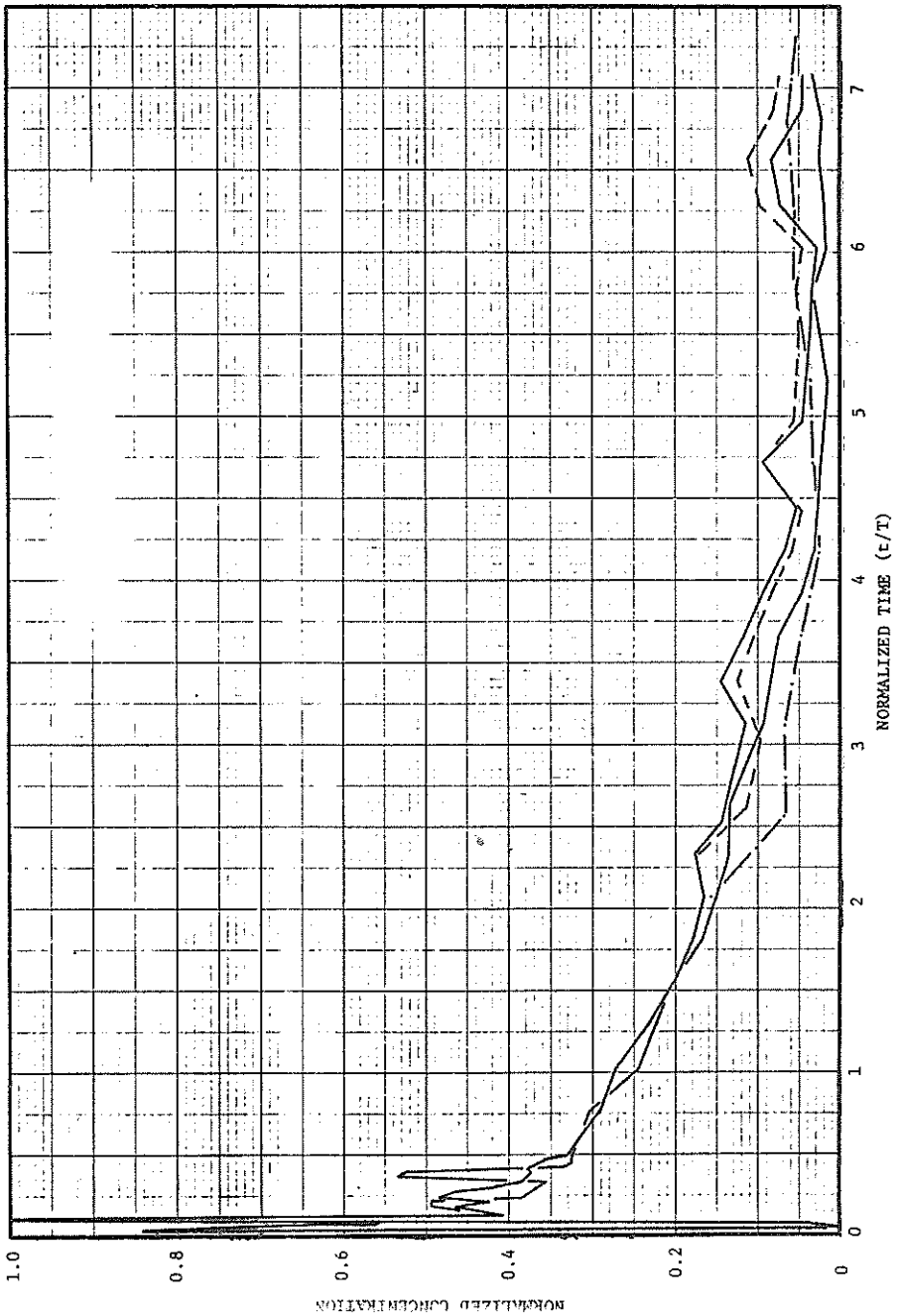

Figure 30-Dispersion Curve - 24 in., Plain 600 gal/min

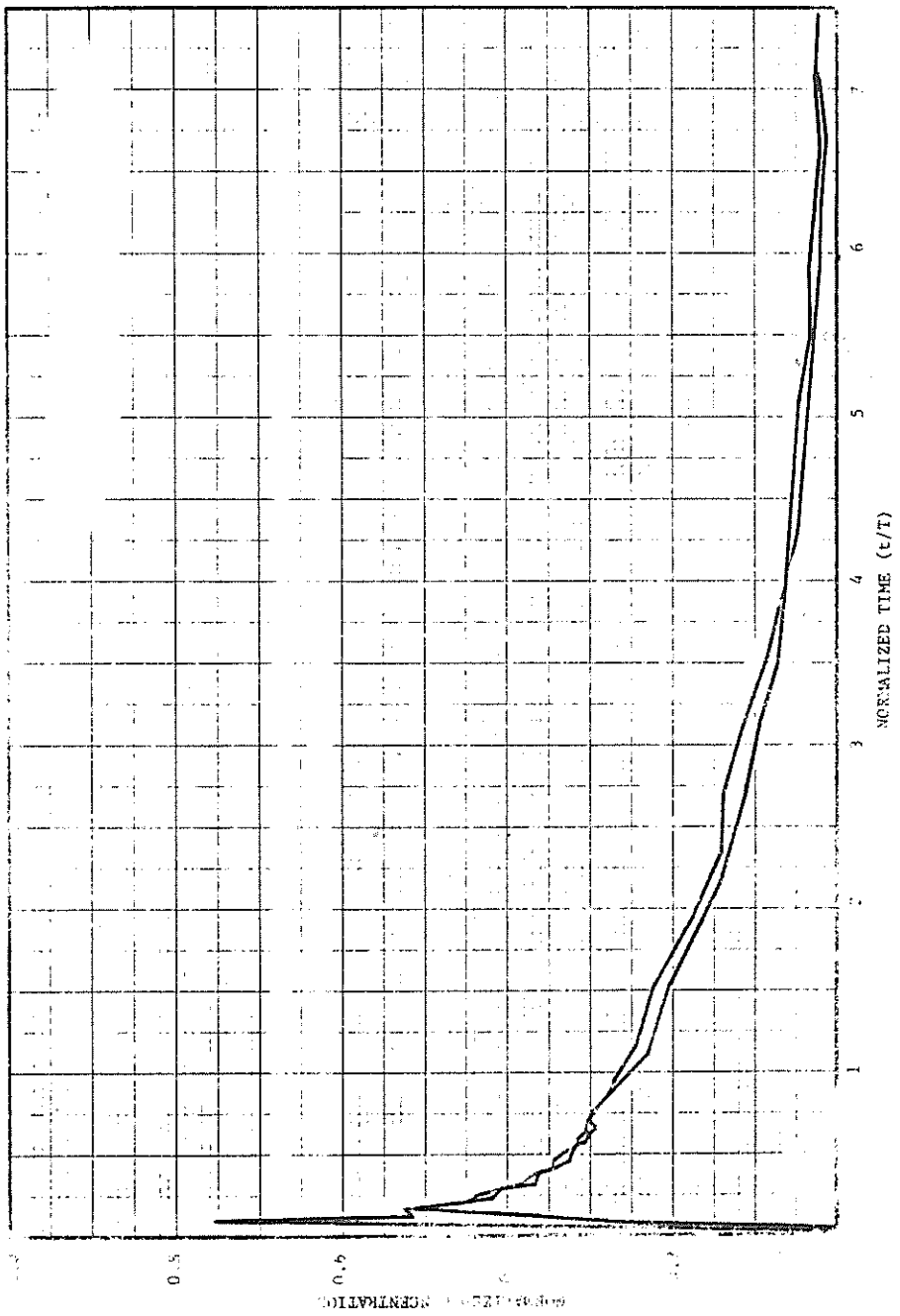

Figure 31-Dispersion Curve - 24 in., Plain 900 gal/min

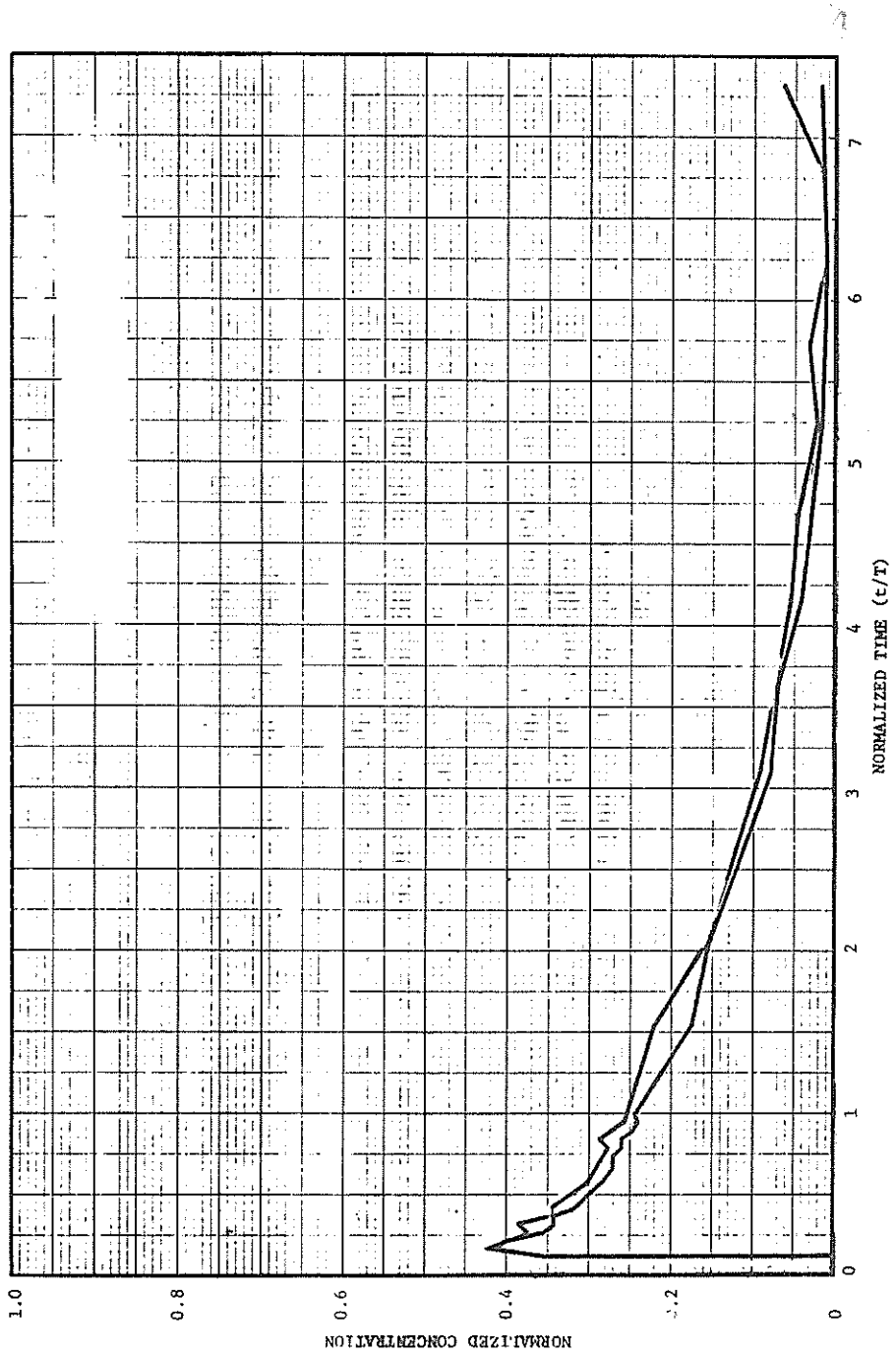

Figure 32-Dispersion Curve - 24 in., Plain 1200 gal/min

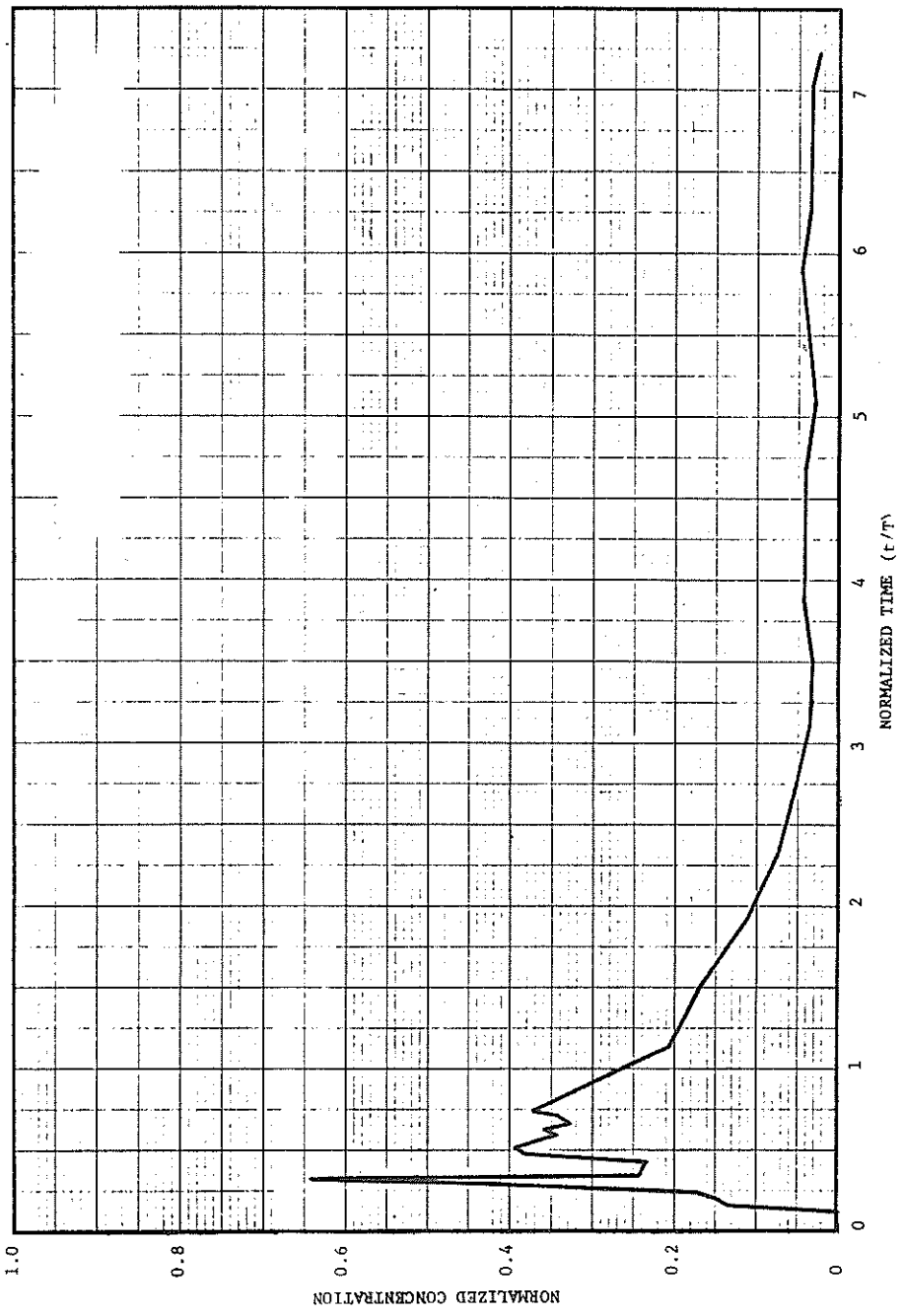

Figure 33-Dispersion Curve - 12 in., 1 Baffle 450 gal/min

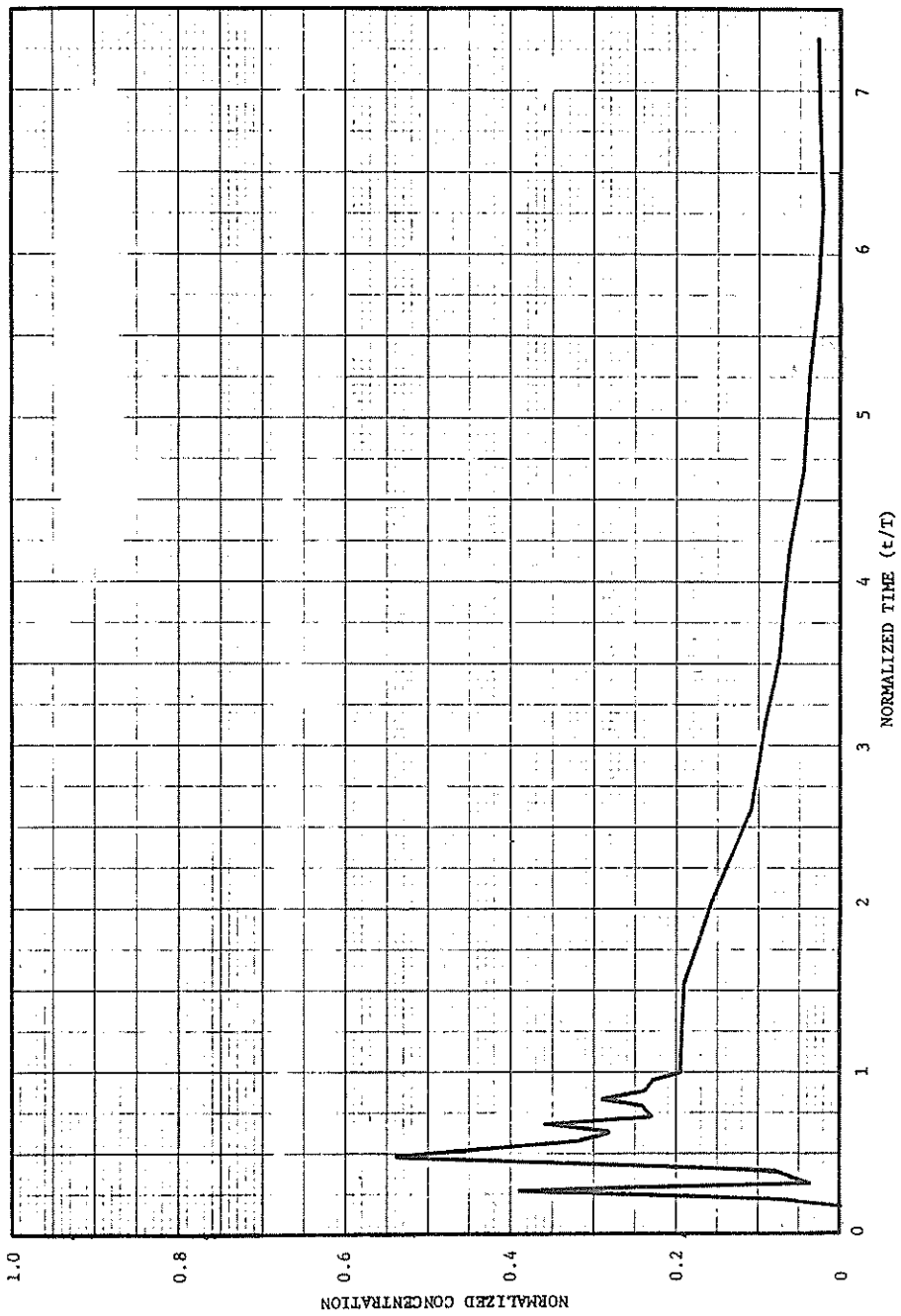

Figure 34-Dispersion Curve - 12 in., 1 Baffle 600 gal/min

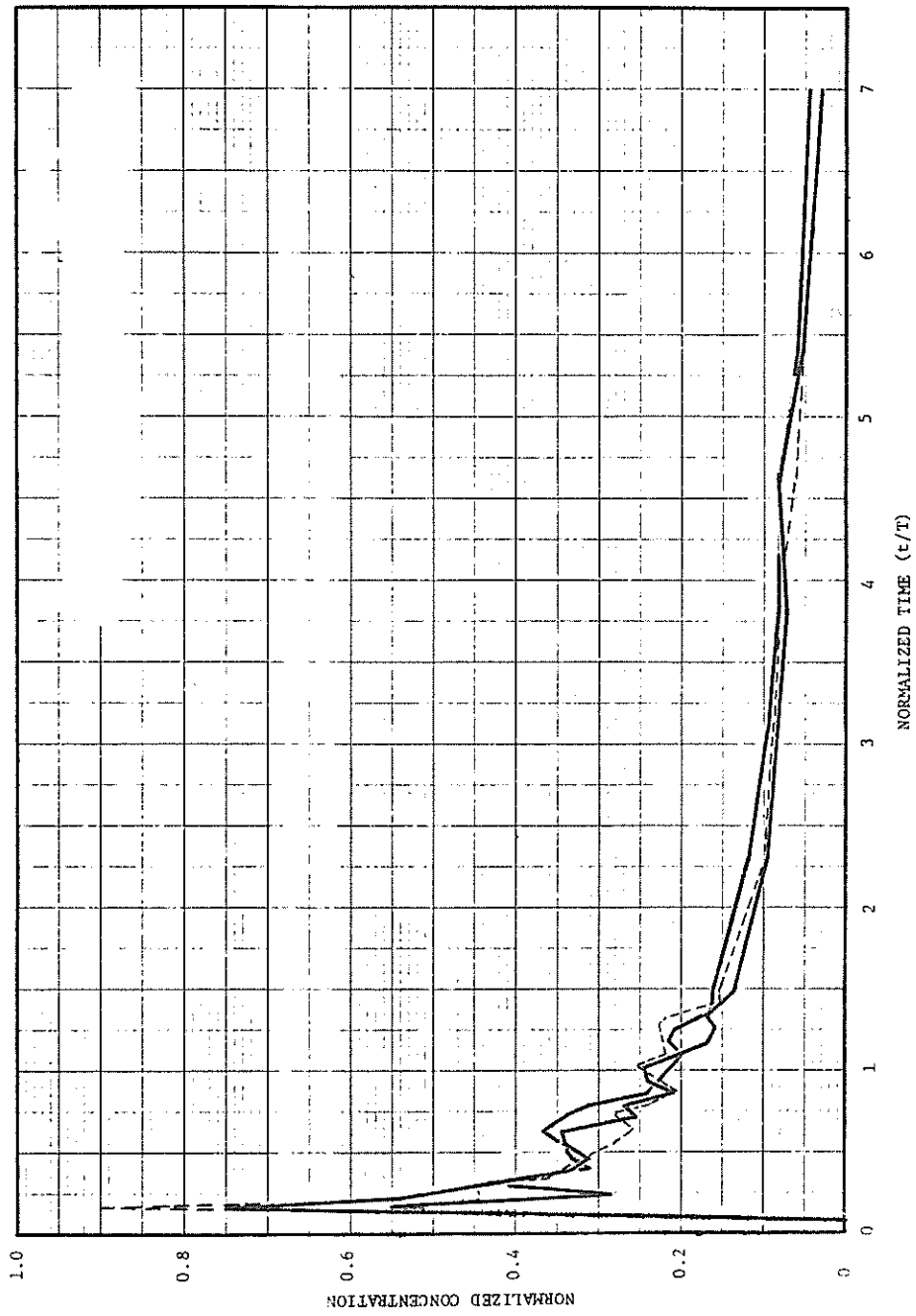

Figure 35-Dispersion Curve - 12 in., 1 Baffle 900 gal/min

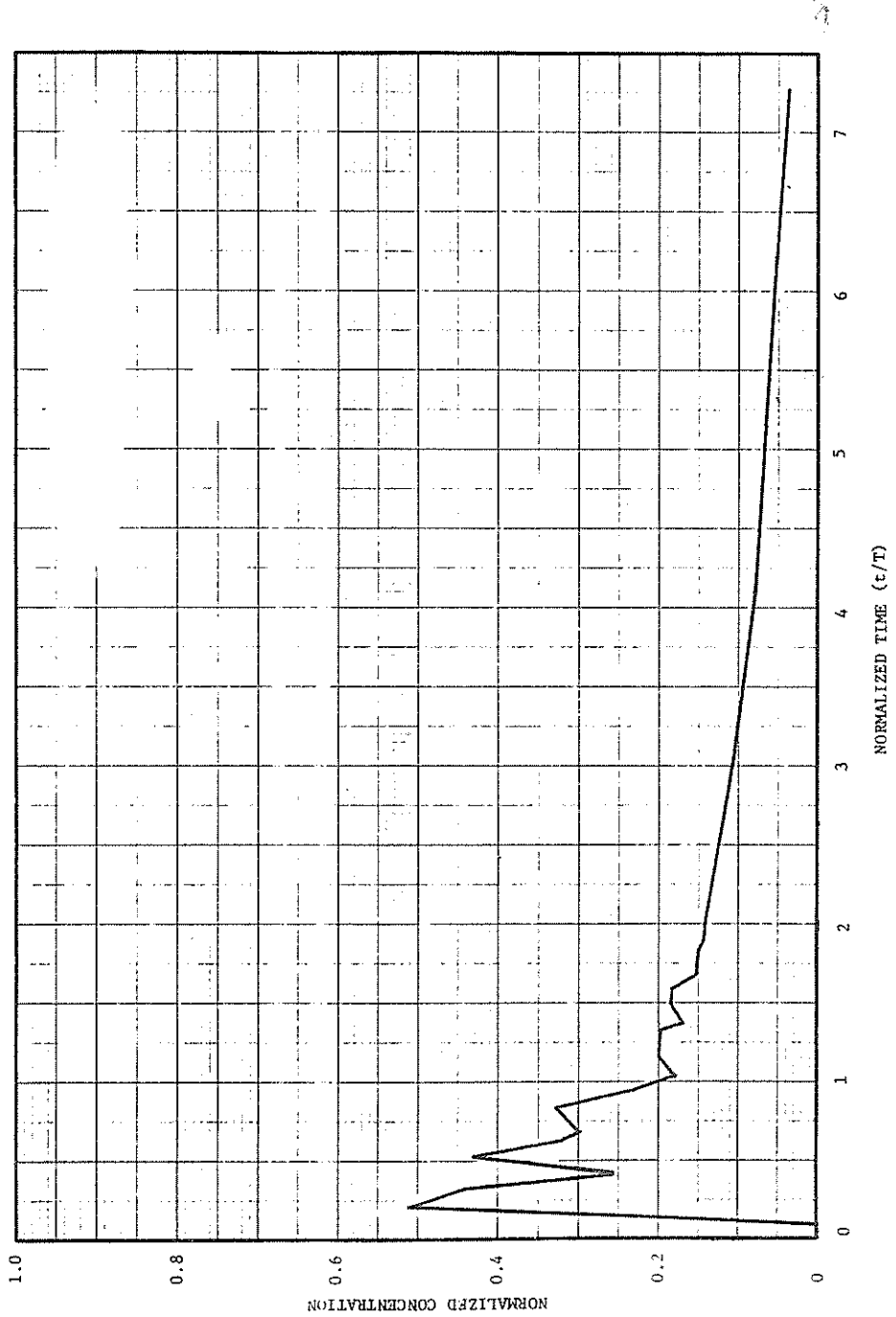

Figure 36-Dispersion Curve - 12 in., 1 Baffle 1200 gal/min

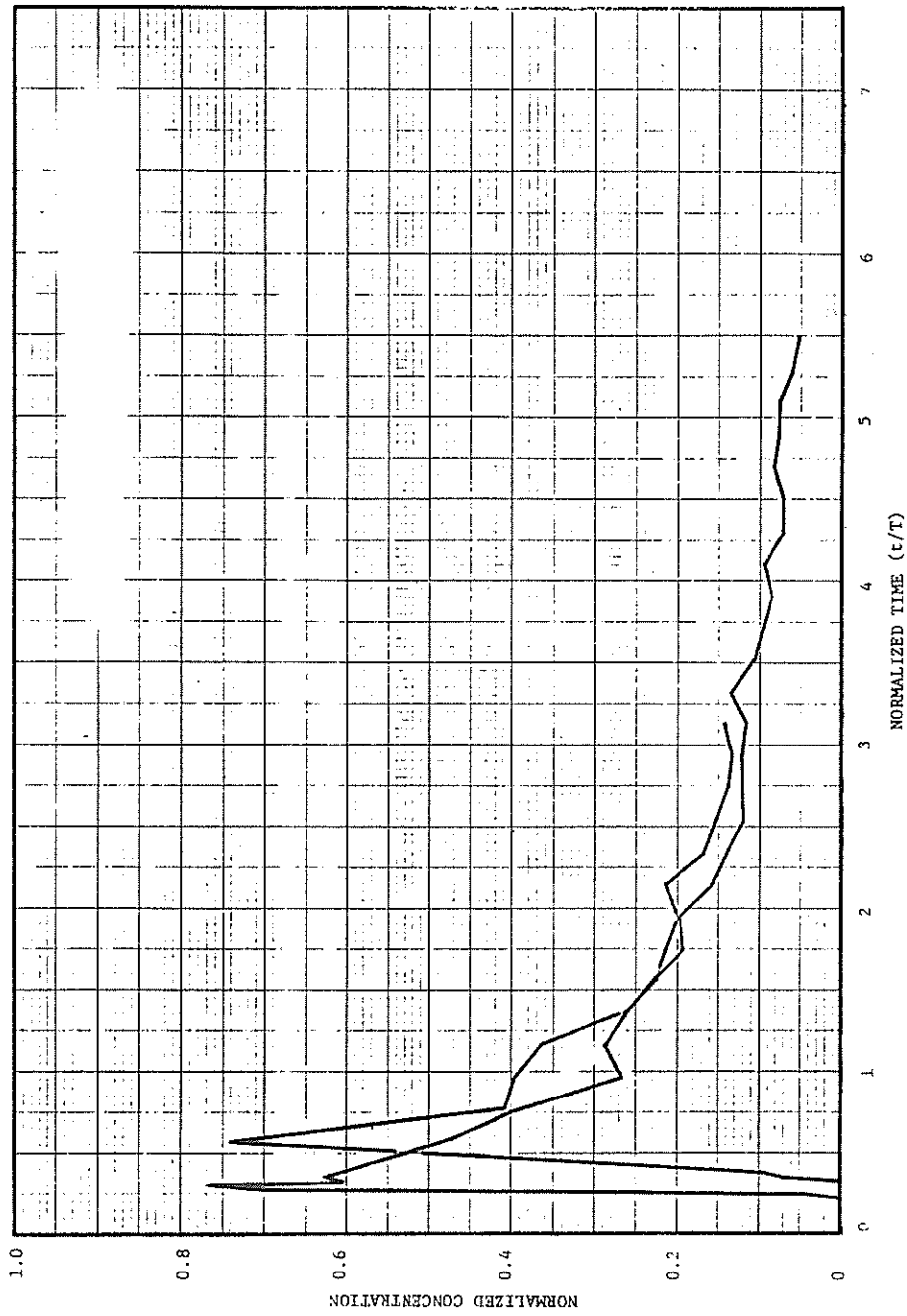

Figure 37-Dispersion Curve - 24 in., 1 Baffle 450 gal/min

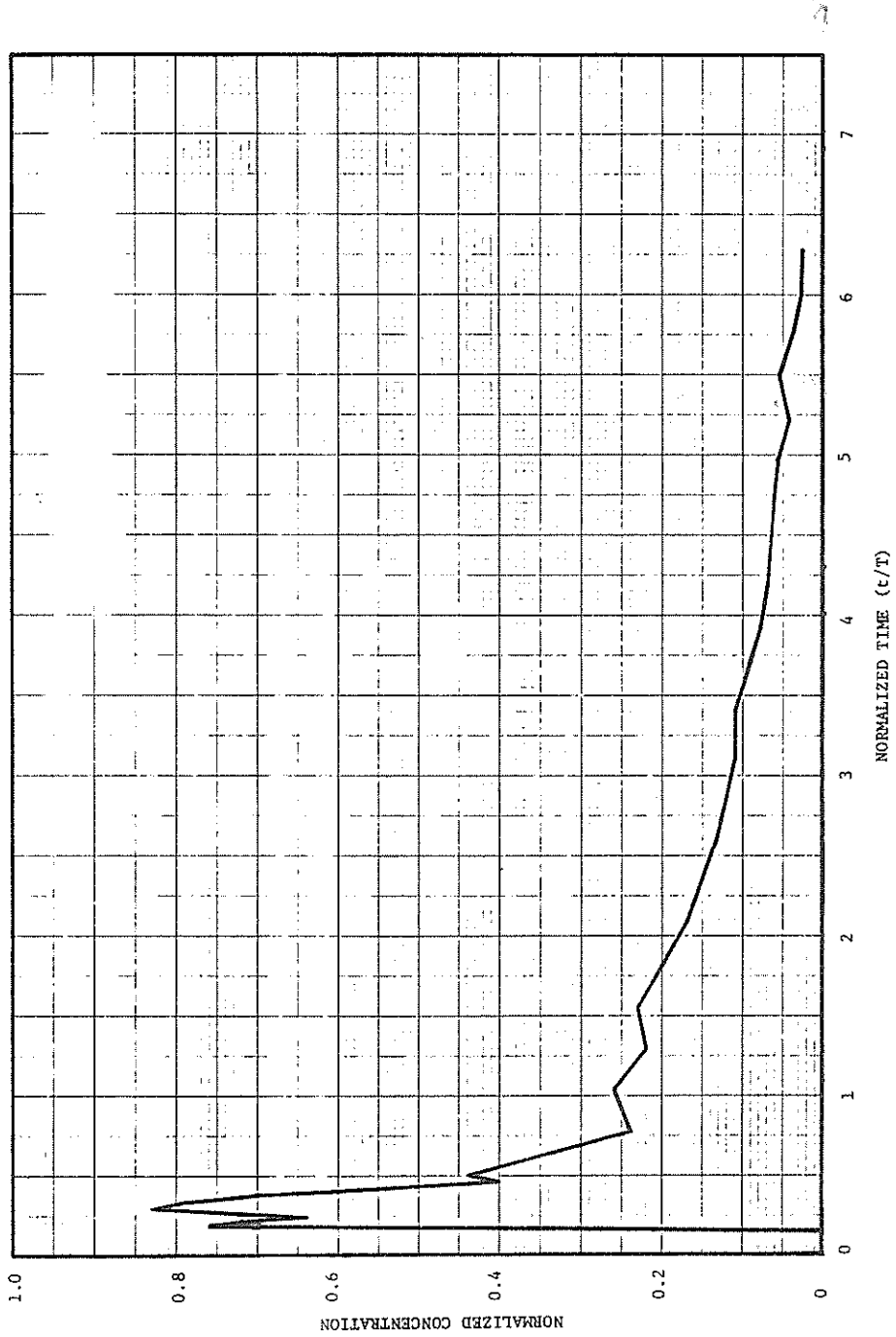

Figure 38. Dispersion Curve - 24 in., 1 Baffle 600 gal/min

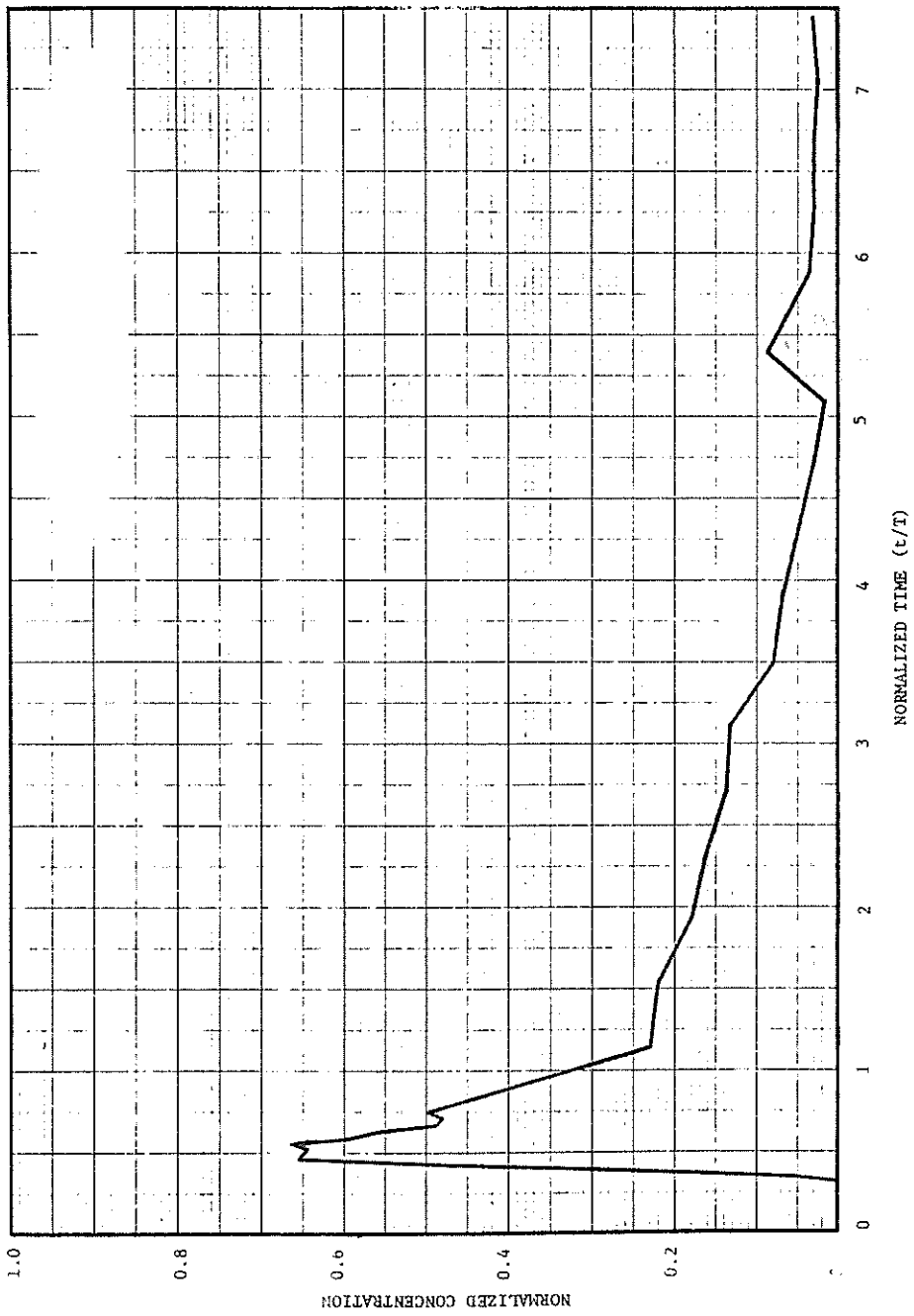

Figure 39-Dispersion Curve - 24 in., 1 Baffle 900 gal/min

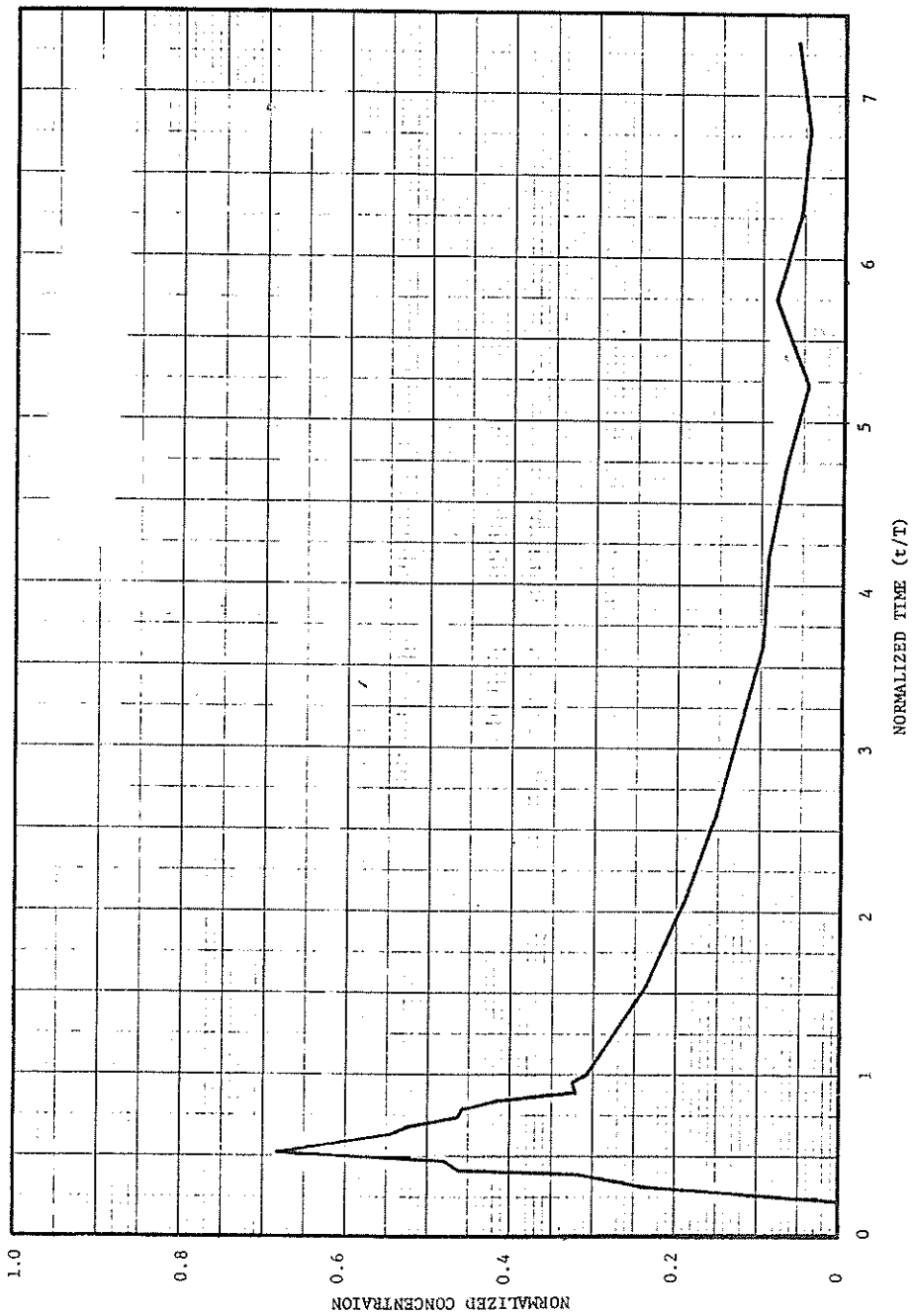

Figure 40-Dispersion Curve - 24 in., 1 Baffle 1200 gal/min

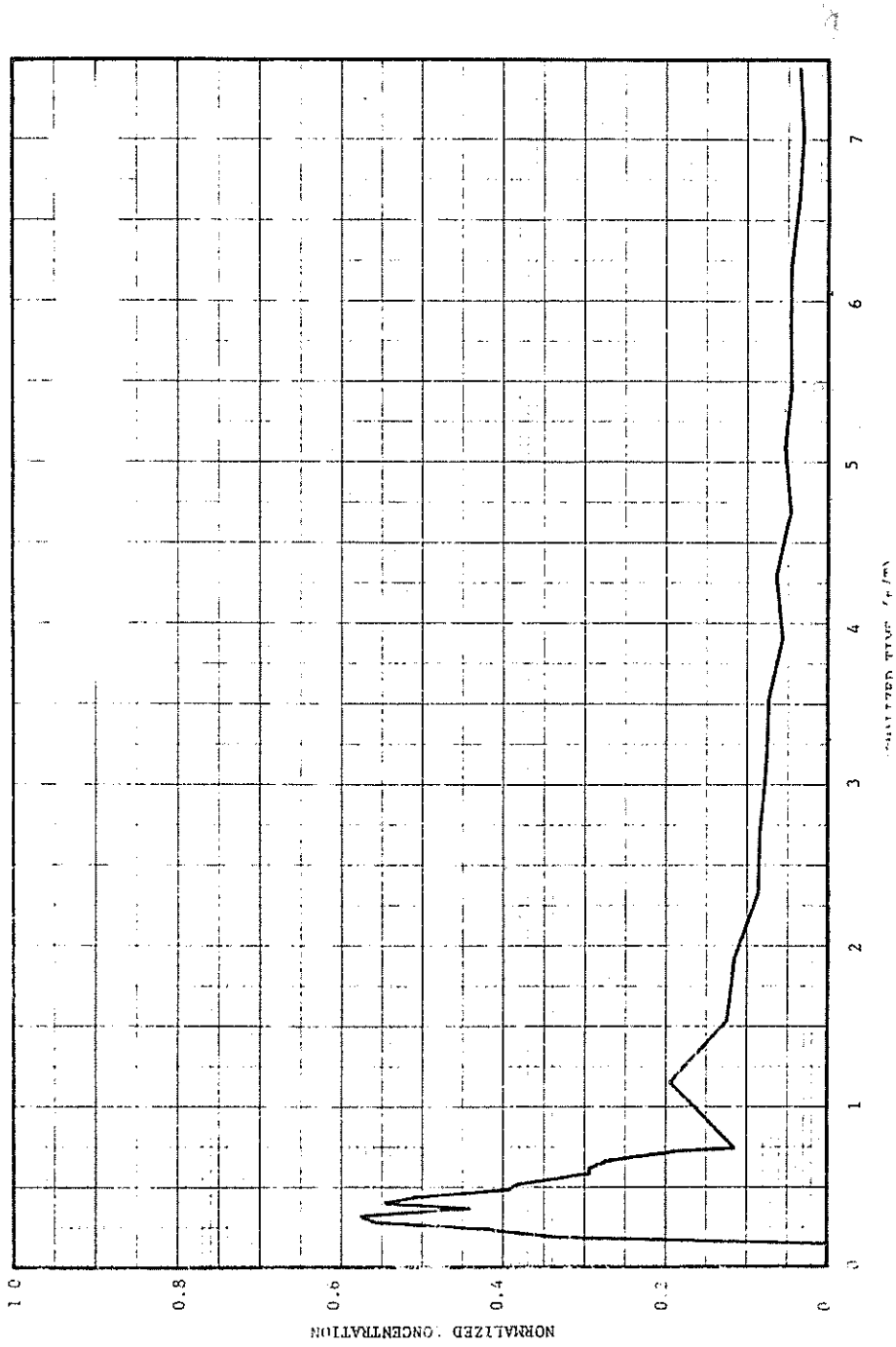

Figure 41-Dispersion Curve - 12 in., 3 Baffles 450 gal/min

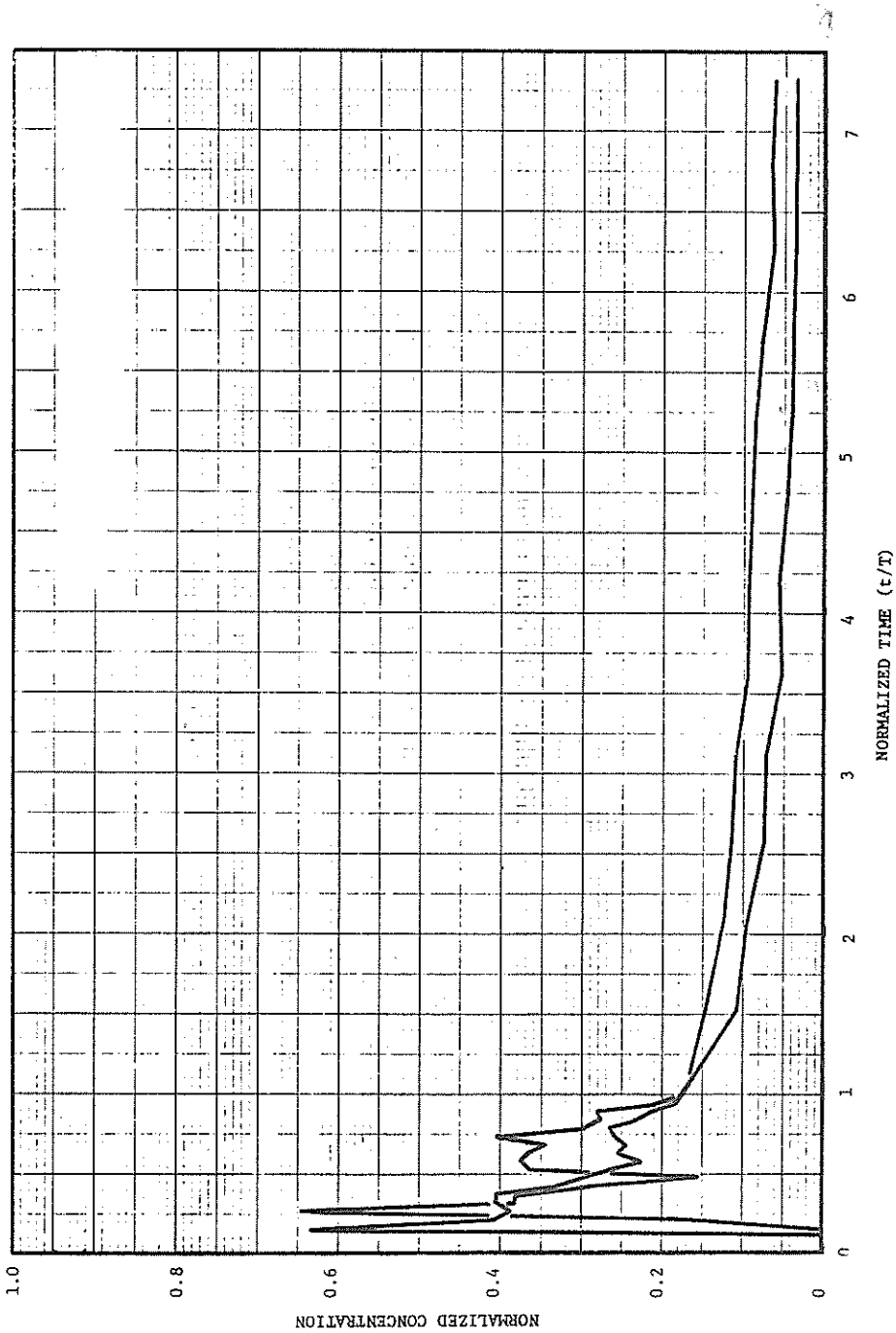

Figure 42-Dispersion Curve - 12 in., 3 Baffles 600 gal/min

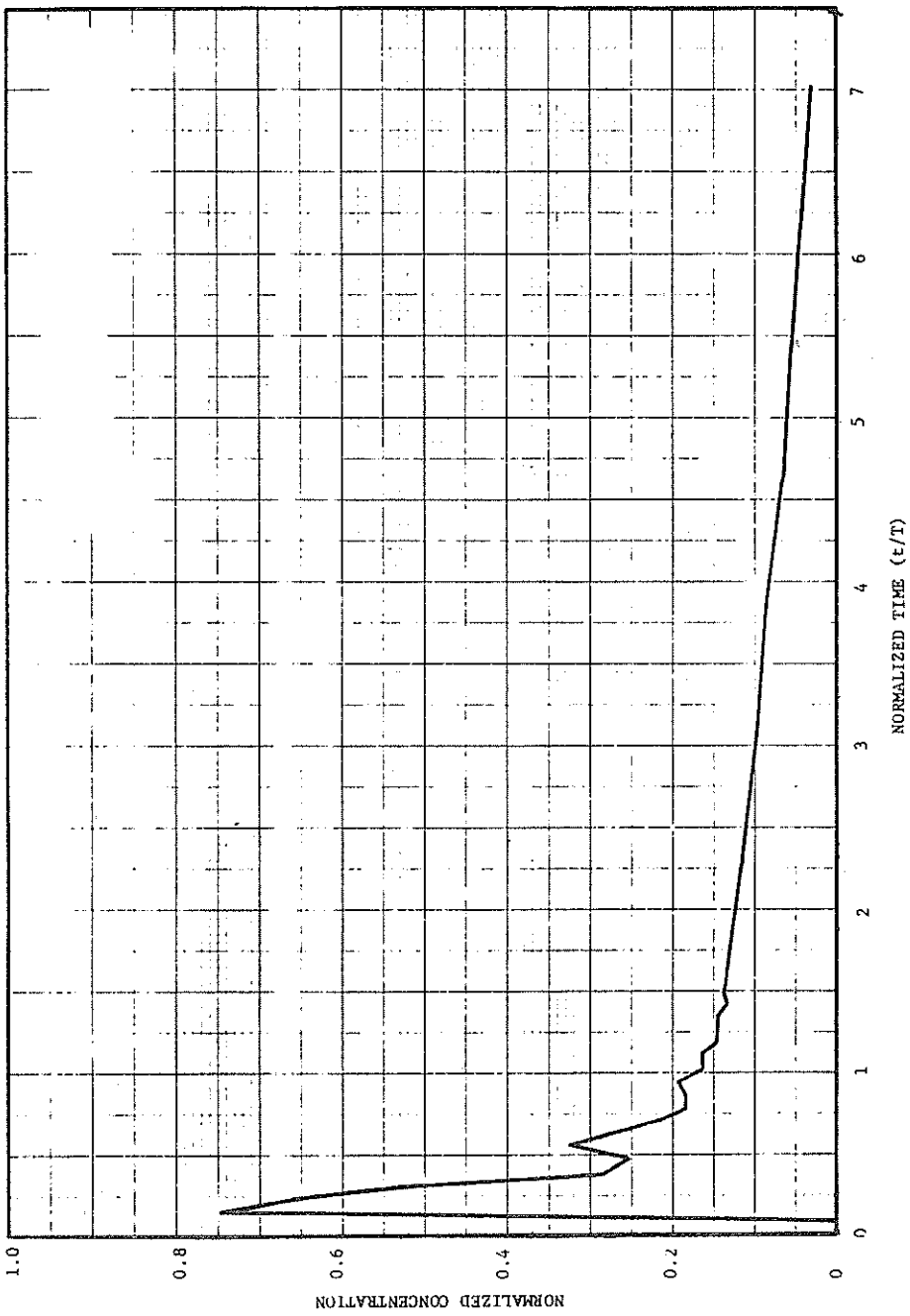

Figure 43-Dispersion Curve - 12 in., 3 Baffles 900 gal/min

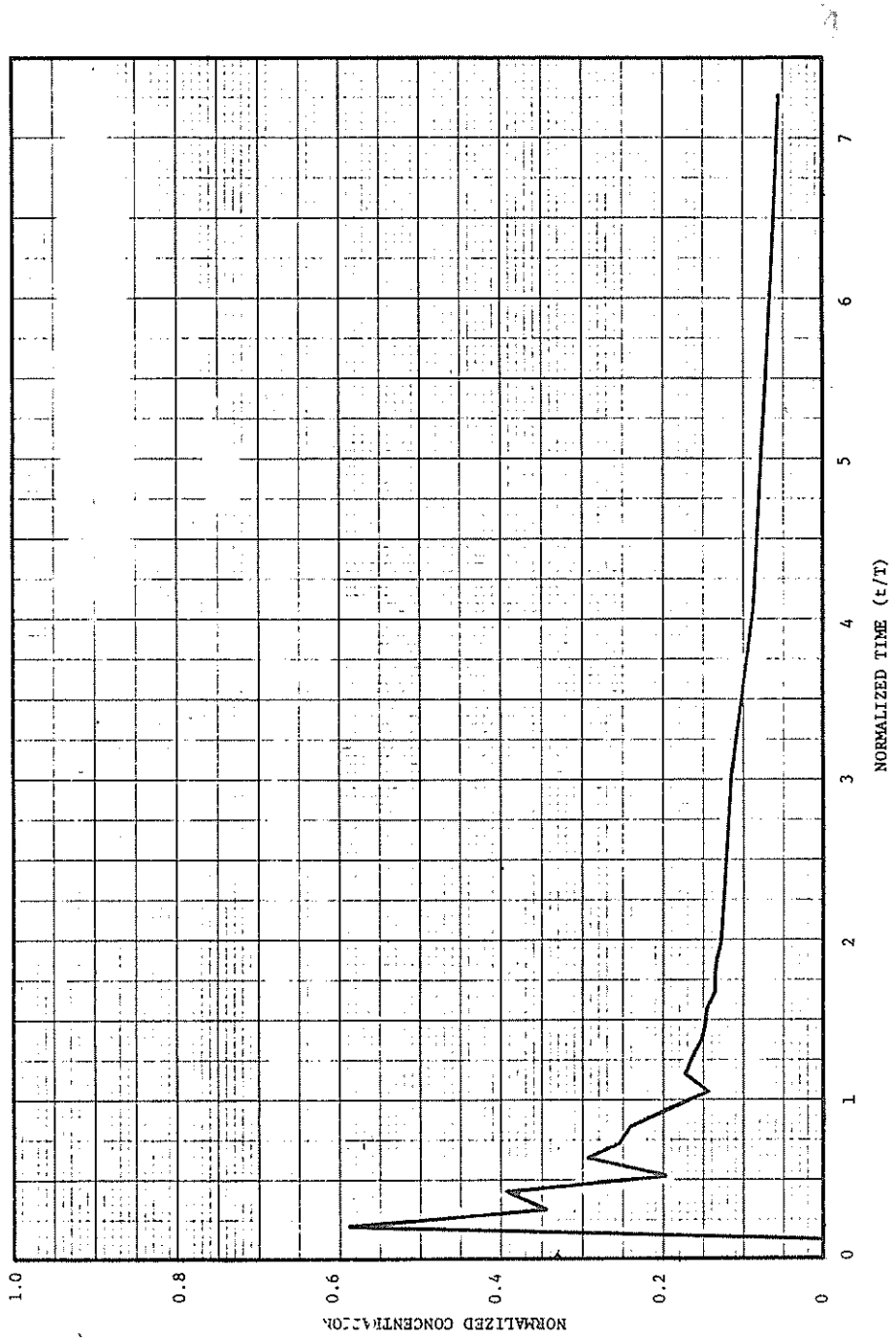

Figure 44-Dispersion Curve - 12 in., 3 Baffles 1200 gal/min

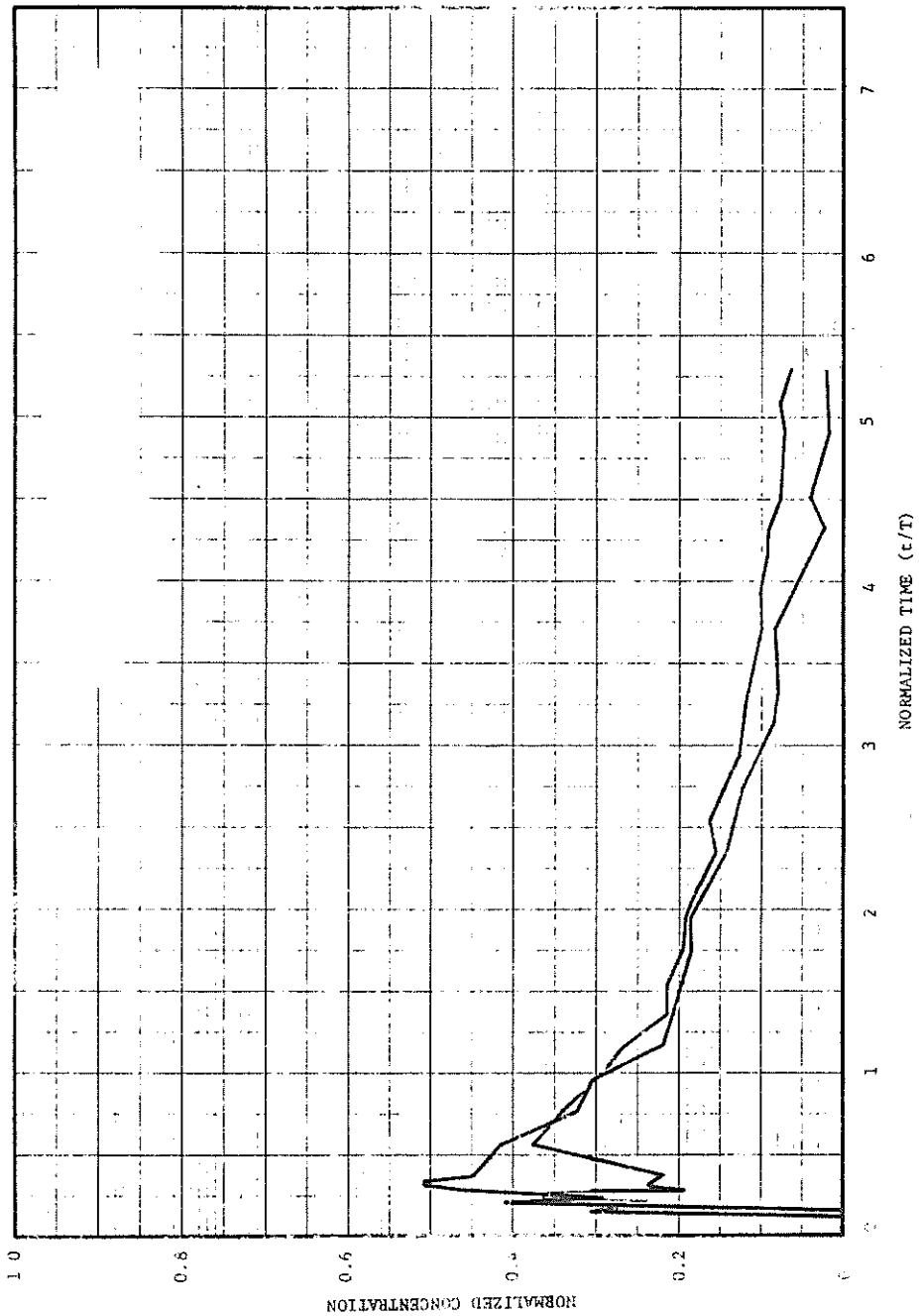

Figure 45-Dispersion Curve - 24 in., 3 Baffles 450 gal/min

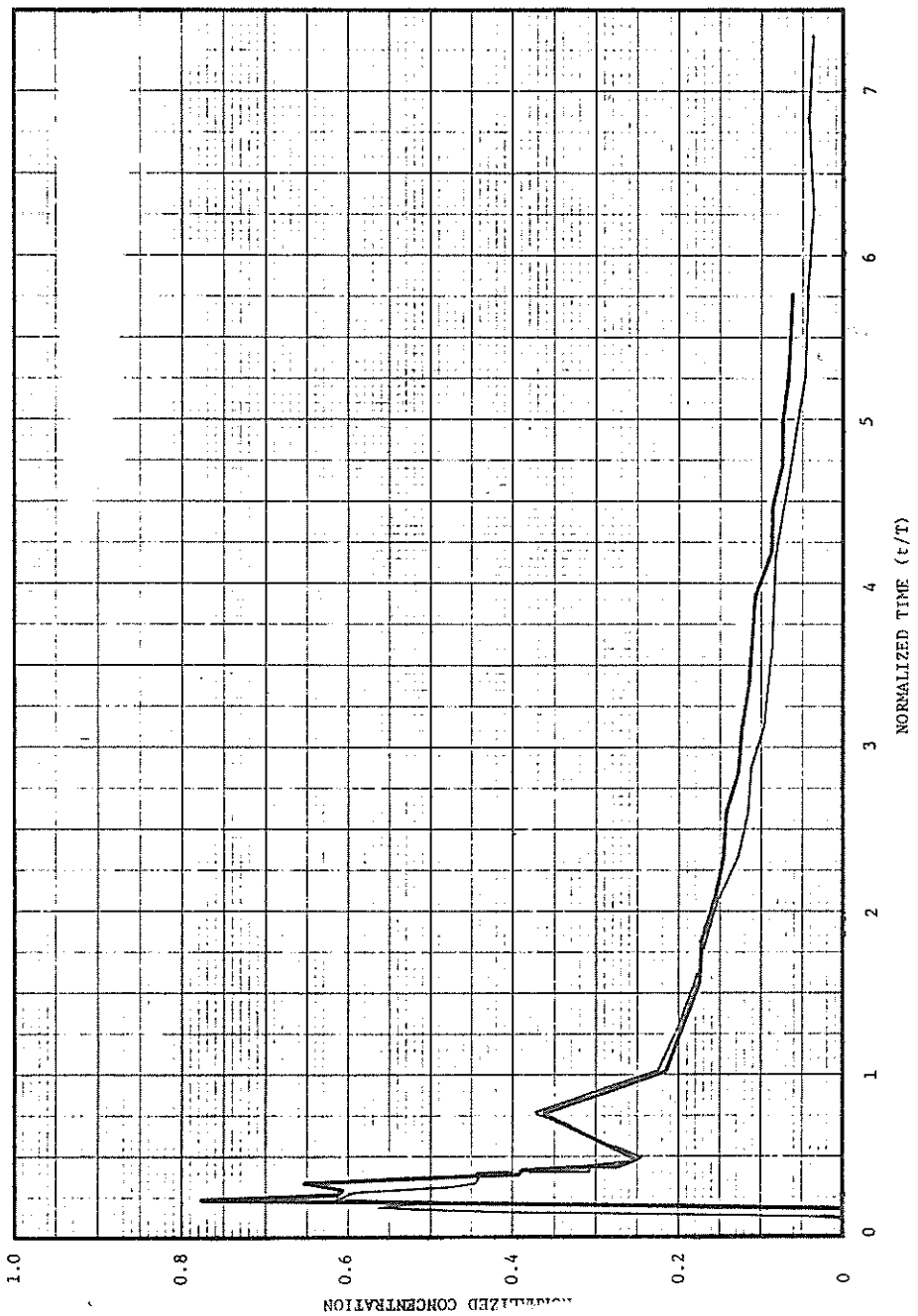

Figure 46-Dispersion Curve - 24 in., 3 Baffles 600 gal/min

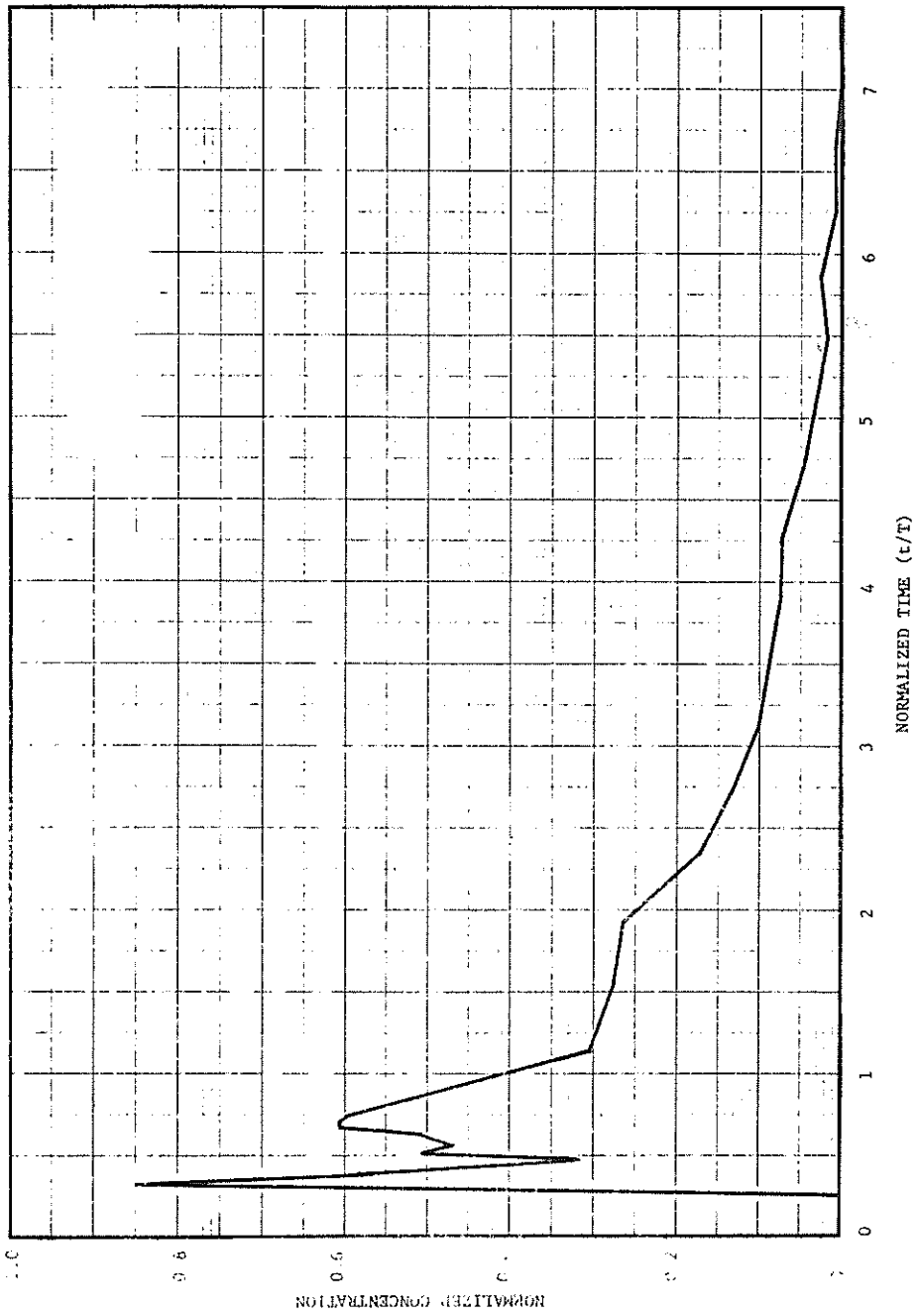

Figure 47-Dispersion Curve - 24 in., 3 Baffles 900 gal/min

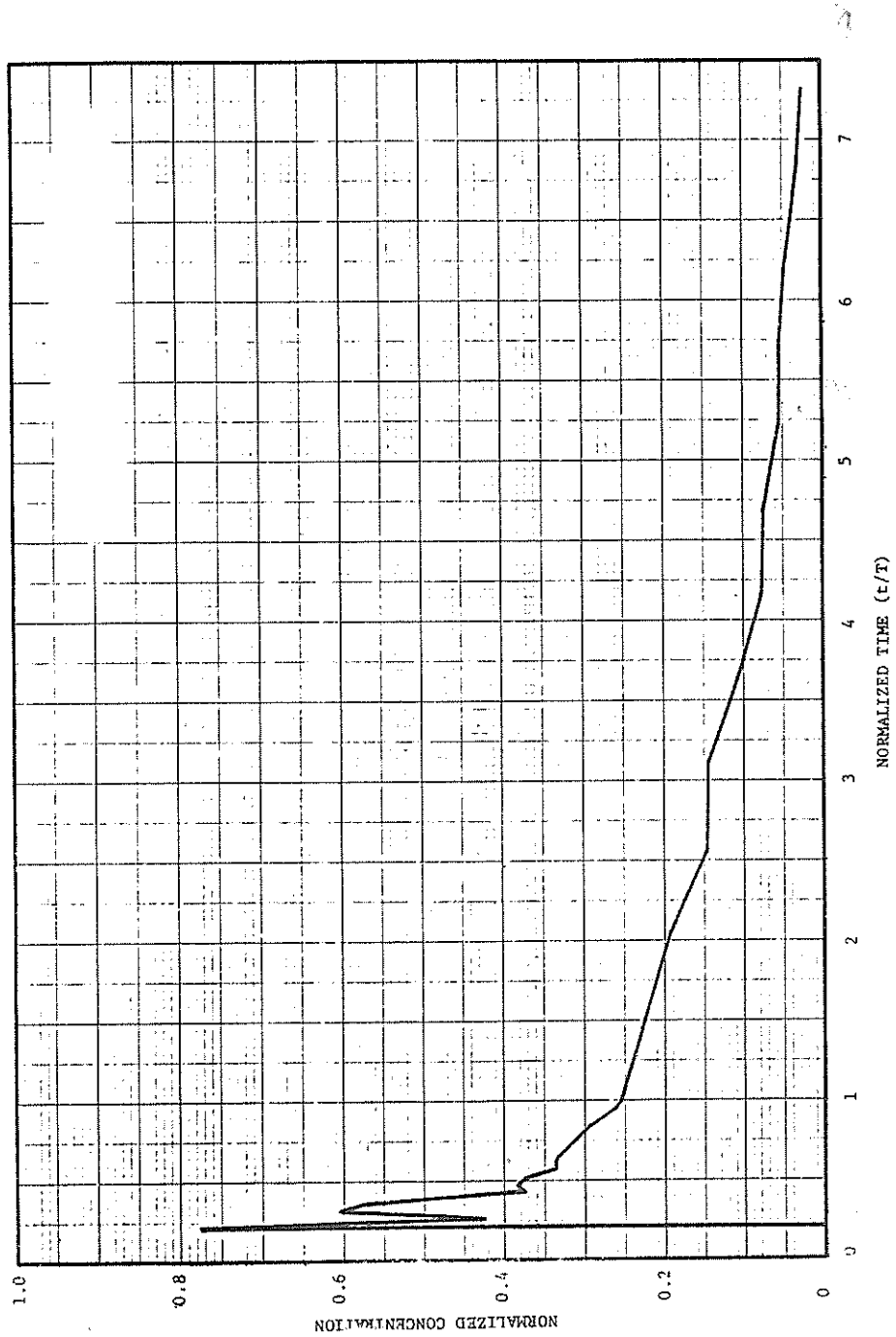

Figure 48-Dispersion Curve - 24 in., 3 Baffles 1200 gal/min

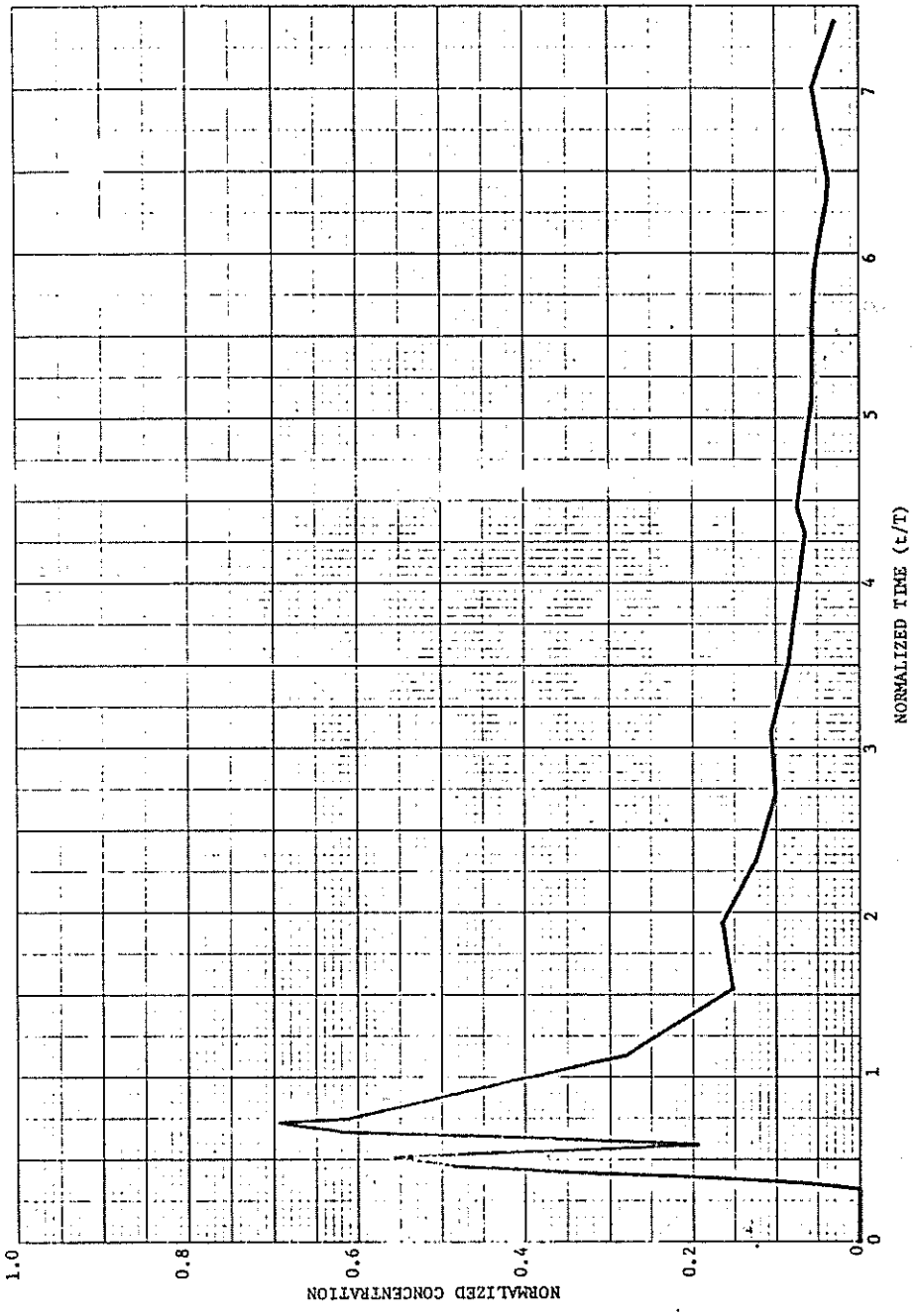

Figure 49. Dispersion Curve - 12 in., Baffle Box 450 gal/min

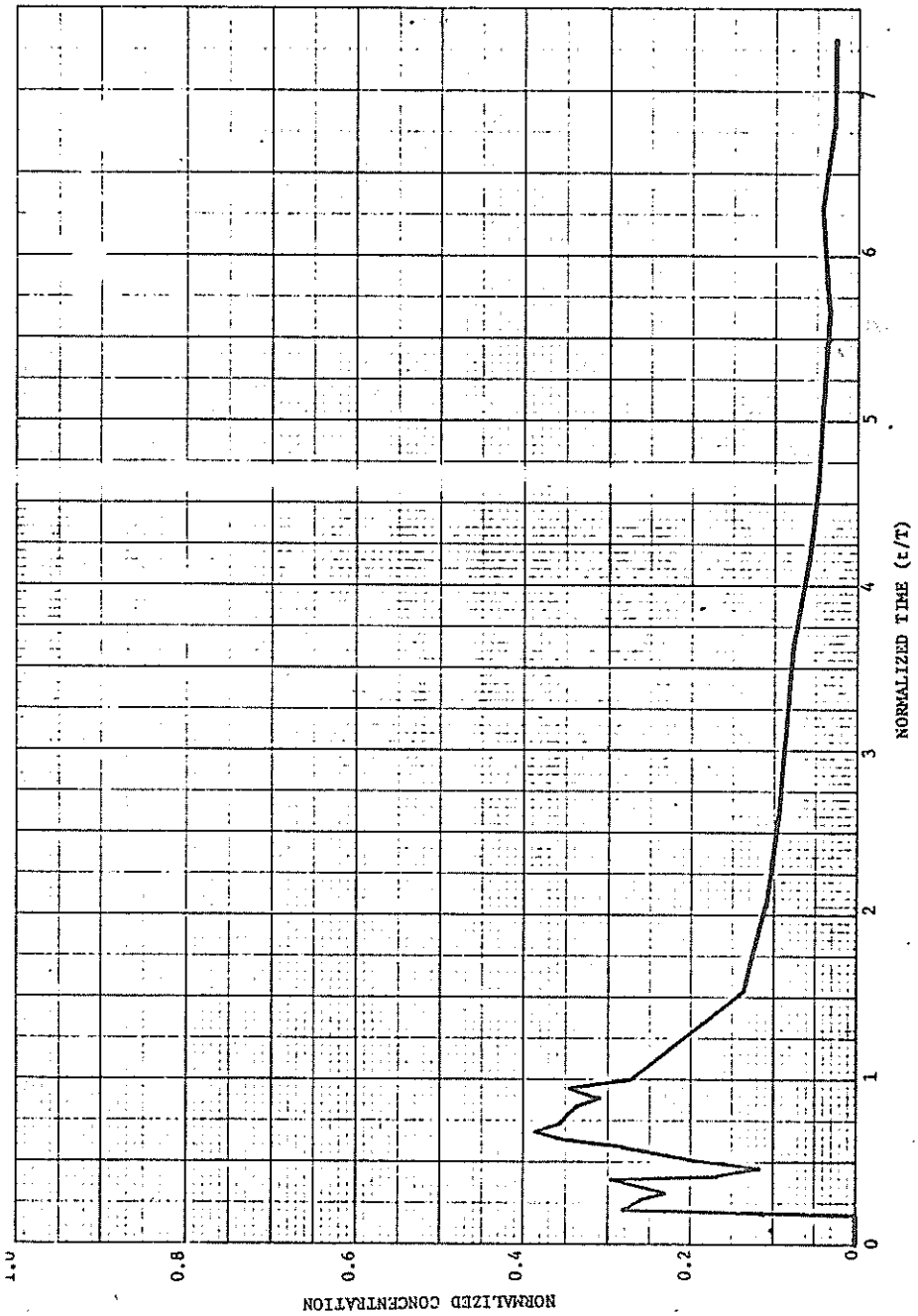

Figure 50. Dispersion Curve - 12 in., Baffle Box 600 gal/min

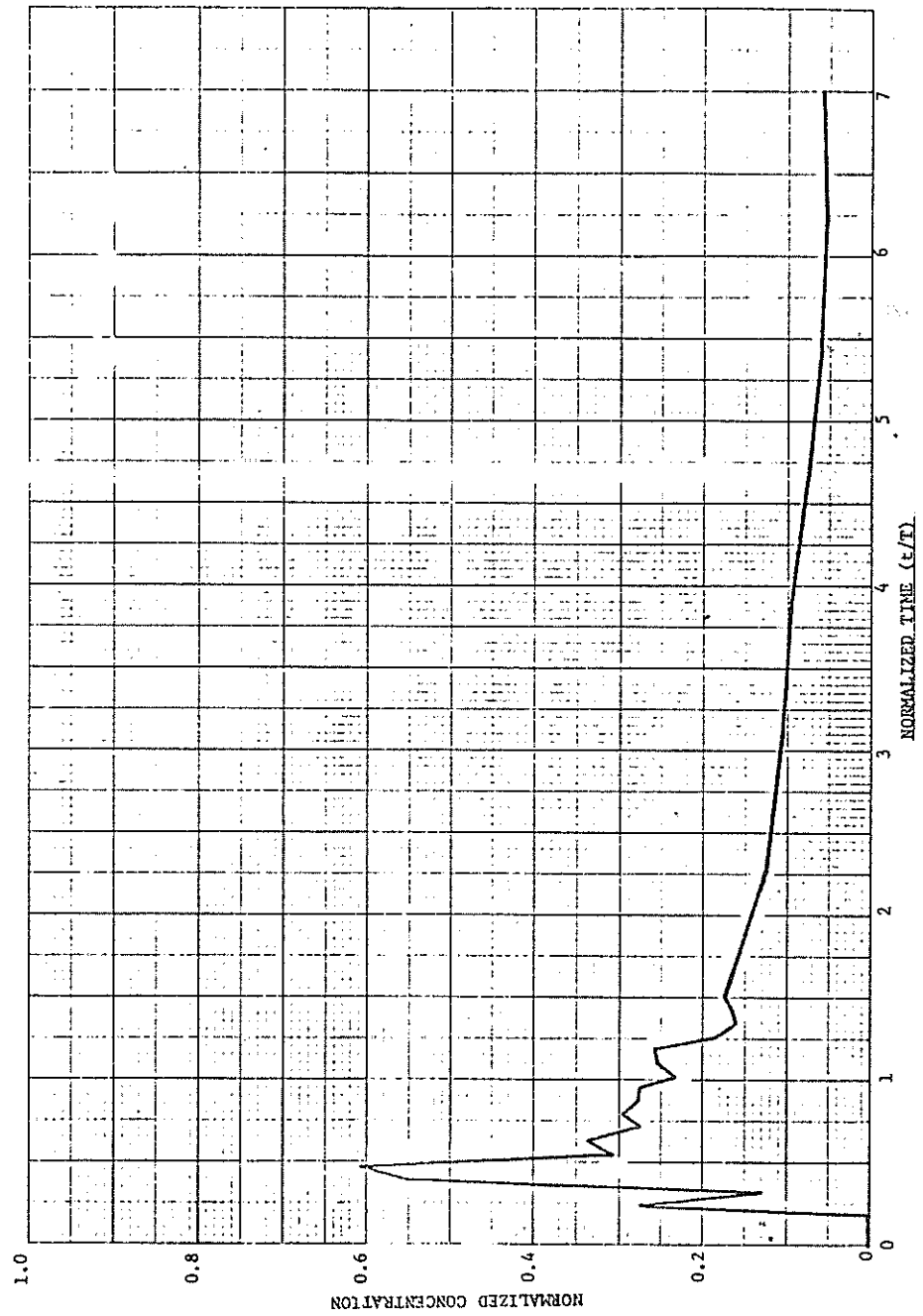

Figure 51. Dispersion Curve - 12 in., Baffle Box 900 gal/min

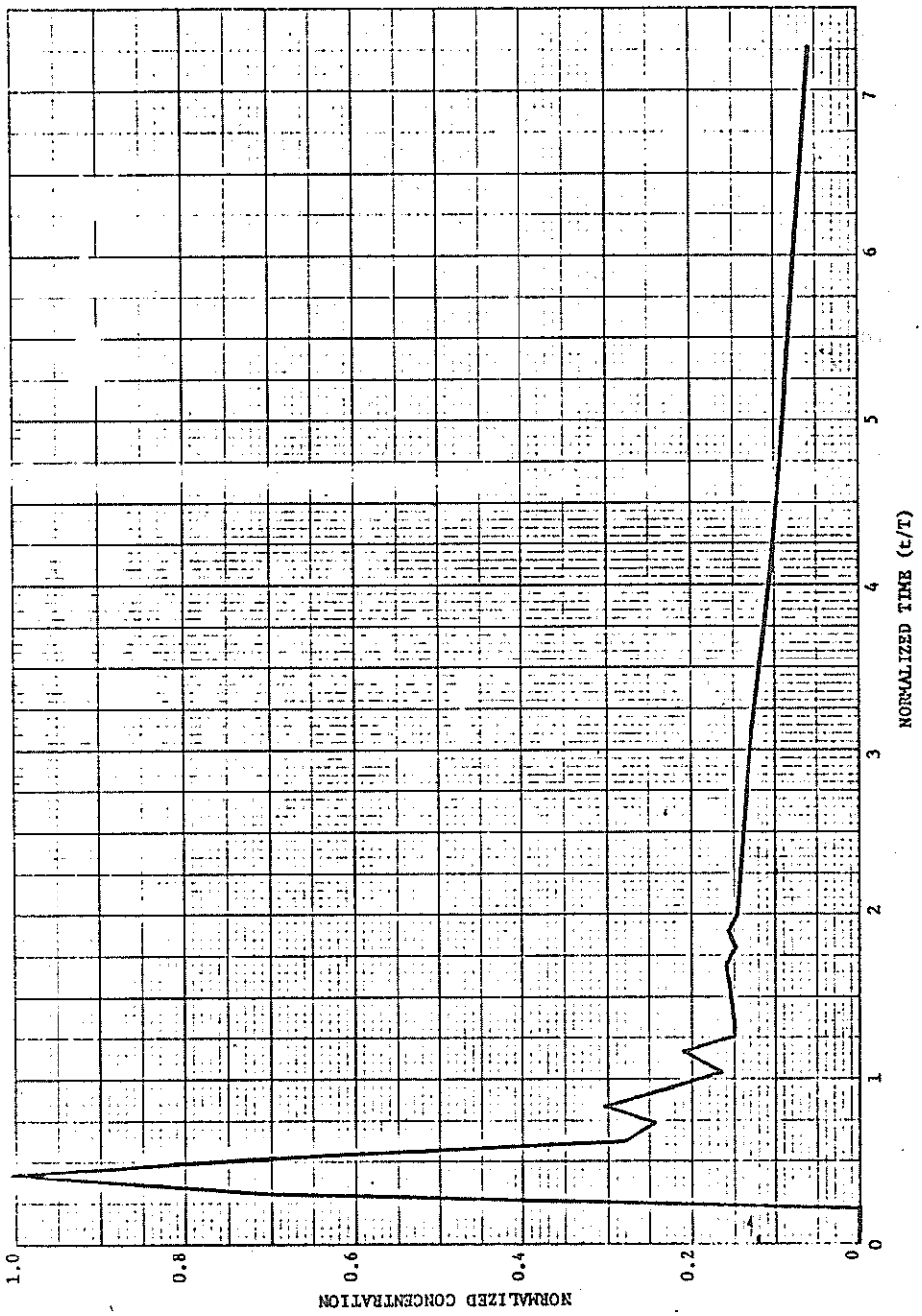

Figure 52. Dispersion Curve - 12 in., Baffle Box 1200 gal/min

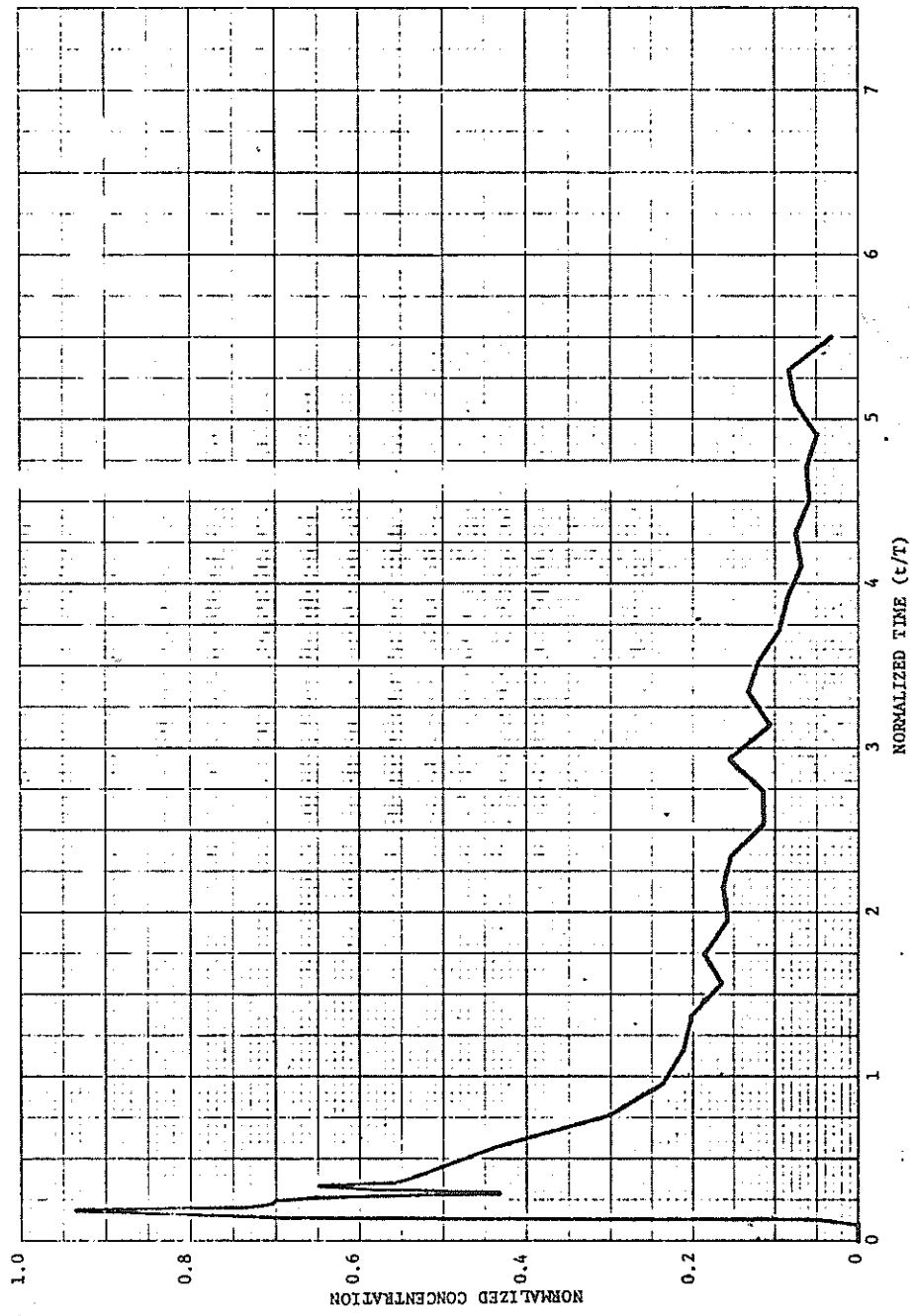

Figure 53. Dispersion Curve - 24 in., Baffle Box 450 gal/min

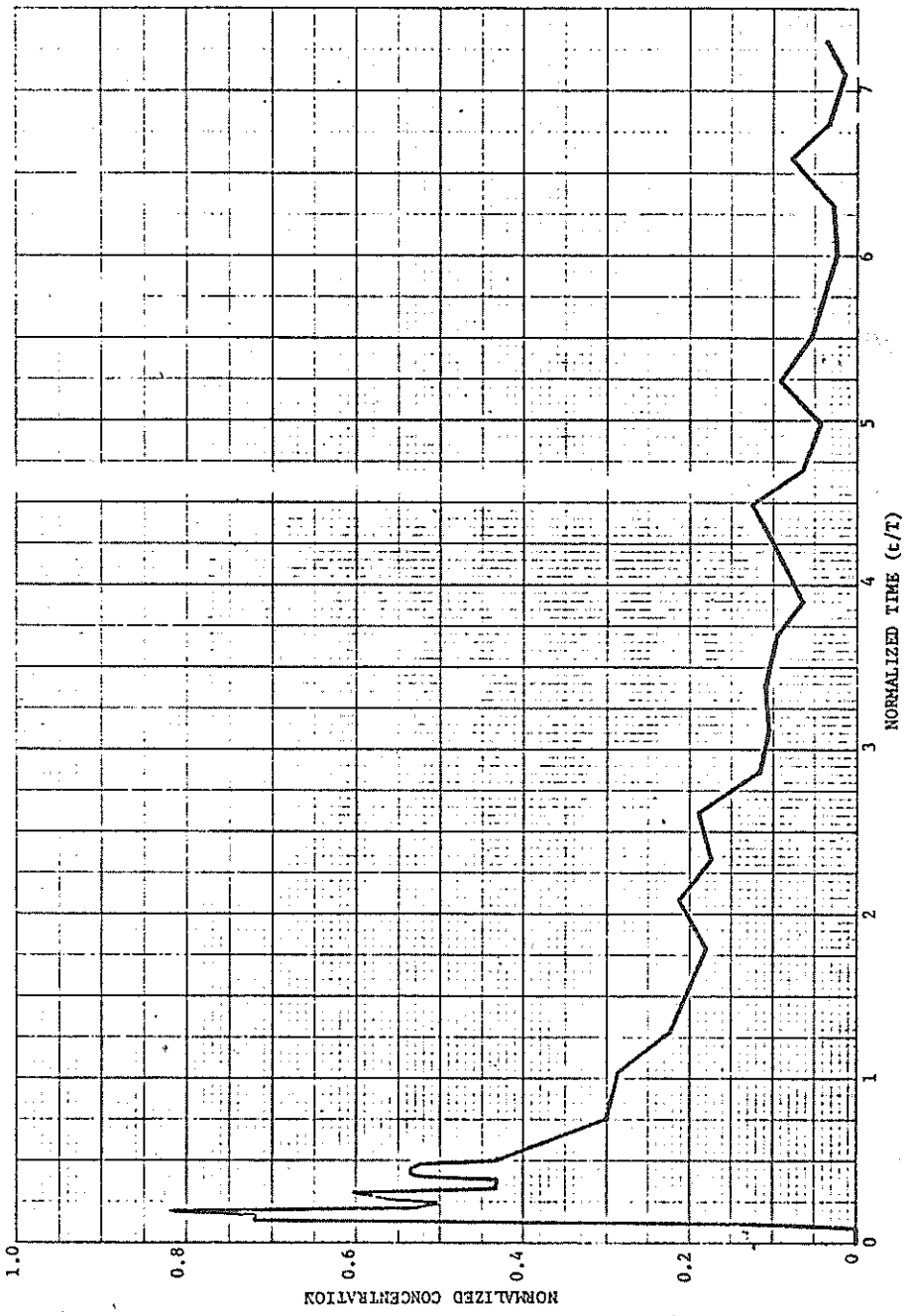

Figure 54. Dispersion Curve - 24 in., Baffle Box 600 gal/min

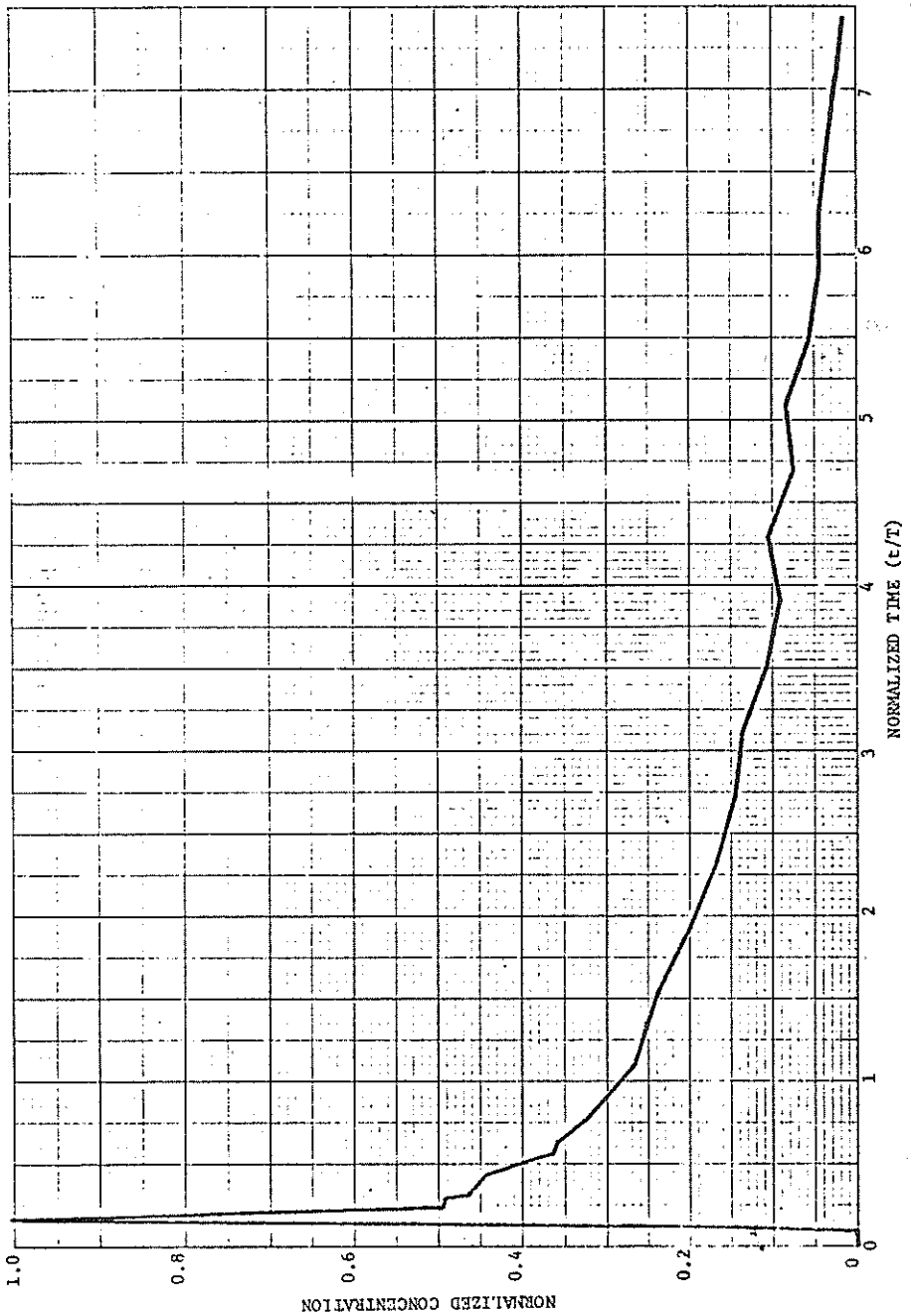

Figure 55. Dispersion Curve - 24 in., Baffle Box 900 gal/min

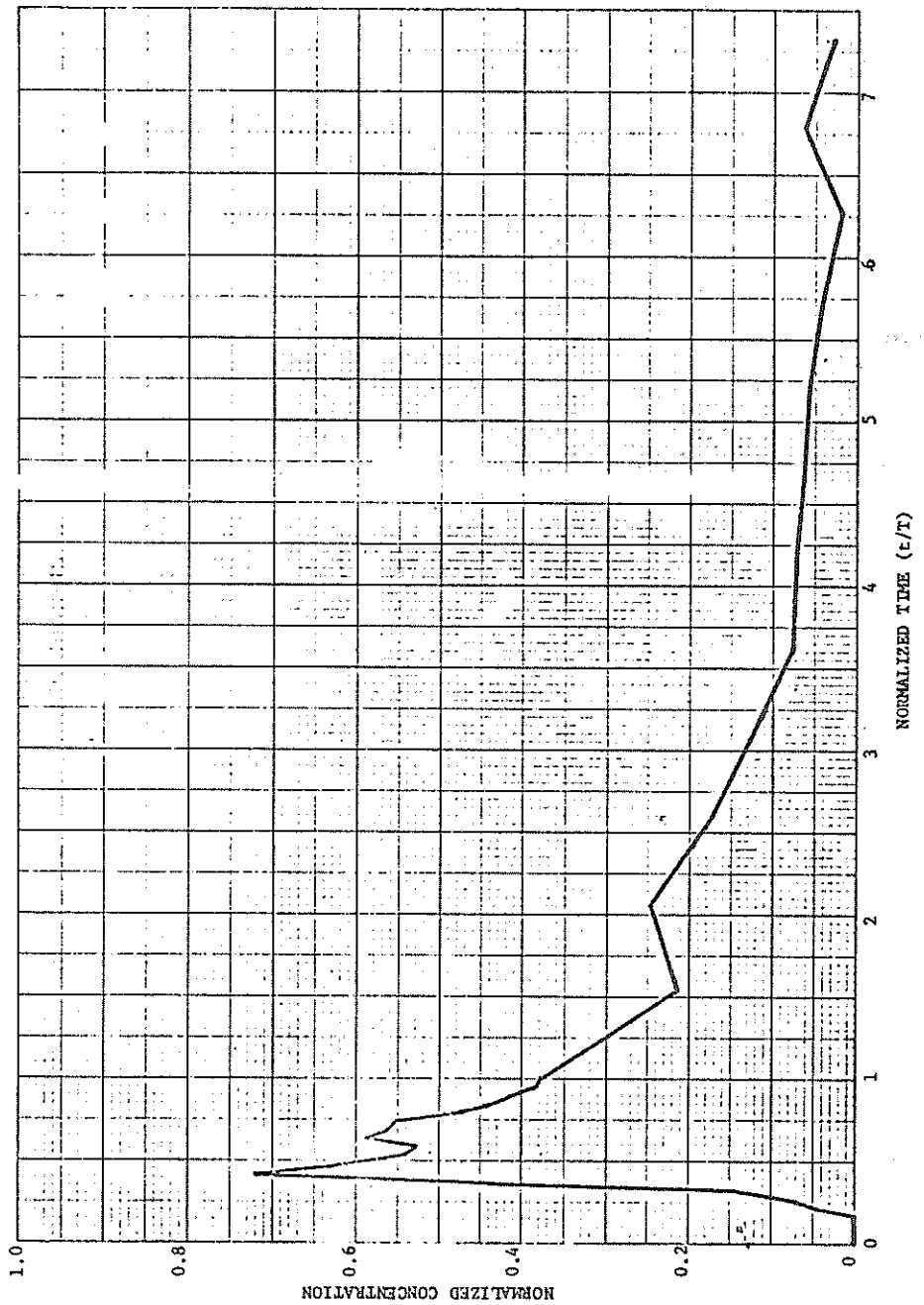

Figure 56. Dispersion Curve - 24 in., Baffle Box 1200 gal/min

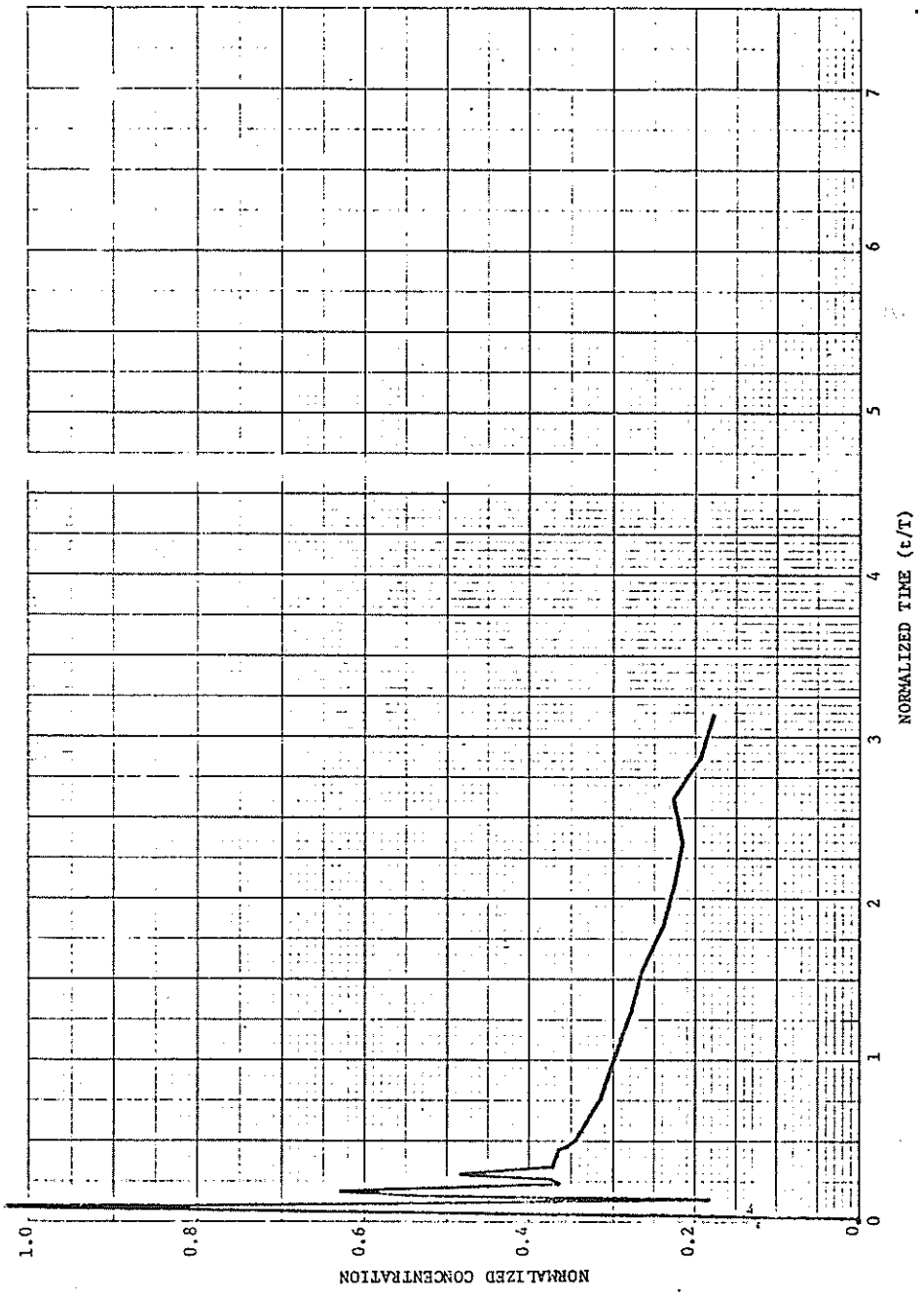

Figure 57. Dispersion Curve - 24 in., Reaction-Jet 600 gal/min

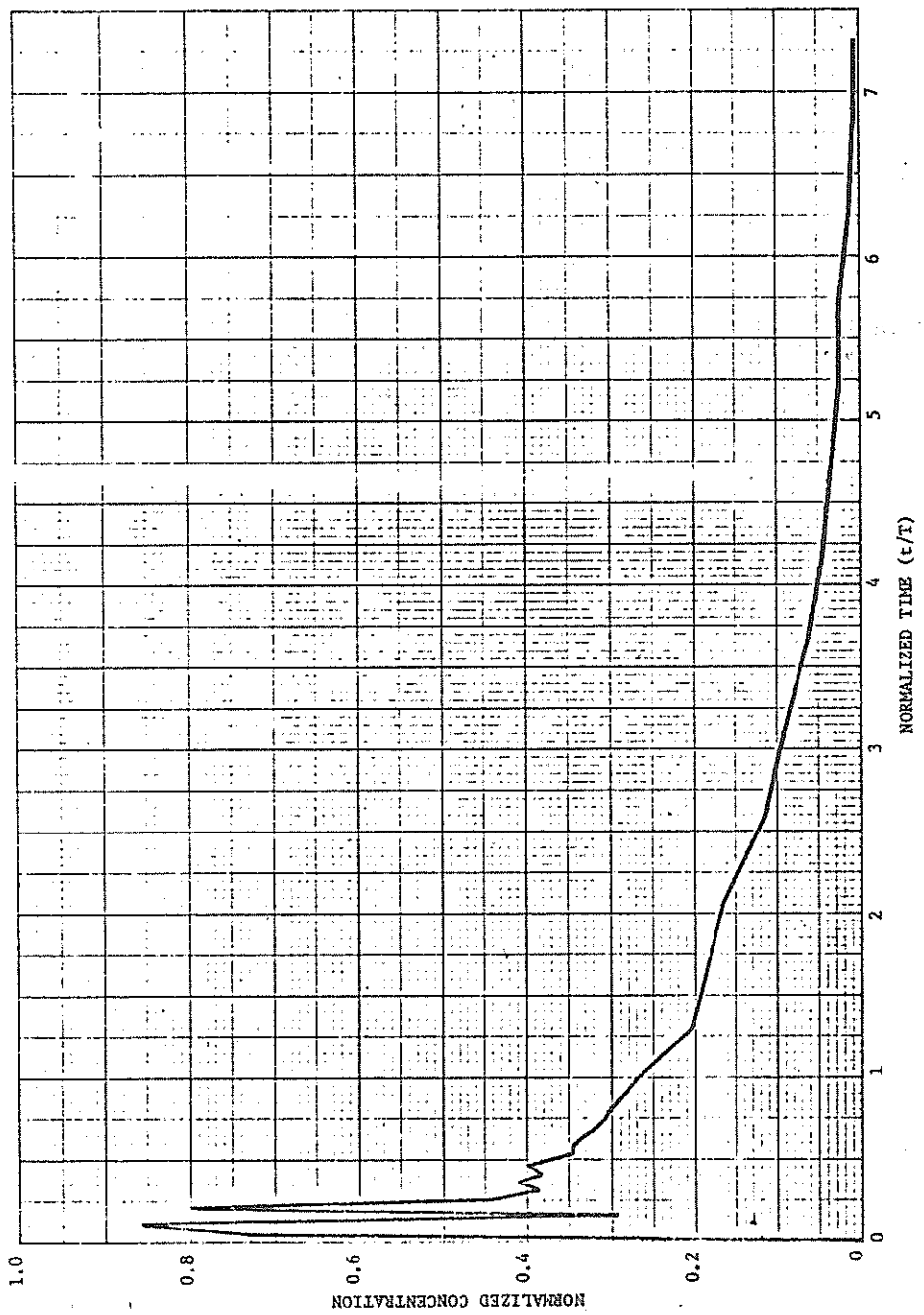

Figure 58. Dispersion Curve - 24 in., Reaction-Jet 1200 gal/min

APPENDIX VI

Calculation of Sediment Removal

The computations followed those explained in Villemonte et al. (19) as previously discussed in section VI

$$R_n = \frac{\sum_{i=1}^{n} S_i H_i \Delta t}{\sum_{i=1}^{n} H_i \Delta t}$$

The values of S_i and H_i were read from the respective graphs at sufficiently small Δt intervals to be suitably representative. For the curves presented in this report a small programmable calculater was programmed to calculate the R_n values for each new S_i and H_i. The following tabulation illustrates the method.

t	t/T	H_i	S_i	R_i
125	0.065	0	0.01	0.01
375	0.197	0	0.05	0.05
625	0.328	0.195	0.19	0.19
875	0.460	0.520	0.57	0.466
1250	0.657	0.662	0.72	0.631
1750	0.921	0.318	0.82	0.676
2250	1.184	0.288	0.86	0.708
2750	1.447	0.258	0.88	0.732
3250	1.710	0.228	0.89	0.749
3750	1.974	0.199	0.90	0.762
6000	3.158	0.126	0.925	0.811
10000	5.623	0.0518	0.956	0.828
14000	7.368	0.0500	0.971	0.841

Calculated for 1200 gpm, 1 baffle, 24 in. depth (see Figure 20, p. 65).

Two changes were made in Δt, at these changes the stored cumulatives were multiplied by the Δt ratio, $(\Delta t)_1/(\Delta t)_2$. The Δt values were not included in the calculation other than at changes in Δt.

The author took 15 to 20 min from start to finish for each such calculation on the already programmed calculator. This time included the extraction of the first four columns.

The method of dividing by the area under the dispersion curve to the time of interest, as opposed to the total area, caused the asymptotic removal value to be approached more quickly. The sequential computation also depended on this formulation.